An enhanced Johnson-Cook strength model for splitting strain rate and temperature effects on lower yield stress and plastic flow

Luca Gambirasio
Università di Bergamo, Dipartimento di Ingegneria e Scienze Applicate, 24044 Dalmine (BG), Italy
luca.gambirasio@unibg.it

Egidio Rizzi*
Università di Bergamo, Dipartimento di Ingegneria e Scienze Applicate, 24044 Dalmine (BG), Italy
egidio.rizzi@unibg.it

* Corresponding Author
Submitted for publication, 31 July 2015; Revised, 28 October 2015

Keywords

Modified Johnson-Cook model; Split Johnson-Cook material parameters; Calibration procedures; Strain rate and temperature sensitivities; Plastic behavior of metals.

Abstract

This paper introduces a new 'strength model', named Split Johnson-Cook (SJC). The model is a generalization of classical Johnson-Cook (JC) and provides a much improved coherence for the plastic material description. Specifically, the new model tackles the issue that the effects of equivalent plastic strain rate and temperature shall not be taken as equal for each equivalent plastic strain, avoiding then heavy modeling errors on the lower yield stress and on the subsequent plastic flow.

The salient features of the original JC model are shortly reviewed first, paying specific attention to possible modeling incoherencies. Two main shortcoming issues are framed and discussed. Further, a review on several modifications of the JC model from the literature is outlined. Then, the new SJC model is introduced in such a framework and thoroughly described. A comprehensive discussion on its calibration strategies follows, by developing three alternative calibration approaches.

The new model is then applied to the material description of three real material cases (a structural steel, a commercially pure metal and a stainless steel), by considering literature sets of hardening functions recorded at different equivalent plastic strain rates and temperatures. SJC predicted trends are checked against experimental data, for each calibration strategy, by evaluating the material prediction on both lower yield stress and plastic flow. Obtained results are also compared to those provided by plain JC.

The SJC model shows the capability to remarkably improve the material description, as compared to plain JC. Moreover, the fact of presenting a form very similar to that of the original JC model allows to possibly reusing some of the JC material parameters, which may be already known from available calibrations. Also, the SJC model keeps the same computational appeal of the original JC model and need of experimental data towards calibration, while heaviness of calibration and computational weight remain almost unchanged.

1. Introduction

The present paper proposes a modification of the so-called Johnson-Cook (JC) strength model (Johnson and Cook, 1983), namely a hardening function describing the material yield stress as a function of equivalent plastic strain, equivalent plastic strain rate and temperature. The new strength model consists in a generalization of the original JC model, towards achieving a better modeling coherence.

The present enhanced model allows to better describe the effects of equivalent plastic strain rate and temperature on the lower yield stress and on the plastic flow. The resulting strength model aims at providing much better results comparing to those achievable from the plain JC model, by working in the same computational framework and by adopting the same type of experimental data available for calibration.

Notice that Johnson and Cook defined also a model for predicting fracture phenomena (Johnson and Cook, 1985). However, fracture effects are not considered in this paper so far, which focuses on strength models only. On the other hand, a large strain framework is considered. Basic contexts, concepts and notations adopted in the paper follow preliminary earlier work on a doctoral dissertation (Gambirasio, 2013) and results complement those on plain JC produced in a companion paper (Gambirasio and Rizzi, 2014).

The JC hardening function fits in the classic elastoplastic framework (see, Hill, 1950, Kachanov, 1971, Chaboche, 2008, and Bigoni, 2012), by handling the stress deviator evolution only, while a separate equation of state rules the volumetric behavior. On this, computational implementation issues may be found in Wilkins, 1963, 1978, and in Benson, 1992. Also, for a discussion on issues related to constitutive model objectivity in computational implementations, see Gambirasio et al., 2014.

Before introducing the new strength model, a short introduction on the original JC model is presented next, in order to recall some key aspects that take a central role for the subsequent definitions in the enhanced model. Such discussion mainly relies on what exposed in companion paper Gambirasio and Rizzi, 2014, in which a wider discussion on the JC model and on its calibration strategies may be found, together with a review on the bulge of the extensive literature devoted to that.

Subsequently, Section 2 presents a mini review on several modifications of the JC model proposed in the literature, useful for collocation of the present enhanced model and for appreciating its novelty. Then, Section 3 presents the new Split Johnson-Cook model and widely discusses its calibration, outlined on three real material cases, by showing much improved performance with respect to plain JC. Finally, Section 4 outlines the closing considerations and lists the crucial points of this study.

1.1. Johnson-Cook model framework and shortcomings

Johnson and Cook, 1983, introduced a strength model for describing isotropic elastoplastic hardening under large strains, within certain ranges of equivalent plastic strain rates and temperatures. One main target of the JC model was making it suitable for FEM implementation and computational use. Hardening outcomes were exposed in terms of Cauchy stress vs. true strain (logarithmic strain measure). In the JC model, the yield stress is expressed as a power function of the equivalent plastic strain and as a natural logarithmic variation of the yield stress on the dimensionless equivalent plastic strain rate $\dot{\bar{\varepsilon}}^*$

$$\dot{\bar{\varepsilon}}^* = \frac{\dot{\bar{\varepsilon}}_p}{\dot{\bar{\varepsilon}}_p^0}, \tag{1}$$

where $\dot{\bar{\varepsilon}}_p$ is the current equivalent plastic strain rate and $\dot{\bar{\varepsilon}}_p^0$ a fixed reference value of it. Concerning temperature effects, a power dependence of the yield stress on the homologous or homogeneous temperature T^*

$$T^* = \frac{T - T_0}{T_m - T_0}, \tag{2}$$

is assumed, where T_m is the melting temperature and T_0 a reference fixed value of temperature.

According to these assumptions, the JC model was multiplicatively represented by the following hardening equation, expressed as the von Mises yield stress as a function of equivalent plastic strain, dimensionless equivalent plastic strain rate and homologous temperature

$$\bar{s} = \left(A + B \cdot \bar{\varepsilon}_p^n\right) \cdot \left(1 + C \cdot \ln \frac{\dot{\bar{\varepsilon}}_p}{\dot{\bar{\varepsilon}}_p^0}\right) \cdot \left(1 - \left(\frac{T - T_0}{T_m - T_0}\right)^m\right). \tag{3}$$

with eight JC material parameters A, B, n, C, $\dot{\bar{\varepsilon}}_p^0$, T_0, T_m, m of dimensions and possible units as reported in Table 1. Appropriate experimental tests are needed for their calibration.

A	Stress [MPa]	n	Dimensionless	$\dot{\bar{\varepsilon}}_p^0$	Strain rate [s^{-1}]	T_m	Temperature [K]
B	Stress [MPa]	C	Dimensionless	T_0	Temperature [K]	M	Dimensionless

Table 1. JC parameters dimensions and possible units.

The JC strength model conceives a multiplicative decomposition of the current yield stress in the three terms visible in Eq. (3). They set, respectively: a power hardening law (quasi-static term), a log function on the dimensionless equivalent plastic strain rate (strain rate term), a power variation on the homologous temperature (temperature term). Regarding the latter, when the melting temperature is reached, the temperature term vanishes, so that the material loses its deviatoric strength. Above the melting temperature the yield stress may be set to zero or a different strength function may be considered, appropriate for describing the arising material phases.

The JC model has been largely used by several authors, for successfully modeling of different materials. As instances, the JC model has been adopted for the modeling of Ti-6Al-4V titanium alloy (Lee and Lin, 1998, Lesuer, 1999, Khan et al., 2004, Akbari Mousavi et al., 2008, Kotkunde et al., 2014 a), structural steel (Batra and Kim, 1991), XC48 steel (Langrand et al., 1999), HSLA-65 steel (Nemat-Nasser and Guo, 2005), sheet steel (Rusinek et al., 2005), mild steels (Rusinek et al., 2007), ultra-fine-grained copper (Mishra et al., 2008), Hastelloy X (Abotula et al., 2011), 304 stainless steel (Chen et al., 2011), quenched and self-tempered reinforcing steel (Cadoni et al., 2013), 2024-T351 aluminum (Seidt and Gilat, 2013) and advanced high-strength steel sheets (Roth and Mohr, 2014). Among the many applications of the JC model, quite a few consider the modeling of structures under high velocity impacts and blast loadings (see, e.g., Pappu and Murr, 2002, Valerio-Flores et al., 2004, and Teng and Wierzbicki, 2005).

The formulation of the JC model starts from an empirical basis and provides a fairly simple model, which may not always give precise predictions of the material hardening behavior. This aspect was somehow indicated also in Johnson and Cook, 1983. Anyway, this simplicity entails several positive points. In fact, it achieves a reasonable compromise between modeling simplicity, prediction coherency, quest of dedicated experimental data and computational requirements. Regarding negative aspects, it may be said that the simplicity of the JC strength model is paid by introducing some drawbacks in the formulation. In particular, *two main flaws may be identified*:

- The first flaw consists in the fact that the log variation of the yield stress on the dimensionless equivalent plastic strain rate may not be suitable to fit the strain rate sensitivity of some materials.

Analogously, the yield stress power function of the homologous temperature may present the same shortcoming. These aspects might lead to heavy modeling errors in practical cases.

- The second flaw consists in the fact the effects of equivalent plastic strain, equivalent plastic strain rate and temperature on the yield stress are totally independent from each other. This is a direct consequence of the choice of adopting a hardening function designed in a multiplicative way, in which the three factors independently represent the three effects on the yield stress. For instance, for a given equivalent plastic strain, its effect on the yield stress is the same whatever the equivalent plastic strain rate and temperature. This may imply heavy modeling errors, either on the lower yield stress or on the subsequent plastic flow, or even on both. Thus, this simplistic approach may lead to considerable modeling errors, which actually add to the ones due to the first flaw.

The next section aims at better evaluating the magnitude of these two main detrimental issues of plain JC, inspiring then and motivating the present further proposed SJC modification later outlined in Section 3.

2. Assessment of Modeling Incoherencies of the Plain JC Model and Critical Review on Several Proposed Modifications

Considering what stated at the end of Section 1, there arise questions about the relevance of the identified flaws, i.e. how much they may negatively affect the coherence of the JC strength model. It appears that, due to its nature, the JC model may occasionally be incapable to coherently predict the hardening material behavior, in particular over wide ranges of equivalent plastic strain rate and temperature. More in detail, fittings may be appropriate only for selected ranges, but not overall and the JC hardening function may not be good enough to describe the available data in order to reproduce results fruitfully usable for engineering purposes.

The belief that the JC model may sometimes produce notably incoherent predictions appears to be confirmed in analyzing the strain rate and temperature dependent hardening response of different materials, through experimental results from the literature. Some examples of such references are Krafft et al., 1954, which presented studies on iron and steel plastic flows in the dependence of strain rate and temperature; Hoge and Mukherjee, 1977, which proposed an investigation on the temperature and strain rate dependence of the flow stress of tantalum; Nemat-Nasser and Guo, 2003, which proposed a wide strain rate and temperature investigation on the plastic flow behavior of a structural steel; Rusinek et al., 2009, which presented similar investigations for six high-strength steels. Basically, it appears that the form of the JC model may not be suitable to fit such behaviors.

The two previously presented main issues of the JC strength model did not pass unnoticed in the scientific community. Indeed, the model has been the subject of several reviews and modifications. The aims were those of solving or mitigating the negative effects due to the two main drawbacks above. The following exposition aims at briefly reviewing the main proposed contributions. Publications dealing with the first JC issue are presented first, while those dealing with the second issue are presented second. Actually, it may be said that the relevance of the JC model is further proven by the large number of revisions and enhancements that have been proposed since its first publication in 1983.

The following mini review allows to appreciate also how the present SJC model is clearly different from all the other previous JC modifications proposed in the literature and thus reveals its novelty in the potential application for several scientific and technological applications, as those where plain JC and modified JC models have been used, specifically in computational modeling environments.

2.1. Modifications on the First Drawback Issue

The first detrimental JC issue outlines at the end of Section 1 addresses the fact that a material may not present a yield stress log variation on the dimensionless equivalent plastic strain rate and a power law on the homologous temperature. Several authors have proposed modifications of the original JC strain rate and

temperature terms, for improving the coherence of the hardening function. Some of the proposed modifications are analyzed in the following.

For what it concerns the strain rate term, a first modification regards the substitution of the original JC strain rate term with the so-called Cowper-Symonds strain rate term (see, e.g., Symonds, 1967, and Schwer, 2007). This was conceived years before the proposal of Johnson and Cook, 1983. However, such a term may be adopted for replacing the JC strain rate term, leading to the following strength model

$$\bar{s} = \left(A + B \cdot \bar{\varepsilon}_p^{\,n}\right) \cdot \left(1 + \left(\frac{\dot{\bar{\varepsilon}}_p}{D}\right)^{\frac{1}{P}}\right) \cdot \left(1 - \left(\frac{T - T_0}{T_m - T_0}\right)^m\right). \tag{4}$$

The model still uses eight parameters, but the two strain rate parameters are now represented by D and P. Such modification of the JC original model is quite popular, including for implementations in FEM codes.

Another modification of the strain rate term was presented by Holmquist and Johnson, 1991. These authors pointed-out how the yield stress log dependence on the dimensionless equivalent plastic strain rate could be replaced by a power variation. In detail, the original JC strength model was substituted by the following one

$$\bar{s} = \left(A + B \cdot \bar{\varepsilon}_p^{\,n}\right) \cdot \left(\frac{\dot{\bar{\varepsilon}}_p}{\dot{\bar{\varepsilon}}_p^{\,0}}\right)^D \cdot \left(1 - \left(\frac{T - T_0}{T_m - T_0}\right)^m\right). \tag{5}$$

This model still uses eight parameters, with the parameter D playing the role of the exponent in the strain rate term. Holmquist and Johnson, 1991, presented a FEM implementation of this modified JC model, with the aim of computationally reproduce some available experimental data. The modified model provided a better data fitting as compared to the original JC model, although the differences appeared quite marginal. This modified JC model is considered also in Allen et al., 1997, and in Schwer, 2007, in the context of FEM computations.

Couque et al., 1995, proposed another modification of the JC strain rate term. The authors pointed-out that the original JC model may be capable to provide good results when equivalent plastic strain rates lower than 10^3 s^{-1} are involved. However, it was also pointed-out that the model may lack in coherence when higher equivalent plastic strain rates occur. To better account for this effect, the original JC model was modified with the introduction of a power strain rate component added to the log strain rate term, leading to a model with eleven parameters, as represented in the following equation

$$\bar{s} = \left(A + B \cdot \bar{\varepsilon}_p^{\,n}\right) \cdot \left(1 + D \cdot \ln\frac{\dot{\bar{\varepsilon}}_p}{\dot{\bar{\varepsilon}}_p^{\,0}} + E \cdot \left(\frac{\dot{\bar{\varepsilon}}_p}{\dot{\bar{\varepsilon}}_p^{\,1}}\right)^k\right) \cdot \left(1 - \left(\frac{T - T_0}{T_m - T_0}\right)^m\right). \tag{6}$$

In this equation, $\dot{\bar{\varepsilon}}_p^{\,1}$ represents an equivalent plastic strain rate value which determines the transition between the so-called thermally-activated regime and the so-called viscous regime. This value was stated to be about 10^3 s^{-1}. The strain rate term now involves five parameters, instead of two like in the original JC strain rate term. The modified model was evaluated through numerical simulations for reproducing the strain rate behavior of pure nickel and a high-strength nickel alloy. Comparing to plain JC, the outcomes proved the modified model to display an improved coherence in reproducing experimental data at high equivalent plastic strain rates. An application of this modified JC model may be also found in Hussain et al., 2013, in the context of FEM simulations of explosively formed projectiles.

Camacho and Ortiz, 1997, used a modified strain rate term conceived in a way very similar to that proposed by Holmquist and Johnson, 1991 in Eq. (5). The model is expressed as

$$\bar{s} = \left(A + B \cdot \bar{\varepsilon}_p^n\right) \cdot \left(1 + \frac{\dot{\bar{\varepsilon}}_p}{\dot{\bar{\varepsilon}}_p^0}\right)^D \cdot \left(1 - \left(\frac{T - T_0}{T_m - T_0}\right)^m\right). \tag{7}$$

As in Holmquist and Johnson, 1991, the yield stress log variation on the dimensionless equivalent plastic strain rate is replaced by a power dependence. The only difference consists in the fact that the dimensionless equivalent plastic strain rate is augmented by 1 before being raised to the exponent D. Further uses of such a modified model are reported, e.g., in Børvik et al., 2001, Clausen et al., 2004, Dey et al., 2007, and Gruben et al., 2011.

Another modification of the strain rate multiplicative term was proposed by Rule and Jones, 1998. The point was that of modifying the original JC strain rate term to more closely match observed material behaviors at high strain rates. Similarly to what stated by Couque et al., 1995, the two authors pointed-out that the yield strength may increase more rapidly with the equivalent plastic strain rate than what determined for the original JC hardening function, in particular for equivalent plastic strain rates exceeding 10^3 s^{-1}. On this basis, Rule and Jones, 1998, proposed to modify the original JC model in the following way

$$\bar{s} = \left(A + B \cdot \bar{\varepsilon}_p^n\right) \cdot \left(1 + D \cdot \ln \frac{\dot{\bar{\varepsilon}}_p}{\dot{\bar{\varepsilon}}_p^0} + E_1 \left(\frac{1}{E_2 - \ln \frac{\dot{\bar{\varepsilon}}_p}{\dot{\bar{\varepsilon}}_p^0}} - \frac{1}{E_2}\right)\right) \cdot \left(1 - \left(\frac{T - T_0}{T_m - T_0}\right)^m\right). \tag{8}$$

In this equation, E_1 and E_2 are additional material parameters, obtainable from experimental data. Thus, the number of model parameters amounts to eleven. Rule and Jones, 1998, proposed also a calibration procedure for the model parameters, with application to four metals, through the evaluation of different experimental tests. This new model was then proven of providing a good fit of the yield stress at elevated equivalent plastic strain rates for some available experimental data.

Kang et al., 1999, pointed-out that the original JC strain rate term, which determines a linear dependence of the yield stress on the natural logarithm of the dimensionless equivalent plastic strain rate, may need to be enriched with a term that adds a quadratic dependence as well. This assumption was motivated with reference to some presented experimental data. In particular, it was shown that the quadratic term may be necessary to correctly represent the material behavior at low equivalent plastic strain rates, specifically lower than 1 s^{-1}. The JC hardening function was then modified in the following way

$$\bar{s} = \left(A + B \cdot \bar{\varepsilon}_p^n\right) \cdot \left(1 + D \cdot \ln \frac{\dot{\bar{\varepsilon}}_p}{\dot{\bar{\varepsilon}}_p^0} + D_1 \cdot \left(\ln \frac{\dot{\bar{\varepsilon}}_p}{\dot{\bar{\varepsilon}}_p^0}\right)^2\right) \cdot \left(1 - \left(\frac{T - T_0}{T_m - T_0}\right)^m\right). \tag{9}$$

This model uses nine parameters. A new parameter is introduced in the model, denoted by D_1. It determines the weight of the quadratic strain rate term. Considerations on this specific modified JC model may also be found in Schwer, 2007.

Johnson et al., 2006, proposed another modification of the strain rate term by introducing a power term that enriches the modeling of the yield stress variation on the equivalent plastic strain rate. The following form was then proposed and called high-rate JC model

$$\bar{s} = \left(A + B \cdot \bar{\varepsilon}_p^{\,n}\right) \cdot \left(1 + D \cdot \ln \frac{\dot{\bar{\varepsilon}}_p}{\dot{\bar{\varepsilon}}_p^{\,0}} + D_1 \cdot \left(\ln \frac{\dot{\bar{\varepsilon}}_p}{\dot{\bar{\varepsilon}}_p^{\,0}}\right)^{D_2}\right) \cdot \left(1 - \left(\frac{T - T_0}{T_m - T_0}\right)^m\right). \tag{10}$$

It may be pointed-out that this strength model appears as a generalization of the model proposed by Kang et al., 1999, i.e. that represented in Eq. (9). Comparing to plain JC, this approach introduces two additional parameters, denoted by D_1 and D_2, leading to a total of ten parameters. Applications of this model and comparisons to plain JC have been provided in the same reference, i.e. Johnson et al., 2006. Referring to the original JC model, the high-rate JC model showed an improved coherence.

Some modifications have been proposed for the JC temperature term as well, with different authors pointing-out difficulties of the original JC model to fit specific temperature dependent plastic flow data, such as, e.g., Samantaray et al., 2009, which pointed-out how the original JC model presents problems in fitting the temperature dependent plastic flow of a modified 9Cr-1Mo steel. However, no modifies to the JC temperature term were proposed in this publication.

A modification of the temperature term was actually proposed by Maheshwari et al., 2010, by relying on high temperature experimental data of aluminum alloy Al-2024, considering also the strain rate term modification proposed by Holmquist and Johnson, 1991, i.e. the power dependence. The following hardening function was then proposed

$$\bar{s} = \left(A + B \cdot \bar{\varepsilon}_p^{\,n}\right) \cdot \left(\frac{\dot{\bar{\varepsilon}}_p}{\dot{\bar{\varepsilon}}_p^{\,0}}\right)^C \cdot \left(1 + \left(\frac{\bar{s}_m}{\bar{s}_y} - 1\right) e^{-\alpha\left(\frac{T - T_0}{T_m - T_0}\right)^\beta}\right). \tag{11}$$

In this equation, $\bar{s}_m$, $\bar{s}_y$, α and β represent additional model parameters. The total number of parameters becomes then eleven. Maheshwari et al., 2010, presented some applications of the model that demonstrated a more coherent fitting of some temperature sensitive experimental data, when comparing to the original JC hardening function, in particular at high temperatures.

Hou and Wang, 2010, introduced a modification of the temperature term for better prediction when the range of temperatures is particularly wide. The focus was on a hot-extruded Mg-10Gd-2Y-0.5Zr alloy. Such modified hardening function uses eight parameters. The proposed model is reported in the following equation

$$\bar{s} = \left(A + B \cdot \bar{\varepsilon}_p^{\,n}\right) \cdot \left(1 + C \cdot \ln \frac{\dot{\bar{\varepsilon}}_p}{\dot{\bar{\varepsilon}}_p^{\,0}}\right) \cdot \left(1 - \lambda \frac{e^{\frac{T}{T_m}} - e^{\frac{T_0}{T_m}}}{e - e^{\frac{T_0}{T_m}}}\right). \tag{12}$$

Beyond the introduction of a new parameter, denoted by λ, the other seven parameters are claimed to be the same adopted for the original JC model.

Nguyen et al., 2012, considered replacements of the power quasi-static term with two other forms and then elaborated the temperature dependence of the yield stress by adopting a series of temperature terms similar to that of the original JC model, in the context of the prediction of boron steel sheets behavior at elevated and cooling temperatures. Also, the strain rate part of the model was neglected. Due to these aspects, the resulting hardening functions do not strictly appear as modifications of the original JC model, although Nguyen et al., 2012, referred to them as modified JC models. Rather, these models may be considered as belonging to other families of hardening functions. Therefore, they are not considered in the present list of proposed JC modified models.

As proven by the brief review presented here, many modifications of the original JC model strain rate and temperature terms have been proposed. In general, it may be said that the first issue of the JC model is partially solved, or mitigated, by the possibility of choosing between different strain rate and temperature terms, with the aim of better fitting the experimental data of the considered material, by taking into account specific equivalent plastic strain rate and temperature ranges. Incidentally, some commercial FEM codes allow to choose between some of the different strain rate and temperature terms described above.

2.2. Modifications on the Second Drawback Issue

For what it concerns the second JC issue, outlined at the end of Section 1, the point was that of considering the effects on the yield stress of equivalent plastic strain, equivalent plastic strain rate and temperature as totally independent from each other. In this regard, some authors proposed modifications apt to partially introduce the synergic dependence of strain rate and temperature effects.

For instance, Lin and Chen, 2010a and 2010b, introduced a modified JC model involving a mixed strain rate and temperature term, like

$$\bar{s} = \left(A + B \cdot \bar{\varepsilon}_p\right) \cdot e^{\left(-D_1 \cdot T + D_2 \cdot T \cdot \ln \frac{\dot{\bar{\varepsilon}}_p}{\dot{\bar{\varepsilon}}_p^0}\right)}. \tag{13}$$

The strain rate and temperature terms are merged in a single exponential term, in which both the temperature and the dimensionless equivalent plastic strain rate are involved, allowing for a coupling of strain rate and temperature effects. The model was introduced in the context of predicting the behavior of hot compressed typical high-strength alloy steels. Prediction results presented a good agreement with experimental data. Lin and Chen, 2010a, called this model combined JC and Zerilli-Armstrong model, since it partly derives from considerations due to the Zerilli-Armstrong strength model (Zerilli and Armstrong, 1987).

Lin et al., 2010, proposed a modified JC model in which another mixed strain rate and temperature term is introduced, in a more complex fashion than that proposed by Lin and Chen, 2010a, in Eq. (13). The proposed model assumed the following form

$$\bar{s} = \left(A + B_1 \cdot \bar{\varepsilon}_p + B_2 \cdot \bar{\varepsilon}_p^2\right) \cdot \left(1 + D \cdot \ln \frac{\dot{\bar{\varepsilon}}_p}{\dot{\bar{\varepsilon}}_p^0}\right) \cdot e^{\left(\lambda_1 + \lambda_2 \cdot \ln \frac{\dot{\bar{\varepsilon}}_p}{\dot{\bar{\varepsilon}}_p^0}\right) \cdot \left(T - T_r\right)}. \tag{14}$$

The power quasi-static term is replaced by a form that involves a second-order trend with respect to the equivalent plastic strain. Parameters B_1, B_2 replace original JC parameters B and n. Their role is that of describing the quasi-static behavior. However, this is only another form to fit data throughout the equivalent plastic strain range, and the point here is on the strain rate and temperature terms. The strain rate term is maintained the same as in the original JC model. The temperature term is substituted with an exponential term which involves the dimensionless equivalent plastic strain rate and the temperature. Two new parameters are introduced, denoted by λ_1 and λ_2, while parameters T_m and m are no longer present, thus keeping a total number of parameters equal to eight. The proposed model was applied to predict the tensile behavior of a high-strength alloy steel, showing a good fitting of experimental results. The modified JC model defined in Eq. (14) was also used by He et al., 2013, for modeling the high temperature plastic flow of 20Cr-Mo steel, by Li et al., 2013, for predicting the hot deformation behavior of 28Cr-Mn-Mo-V steel, and by Kotkunde et al., 2014b, and Cai et al., 2015, in the context of modeling of Ti-6Al-4V titanium alloy.

Wang et al., 2011, proposed a modification similar to the one introduced by Lin et al., 2010, with some variations of the quasi-static and strain rate terms, as in the following

$$\bar{s} = \left(A - B_1 \cdot e^{-B_2 \cdot \bar{\varepsilon}_p}\right) \cdot \left(1 + \left(D_1 + D_2 \bar{\varepsilon}_p\right) \cdot \ln \frac{\dot{\bar{\varepsilon}}_p}{\dot{\bar{\varepsilon}}_p^0}\right) \cdot e^{\left(\lambda_1 + \lambda_2 \cdot \ln \frac{\dot{\bar{\varepsilon}}_p}{\dot{\bar{\varepsilon}}_p^0}\right) \cdot \left(T - T_r\right)} . \quad (15)$$

The context was that of modeling the behavior of a 30Cr2Ni4MoV rotor steel over a large range of temperatures and strain rates. The obtained results showed how the developed constitutive equation may provide a quite accurate prediction of plastic flow for the considered material.

Lin et al., 2012a, introduced a modification of the JC model defined as follows

$$\bar{s} = \left(A + B\left\{\dot{\bar{\varepsilon}}_p\right\} \cdot \bar{\varepsilon}_p^{n\left\{\dot{\bar{\varepsilon}}_p\right\}}\right) \cdot \left(1 - \left(\frac{T - T_0}{T_m - T_0}\right)^{m\left\{\dot{\bar{\varepsilon}}_p\right\}}\right), \quad (16)$$

where parameters B, n and m are functions of the equivalent plastic strain rate. Such model was used for describing the high temperature behavior of a Al-Zn-Mg-Cu alloy, obtaining good correlation with experimental results.

In a similar fashion, Lin et al., 2012b, defined a modified JC model for describing the high temperature flow stress of a Al-Cu-Mg alloy. The proposal was as follows

$$\bar{s} = \left(A + B\{t\} \cdot \bar{\varepsilon}_p^{n\{t\}}\right) \cdot \left(1 + D\{t\} \cdot \ln \frac{\dot{\bar{\varepsilon}}_p}{\dot{\bar{\varepsilon}}_p^0}\right), \quad (17)$$

where parameters B, n and D become now functions of the temperature. The proposed model successfully predicted the behavior of the considered alloy. Also, Lin et al., 2012c, used the same model for modeling the hot compressive deformation behavior of a 7075 Al alloy at elevated temperatures, obtaining very good correlation with experimental data over wide ranges of strain rate and temperature.

Qingdong et al., 2014, introduced a modification aiming at characterizing the coupling effect of temperature and strain on the hardening behavior for advanced high-strength steels over a large range of temperatures, without considering the strain rate term, i.e. without accounting for strain rate effects. The model assumed the following form, in which T* denotes the homologous temperature in Eq. (2)

$$\bar{s} = A\left(1 - p \cdot T^{*m}\right) + B\{T^*\} \cdot \bar{\varepsilon}_p^{n\{T^*\}}, \quad (18)$$

where functions are denoted by writing first the dependent variable and then the independent variable, gathered by curly brackets. Thus, this model generalizes parameters B and n as functions of the homologous temperature. These functions may be polynomials of some order, so that the number of parameters of this model is not established a priori.

Despite these efforts, the second JC issue appears to be still present, in particular in its heaviest problematics, i.e. the fact that the effects of equivalent plastic strain rate and temperature need to be assumed as equal for each equivalent plastic strain, a point which may lead to heavy mismatches on the lower yield stress or on the plastic flow predictions. In this context, following Section 3 introduces the present new formulation apt to mitigate this important shortcoming.

3. New Split Johnson-Cook Strength Model

In this section, a new hardening model is introduced, which is referred to as Split Johnson-Cook (SJC) strength model. Since the new model derives from the classical JC model, it keeps an empirical nature. This aspect is central in order to properly frame the context in which the new model lies. Indeed, the target here is that of defining an empirical model not involving material parameters potentially hard to be determined, e.g. possibly stemming from micromechanical issues, thus following the main idea of the original JC model.

The aim here is that of setting-up a hardening function by relying only on already available experimental data, as assumed for plain JC. On these bases, the new model shall be capable to better reproduce experimental data, by providing an improvement of the description capabilities. The SJC model shall also strive to maintain the same computational appeal of the original JC model, i.e. it shall operate by requiring information only from equivalent plastic strain, equivalent plastic strain rate and temperature, thus allowing to perfectly fit in the same computational framework of plain JC.

3.1. Formulation of the Split JC Model

The SJC model specifies a hardening function which takes the following additively-split form

$$\bar{s} = A \cdot \left(1 + C_1 \cdot \ln \frac{\dot{\bar{\varepsilon}}_p}{\dot{\bar{\varepsilon}}^0_{p_1}}\right) \cdot \left(1 - \left(\frac{T - T_{0_1}}{T_m - T_{0_1}}\right)^{m_1}\right) + B \cdot \bar{\varepsilon}_p^n \cdot \left(1 + C_2 \cdot \ln \frac{\dot{\bar{\varepsilon}}_p}{\dot{\bar{\varepsilon}}^0_{p_2}}\right) \cdot \left(1 - \left(\frac{T - T_{0_2}}{T_m - T_{0_2}}\right)^{m_2}\right). \quad (19)$$

The twelve parameters denoted by A, C_1, $\dot{\bar{\varepsilon}}^0_{p_1}$, m_1, T_{0_1}, B, n, C_2, $\dot{\bar{\varepsilon}}^0_{p_2}$, m_2, T_{0_2}, T_m are the parameters of the SJC hardening function. Table 2 reports their dimensions and possible units.

A	Stress [MPa]	n	Dimensionless	B	Stress [MPa]	T_m	Temperature [K]
C_1	Dimensionless	m_1	Dimensionless	$\dot{\bar{\varepsilon}}^0_{p_1}$	Strain rate [s^{-1}]	T_{0_1}	Temperature [K]
C_2	Dimensionless	m_2	Dimensionless	$\dot{\bar{\varepsilon}}^0_{p_2}$	Strain rate [s^{-1}]	T_{0_2}	Temperature [K]

Table 2. SJC parameters dimensions and possible units.

The proposed hardening description keeps the same multiplicative way in plain JC, with the same strain rate and temperature terms, but the equivalent plastic strain rate and temperature effects are now separated for the lower yield stress, described by parameter A, and for the plastic flow, described by parameters B and n. The name Split Johnson-Cook model actually refers to this aspect. Thus, parameter A is called lower yield stress parameter and parameters B and n are called plastic flow parameters. Regarding the dependence of the yield stress on the equivalent plastic strain, the same power law from plain JC is kept. Parameters C, m and the values of reference equivalent plastic strain rate and temperature are doubled, yielding a total number of twelve parameters, i.e. (only) four parameters more than for plain JC.

The SJC model appears as a generalization of the original JC model, which in fact is recovered if parameters C_1 and C_2 are set equal, if parameters m_1 and m_2 are set equal and if values of reference equivalent plastic strain rates and temperatures are set equal. On the other hand, when these parameters are different from each other, it is possible to independently model the effects of strain rate and temperature on lower yield stress and plastic flow. In general, parameters C_1 and C_2 and parameters m_1 and m_2 become equal only in very particular cases, i.e. cases in which the material presents the same lower yield stress and plastic flow dependencies on equivalent plastic strain rate and temperature. More in general, parameters C_1 and C_2

may be quite different, as for parameters m_1 and m_2. Beyond the considered splitting of equivalent plastic strain rate and temperature effects, the way in which these effects are introduced in the hardening function is exactly the same as that in the original JC model, i.e. through natural logarithmic and power dependencies. This is a point of force of the present proposal, because, while keeping the well-known implant of plain JC, the additional parameters, keeping the same physical meaning, allow for much degrees of freedom in the material description of plastic flow in different ranges of strain rates and temperatures. Despite that, the higher level of complexity of the SJC model is really kept to a minimum. Both JC and SJC models can be used to describe the lower yield stress and plastic flow behavior of materials. However, the present SJC model can do such a task in a much better way. Indeed, this is the strongest enhancement introduced by the new model, i.e. it can predict both the lower yield stress and the plastic flow, with much higher coherence as compared to the original JC model. This is mainly due to the fact that the SJC model defines ad hoc material parameters for introducing temperature and strain rate dependence of the lower yield stress and of the plastic flow, in and independent way.

The first additive term of the hardening function describes the lower yield stress over the ranges of equivalent plastic strain rate and temperature. It is then called lower yield stress term. The two multiplicative terms that operate on such lower yield stress term act together to set it. The first one is called lower yield stress strain rate term and introduces a log variation on the lower yield stress dimensionless equivalent plastic strain rate $\dot{\bar{\varepsilon}}_1^*$, which is defined as

$$\dot{\bar{\varepsilon}}_1^* = \frac{\dot{\bar{\varepsilon}}_p}{\dot{\bar{\varepsilon}}_{p_1}^0}, \tag{20}$$

where $\dot{\bar{\varepsilon}}_{p_1}^0$ marks the lower yield stress reference value of the equivalent plastic strain rate.

The second multiplicative term that acts on the first additive term is called lower yield stress temperature term and introduces a power dependence on the so-called lower yield stress homologous temperature T_1^*, which is defined as

$$T_1^* = \frac{T - T_{0_1}}{T_m - T_{0_1}}, \tag{21}$$

where T_m represents the melting temperature and T_{0_1} represents the so-called lower yield stress reference temperature.

The second additive term of the hardening function describes the plastic flow over the ranges of equivalent plastic strain rate and temperature. This is then called plastic flow term. Two multiplicative terms act together to determine the plastic flow. The first one is called plastic flow strain rate term and introduces a log dependence on the plastic flow dimensionless equivalent plastic strain rate $\dot{\bar{\varepsilon}}_2^*$

$$\dot{\bar{\varepsilon}}_2^* = \frac{\dot{\bar{\varepsilon}}_p}{\dot{\bar{\varepsilon}}_{p_2}^0}, \tag{22}$$

where $\dot{\bar{\varepsilon}}_{p_2}^0$ represents the plastic flow reference value of the equivalent plastic strain rate.

The second multiplicative term acting on the second additive term is called plastic flow temperature term and introduces a power law variation on the plastic flow homologous temperature T_2*, which is defined in the following

$$T_2^* = \frac{T - T_{0_2}}{T_m - T_{0_2}}, \tag{23}$$

where T_m represents again the melting temperature and T_{0_2} represents the so-called plastic flow reference temperature.

The lower yield stress strain rate term is defined in such a manner that when the current equivalent plastic strain rate equals the reference value of the lower yield stress equivalent plastic strain rate it turns-out equal to 1, so that no strain rate effects are recorded on the lower yield stress. Otherwise, the strain rate effect is ruled by the current value of the equivalent plastic strain rate and by the reference value of the lower yield stress equivalent plastic strain rate and by parameter C_1. Analogous considerations hold for the plastic flow strain rate term, but considering the reference value of the plastic flow equivalent plastic strain and parameter C_2. This aspect is analogous to what happens for the strain rate term in the original JC model.

Similarly, the lower yield stress temperature term is defined so that when the current temperature equals the reference value of the lower yield stress temperature it becomes equal to 1, so that no temperature effects are recorded on the lower yield stress. Otherwise, the effect of temperature on the lower yield stress is set by the current value of temperature and ruled by the reference lower yield stress temperature, the melting temperature and parameter m_1. Analogous considerations hold for the plastic flow temperature term, but considering the plastic flow reference temperature and parameter m_2. This aspect is analogous to what happens for the temperature term in plain JC.

In general, the reference values of lower yield stress and plastic flow equivalent plastic strain rates and temperatures are not obliged to coincide. Indeed, the SJC model provides better fitting capabilities if these parameters are left to be possibly different. On the other hand, the melting temperature is maintained equal for both lower yield stress and plastic flow additive terms, and in fact it is intended to refer to the real material melting temperature. When the melting temperature is reached, both lower yield stress and plastic flow additive terms vanish and therefore the yield stress is null and the material does not provide additional deviatoric resistance, as for plain JC. If temperatures above the melting value appear, the yield stress is supposed to be no longer determined by the SJC model, which would lead to a negative yield stress, but may be reset to zero or the adopted strength model may be changed, according to the specific material under target.

The proposed form of the SJC model strives to maintain the characteristics of the original JC model but, at the same time, it aims at providing a considerable improvement of the modeling capabilities. In this regard, many possible forms have been set-up and investigated, like, e.g., by allowing lower yield stress parameter A and plastic flow parameters B and n not to be constants but rather functions of equivalent plastic strain rate and temperature. Using this approach, the following strength model would be set-up

$$\bar{s} = A\left\{\dot{\bar{\varepsilon}}, T\right\} + B\left\{\dot{\bar{\varepsilon}}, T\right\} \cdot \bar{\varepsilon}^{n\left\{\dot{\bar{\varepsilon}}, T\right\}}, \tag{24}$$

where functions are denoted by writing first the dependent variable and then the independent variables, gathered by curly brackets and separated by commas. The three functions that define the trends for parameters A, B and n throughout the tested equivalent plastic strain rates and temperatures can be shaped accordingly to the available experimental results and can be enriched where more material information is available. As instance, these functions may be multivariable polynomials or piecewise functions. Simple linear trends are likely incapable of fitting the material behavior with enough coherence. Clearly, this

approach leads to a serious complication of the model, due to the strong increase in the number of parameters needed for representing the three involved functions. This aspect implies a loss of simplicity which is probably the main positive aspect of the JC and SJC models.

Therefore, the proposed form, Eq. (19), is believed to constitute a good compromise between the willing of improving the model coherence and that of maintaining a simple form, similar to that put forward by plain JC. More complex hardening functions have been elaborated and investigated, but they are always affected by the introduction of unwanted complexities, in particular by needing a much larger number of material parameters. The similarity to plain JC allows for some interesting options, such as the possibility to substitute one or more of the lower yield stress and plastic flow terms for strain rate and temperature with some of the proposed substitutive terms, previously reviewed in Section 2. Furthermore, having a form very similar to plain JC, SJC may allow to partially reusing some original JC parameters already determined from previous calibrations.

Concerning the SJC model calibration, i.e. the identification of its material parameters, the first aspect to be appreciated is that experimental data provided by tests of diverse nature may be used. As instance, it is feasible to use experimental data from Hopkinson bar testing (for a description of this testing methodology, one may look at Hopkinson, 1914, Kolsky, 1949, Meyers, 1994, Ramesh and Narasimhan, 1996, Kapoor and Nemat-Nasser, 1998, Kajberg et al., 2004, Kajberg and Wikman, 2007, and Jiang and Vecchio, 2009), Taylor tests (for a description of this testing methodology, one may read Taylor, 1948, Whiffin, 1948, Hawkyard et al., 1968, Hawkyard, 1969, Wilkins and Guinan, 1973, House, 1989, Teng et al., 2005, Brünig and Driemeier, 2007, and Rakvåg et al., 2014) and also other less popular testing methods.

The present treatment defines calibration strategies that make use of experimental hardening functions, namely functions relating yield stress and equivalent plastic strain, for different equivalent plastic strain rates and temperatures. Data of this kind are commonly provided by tensile tests, at low values of equivalent plastic strain rate, and by tests with Hopkinson bar, at mid and high values of equivalent plastic strain rate. Indeed, it appears that nowadays the most popular and reliable way of obtaining high strain rate experimental data is that of performing such kind of testing. Following Section 3.2. introduces appropriate procedures towards achieving best calibration of the SJC model through this kind of data. Some comments on the necessary experimental information needed for each calibration strategy are also outlined.

Anyway, it may be possible to define devoted strategies apt to calibrate the SJC model by using other kinds of experimental data, like, e.g., by relying on some structural parameter achievable from Taylor impact testing. As a matter of fact, it is possible to find several calibration strategies of this kind when dealing with the original JC model. On this, one may consider Johnson and Holmquist, 1988, Holmquist and Johnson, 1988, and 1991, Allen et al., 1997, Rule, 1997, Rohr et al., 2008, Nussbaum and Faderl, 2011, Grązka and Janiszewski, 2012, and Šlais et al., 2012.

3.2. SJC Model Calibration Procedures Based on Experimental Hardening Functions

As for the original JC model, the SJC parameters may be determined by appropriate calibration procedures. In this regard, Gambirasio and Rizzi, 2014, presented five different original JC model calibration strategies, named LYS, OPTLYS, EPS, OPTEPS and GOPTEPS, with systematic applications to real experimental data. In this paper, three different SJC calibration approaches are introduced and carefully discussed, paying particular attention to the analogies between these strategies and those just mentioned for the original JC model. In fact, one aim here is that of describing the three SJC calibration strategies in a way as similar as possible to what done for the five original JC calibration strategies, in order to favor comprehension for readers that are already familiar with the plain JC model, with particular reference to the methodology adopted in Gambirasio and Rizzi, 2014. The three SJC calibration approaches considered here appear to be the most natural and practical, though it is understood that further strategies may be identified and defined as well. For the sake of clarity, a name is associated here to each calibrating approach. The achieved results are

extensively compared and debated, by highlighting several positive issues and negative aspects pertaining to the three different approaches.

To appreciate the concept driving the three calibration strategies, they are systematically applied to three material cases. Underlying experimental outcomes are assumed to consist of nine hardening functions, referring to three equivalent plastic strain rates and to three temperatures, for each considered material case. However, one may consider that the three identified calibration procedures can be adopted independently from the amount of hardening functions that are experimentally available, which shall produce more or less precise calibrations, depending on the richness of the experimental results. On this, the adopted subsets of nine hardening functions look certainly sufficient for the present goals, as well as for avoiding to bring up too much data.

The first material data set is taken from Nemat-Nasser and Guo, 2003, which concerns a high-strength structural steel, labeled DH-36. The selected equivalent plastic strain rates are 0.001 s^{-1}, 0.1 s^{-1} and 3000 s^{-1}, while the considered temperatures are 77 K, 296 K and 800 K. The second material data set is taken from Nemat-Nasser and Guo, 2000, referring to a commercially-pure niobium material. The taken equivalent plastic strain rates are 0.001 s^{-1}, 3300 s^{-1} and 8000 s^{-1}, while the considered temperatures are 296 K, 500 K and 700 K. The third material data set is taken from Nemat-Nasser et al., 2001, in which stainless steel AL-6XN was investigated. The adopted equivalent plastic strain rates are 0.001 s^{-1}, 0.1 s^{-1} and 3500 s^{-1}, while the considered temperatures are 77 K, 296 K and 600 K. Some of these data seemingly present discontinuous yielding phenomena, likely ascribing to the Portevin-Le Chatelier (PLC) effect (see, e.g., Hähner and Rizzi, 2003, and Rizzi and Hähner, 2004).

These three material data sets allow for calibrating the SJC model on three rather dissimilar materials, involving fairly diverse hardening behaviors, over wide equivalent plastic strain rate and temperature ranges. Material data are considered in terms of couples of values of Cauchy stress vs. true (logarithmic) equivalent plastic strain. The specific details about the nature and context of the considered experimental data may be consulted in the relevant papers, i.e. Nemat-Nasser and Guo, 2000, 2003, and Nemat-Nasser et al., 2001.

Such material data sets have been extracted from the original documents through a proper digitalization. Further explanations on how this process has been accomplished are reported in Gambirasio and Rizzi, 2014, which indeed considers the same three sets of experimental data and digitalization process, together with additional information on the considered experimental data, with particular attention to the effect of temperature rising due to plastic work transformed into thermal energy for high strain rate testing. Original JC model calibration results on the same three considered materials are reported in Gambirasio and Rizzi, 2014, by considering five different calibration strategies. This fact allows to compare the present results for the new SJC model to those provided by the original JC model, all against the same experimental data, therefore enabling to much better assess the positive and negative points of the new strength model.

As the original JC model, the SJC model does not account for stress triaxiality effects on the yield stress. Hence, experimental outcomes adopted for calibration purposes may derive from classical mechanical tests, as tensile, compression or torsion tests, as long as results are represented in terms of von Mises stress vs. equivalent plastic strain. Anyway, more or less different model parameters may be calculated when considering one type of test or another, as occurs for the original JC model and somehow indicated by Johnson and Cook, 1983. Yield stress dependence on stress triaxiality looks like a not thoroughly defined aspect and thus it has not been introduced so far in the SJC model. Some comments on the combined effects of stress triaxiality and strain rate are reported in Hopperstad et al., 2003, and in Børvik et al., 2003.

3.2.1. STA Calibration Strategy

The STA (STAndard) calibration strategy is likely the simplest approach apt to set the twelve SJC parameters, among the three strategies introduced in the present paper. This calibration strategy plays the same role taken by the so-called LYS and EPS approaches for the original JC model, since it follows similar considerations.

Melting temperature is to be determined first. Then, the lower yield stress term parameters are calculated. Clearly, the parameters relative to the lower yield stress term are determined by considering experimental data at zero equivalent plastic strain, i.e. with a vanishing plastic flow additive term. In these conditions, the SJC model reduces to the following form

$$\overline{s} = A \cdot \left(1 + C_1 \cdot \ln \frac{\dot{\overline{\varepsilon}}_p}{\dot{\overline{\varepsilon}}^0_{p_1}} \right) \cdot \left(1 - \left(\frac{T - T_{0_1}}{T_m - T_{0_1}} \right)^{m_1} \right). \tag{25}$$

This is totally analogous to that of plain JC, when the equivalent plastic strain vanishes.

At first, the testing equivalent plastic strain rates and temperatures have to be selected, to set the reference values of the lower yield stress equivalent plastic strain rate and temperature. The reference value of the lower yield stress equivalent plastic strain rate is set equal to one of the testing equivalent plastic strain rates. No further constraints are introduced, so any of them could be chosen, with a typical choice consisting in adopting the lowest tested value. Concerning the lower yield stress reference temperature, an appropriate choice is that of setting it equal to the lowest testing temperature, to avoid the possible appearance of negative lower yield stress homologous temperatures. In this view, the model should be used by never involving temperatures lower than the reference temperature. This is the same for the temperature term in plain JC.

The subsequent step consists in setting lower yield stress parameter A, as equal to the lower yield stress of the hardening function referring to the lower yield stress reference equivalent plastic strain rate and temperature. In fact, in that case the lower yield stress strain rate and temperature factors become equal to one and the SJC hardening rule reduces to

$$\overline{s} = A\,. \tag{26}$$

The next point determines lower yield stress strain rate parameter C_1. This step is similar to that apt to determine parameter C for the plain JC model by the LYS calibration. Indeed, parameter C_1 can be obtained from experimental data at the lower yield stress reference temperature. This fact implies the vanishing of the lower yield stress temperature factor. Parameter C_1 can then be determined as

$$C_1 = \frac{\dfrac{\overline{s}}{A} - 1}{\ln \dfrac{\dot{\overline{\varepsilon}}_p}{\dot{\overline{\varepsilon}}^0_{p_1}}}\,. \tag{27}$$

At this point, it is possible to compute different values of parameter C_1, by considering all the available hardening functions at the lower yield stress reference temperature for the various tested equivalent plastic strain rates differing from the reference one. When material hardening reproduces a log dependence on the lower yield stress dimensionless equivalent plastic strain rate, the same value of C_1 shall be obtained for all the available tested equivalent plastic strain rates; otherwise, C_1 may be computed as an average value among all the obtained ones.

The next step determines lower yield stress temperature parameter m_1. This step is similar to that for setting parameter m for the original JC model by the LYS calibration. Indeed, m_1 can be obtained from data

at the lower yield stress reference equivalent plastic strain rate. This implies the vanishing of the lower yield stress equivalent plastic strain rate factor and m_1 can be determined as

$$m_1 = \frac{\ln\left(1-\frac{\bar{s}}{A}\right)}{\ln\left(\frac{T-T_{0_1}}{T_m-T_{0_1}}\right)}. \tag{28}$$

Here again it is possible to compute different values of m_1, by considering all the available hardening functions at the lower yield stress reference equivalent plastic strain rate and at the various tested temperatures different from the reference one. When the lower yield stress power dependence on the lower yield stress homologous temperature is reproduced, the same value of m_1 shall be obtained; otherwise, m_1 may be evaluated as an average value.

Material data used for setting lower yield stress parameters A, C_1 and m_1 need not to be purified from structural effects through possible inverse analysis at the sample scale, since at the lower yield stress, spurious structural effects should not arise.

The next step regards the determination of the reference values of plastic flow equivalent plastic strain rate and temperature, together with plastic flow parameters B and n. The reference value of plastic flow equivalent plastic strain rate is set coincident to one of the testing equivalent plastic strain rates. No further constraints are introduced, so any of them can be chosen, with a typical choice in adopting the lowest tested value. The reference value of plastic flow temperature is chosen again as the lowest testing temperature. Hence, the STA calibration procedure sets the reference value of the plastic flow temperature as equal to the reference value of the lower yield stress temperature; the two reference values of the equivalent plastic strain rates could be set equal as well.

Parameters B and n are to be determined next, from data at the reference values of plastic flow equivalent plastic strain rate and temperature. These may be purified from structural effects through FEM inverse analyses of the tests, over the plastic strain range. When the hardening function refers to the reference value of plastic flow equivalent plastic strain rate and temperature, the SJC description reduces to

$$\bar{s} = A\cdot\left(1+C_1\cdot\ln\frac{\dot{\bar{\varepsilon}}_p}{\dot{\bar{\varepsilon}}^0_{p_1}}\right)+B\cdot\bar{\varepsilon}_p^{\,n}\,, \tag{29}$$

where the lower yield stress temperature factor disappears. Incidentally, the log term attached to C_1 would vanish too if $\dot{\bar{\varepsilon}}_p = \dot{\bar{\varepsilon}}^0_{p_1}$. Through appropriate fitting, e.g. by nonlinear regression of Eq. (29) of the experimental points at the reference values of plastic flow equivalent plastic strain rate and temperature, parameters B and n can be calibrated.

The next point aims at calculating plastic flow strain rate parameter C_2. This phase makes use of hardening functions recorded at the reference plastic flow temperature and at equivalent plastic strain rates that are different from the reference value, from the lowest to the highest. Parameter C_2 can be obtained by noting that the plastic flow temperature factor becomes equal to one, leading to

$$\bar{s} = A\cdot\left(1+C_1\cdot\ln\frac{\dot{\bar{\varepsilon}}_p}{\dot{\bar{\varepsilon}}^0_{p_1}}\right)+B\cdot\bar{\varepsilon}_p^{\,n}\cdot\left(1+C_2\cdot\ln\frac{\dot{\bar{\varepsilon}}_p}{\dot{\bar{\varepsilon}}^0_{p_2}}\right), \tag{30}$$

where the factor attached to the lower yield stress temperature is not present since the reference value of the lower yield stress temperature is set equal to the plastic flow reference temperature, as in Eq. (29). It is then possible to determine C_2 through a regression of Eq. (30) on hardening data at a specific equivalent plastic strain rate, different from the reference one. Also at this stage, different values of C_2 may be obtained for each tested equivalent plastic strain rate and they may correspond to each other if the log dependence of plastic flow is really reproduced; otherwise, an average value could be estimated.

The next point considers the determination of plastic flow temperature parameter m_2. This makes use of experimental data obtained at the reference value of plastic flow equivalent plastic strain and at temperatures different from the reference plastic flow one, from the lowest tested to the highest. Parameter m_2 can be obtained by noting that the plastic flow equivalent plastic strain term becomes equal to one so that

$$\overline{s} = A \cdot \left(1 + C_1 \cdot \ln \frac{\dot{\overline{\varepsilon}}_p}{\dot{\overline{\varepsilon}}_{p_1}^0} \right) \cdot \left(1 - \left(\frac{T - T_{0_1}}{T_m - T_{0_1}} \right)^{m_1} \right) + B \cdot \overline{\varepsilon}_p^n \cdot \left(1 - \left(\frac{T - T_{0_2}}{T_m - T_{0_2}} \right)^{m_2} \right). \tag{31}$$

As said, the lower yield stress strain rate term may become equal to 1 too if $\dot{\overline{\varepsilon}}_p = \dot{\overline{\varepsilon}}_{p_1}^0$. It is then possible to set parameter m_2 through a regression of Eq. (31) on hardening function data at a specific temperature, different from the reference one. This evaluates parameter m_2 at each specific temperature. If power low trends are not really reproduced, an average value of m_2 may be determined, among the obtained ones.

In sum, experimental outcomes needed for calculating the SJC parameters through the STA calibration procedure are summarized as follows (assuming melting temperature to be known).

1. A test at reference lower yield stress temperature and equivalent plastic strain rate. Such results are used for determining lower yield stress quasi-static parameter A.
2. Tests at reference lower yield stress temperature and equivalent plastic strain rates different from the reference one. Such outcomes are employed for getting parameter C_1.
3. Tests at reference lower yield stress equivalent plastic strain rate and at temperatures different from the reference one. Such scores are adopted for estimating parameter m_1.
4. A test at reference plastic flow temperature and equivalent plastic strain rate. Such results are used for determining lower yield stress quasi-static parameters B and n.
5. Tests at reference plastic flow temperature and equivalent plastic strain rates different from the reference one. Such data are used for calibrating parameter C_2.
6. Tests at reference plastic flow equivalent plastic strain rate and temperatures different from the reference one. Such results are employed for estimating parameter m_2.

Since for STA calibration the reference temperatures of lower yield stress and plastic flow are assumed to coincide, cases in which the reference equivalent plastic strain rates for lower yield stress and plastic flow are equal too imply that data used for point 5 are the same as those used for point 2 and that data used for point 6 are the same as those used for point 3. Also, concerning points 2, 3, 5 and 6, it is obvious that the more hardening functions are available, the more temperature and equivalent plastic strain rate ranges are covered with proper representation. Moreover, it is worthwhile to mention that if the reference values of lower yield stress and plastic flow parameters are the same, test results required for STA calibration are the same as those needed for calibrating plain JC by the LYS or EPS approaches.

Below, STA calibration is implemented on the three considered material cases. For all of them, the reference values of lower yield stress and plastic flow plastic strain rates and temperatures are taken equal. Regression required to determine parameters B, n, C_1, m_1, C_2 and m_2 has been solved through an implementation within Wolfram Mathematica. The obtained parameters are summarized in following Table 3.

DH-36 steel	$\dot{\bar{\varepsilon}}^{0}_{p_1}$ **[s^{-1}]**	T_{0_1} **[K]**	**T_m [K]**	**A [MPa]**	**C_1**	**m_1**
	0.001	77	1773	915.56	0.0156	0.2268
	$\dot{\bar{\varepsilon}}^{0}_{p_2}$ **[s^{-1}]**	T_{0_2} **[K]**	**n**	**B [MPa]**	**C_2**	**m_2**
	0.001	77	0.6010	760.78	-0.0617	2.8382
Niobium	$\dot{\bar{\varepsilon}}^{0}_{p_1}$ **[s^{-1}]**	T_{0_1} **[K]**	**T_m [K]**	**A [MPa]**	**C_1**	**m_1**
	0.001	296	2750	76.345	0.2788	0.9061
	$\dot{\bar{\varepsilon}}^{0}_{p_2}$ **[s^{-1}]**	T_{0_2} **[K]**	**n**	**B [MPa]**	**C_2**	**m_2**
	0.001	296	0.2877	390.84	-0.0067	0.9453
Al-6XN steel	$\dot{\bar{\varepsilon}}^{0}_{p_1}$ **[s^{-1}]**	T_{0_1} **[K]**	**T_m [K]**	**A [MPa]**	**C_1**	**m_1**
	0.001	77	1673	256.87	-0.0247	0.4926
	$\dot{\bar{\varepsilon}}^{0}_{p_2}$ **[s^{-1}]**	T_{0_2} **[K]**	**n**	**B [MPa]**	**C_2**	**m_2**
	0.001	77	0.4340	2511.9	0.0015	0.4577

Table 3. STA calibration strategy: SJC parameters for the three material cases.

If the reference parameters of lower yield stress and plastic flow are the same, ten out of the twelve STA calibrated SJC parameters are reusable from the parameters of plain JC, calibrated on the same data through LYS calibration. In fact, all STA parameters except for C_2 and m_2 are equal to those of the LYS calibrated original JC model, noting that parameters C_1 and m_1 turn out equal to C and m LYS calibrated JC parameters, respectively.

Figs. 1 to 3 show the hardening functions predicted by the STA calibrated SJC model, for the three considered material cases.

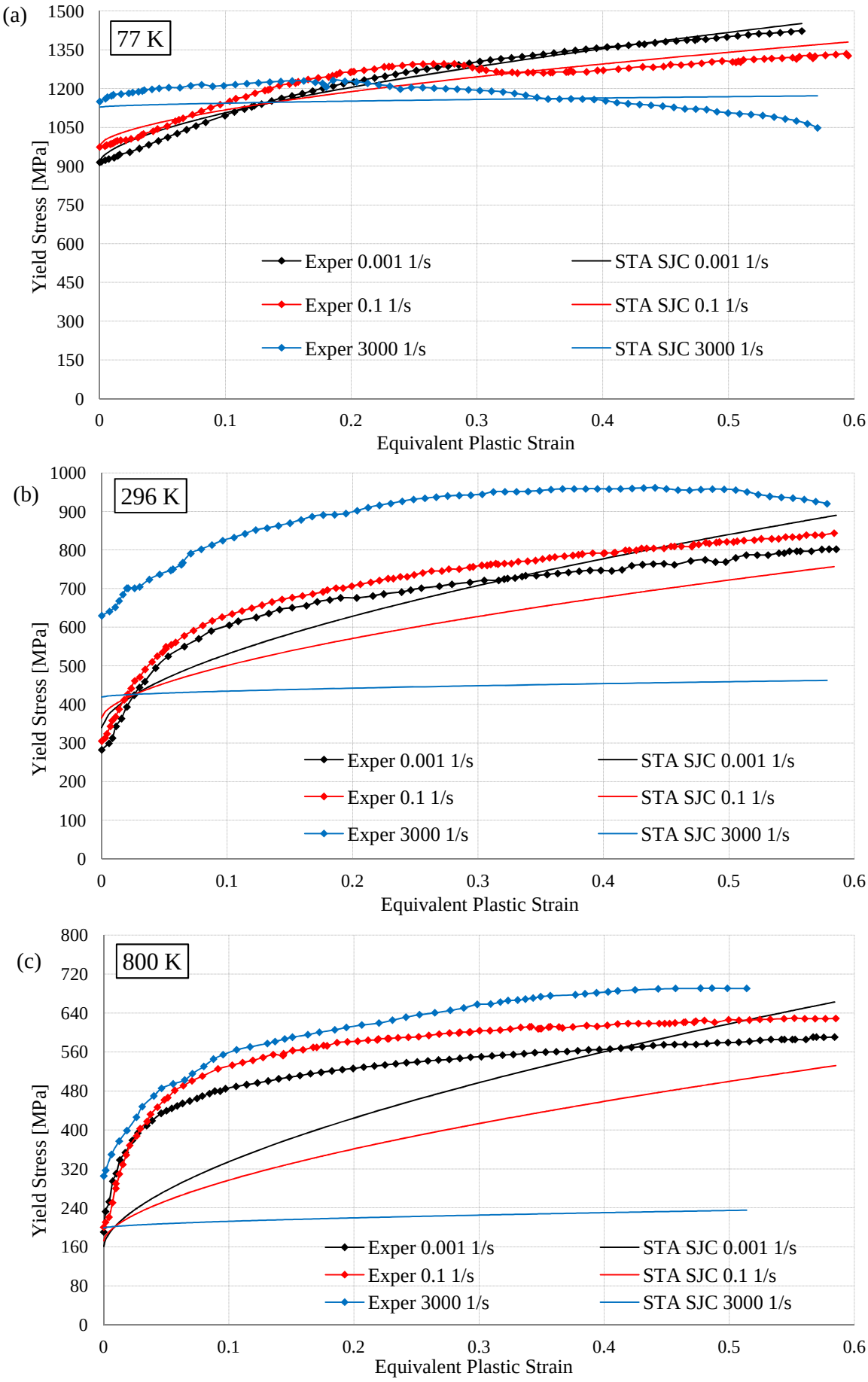

Figure 1. STA calibrated SJC fit for DH-36 steel at 0.001 s^{-1}, 0.1 s^{-1}, 3000 s^{-1} and at (a) 77 K, (b) 296 K, (c) 800 K.

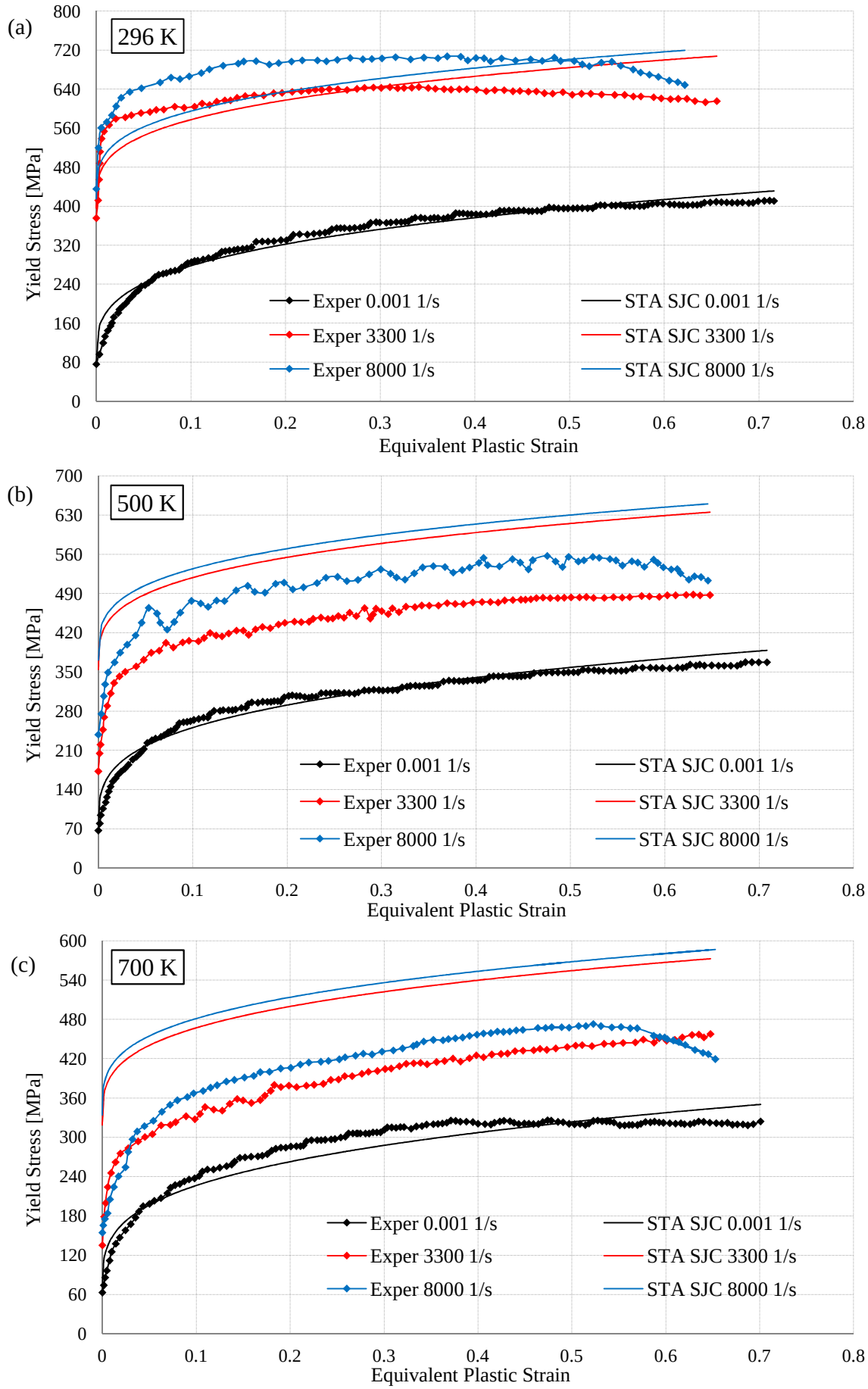

Figure 2. STA calibrated SJC fit for niobium at 0.001 s^{-1}, 3300 s^{-1}, 8000 s^{-1} and at (a) 296 K, (b) 500 K, (c) 700 K.

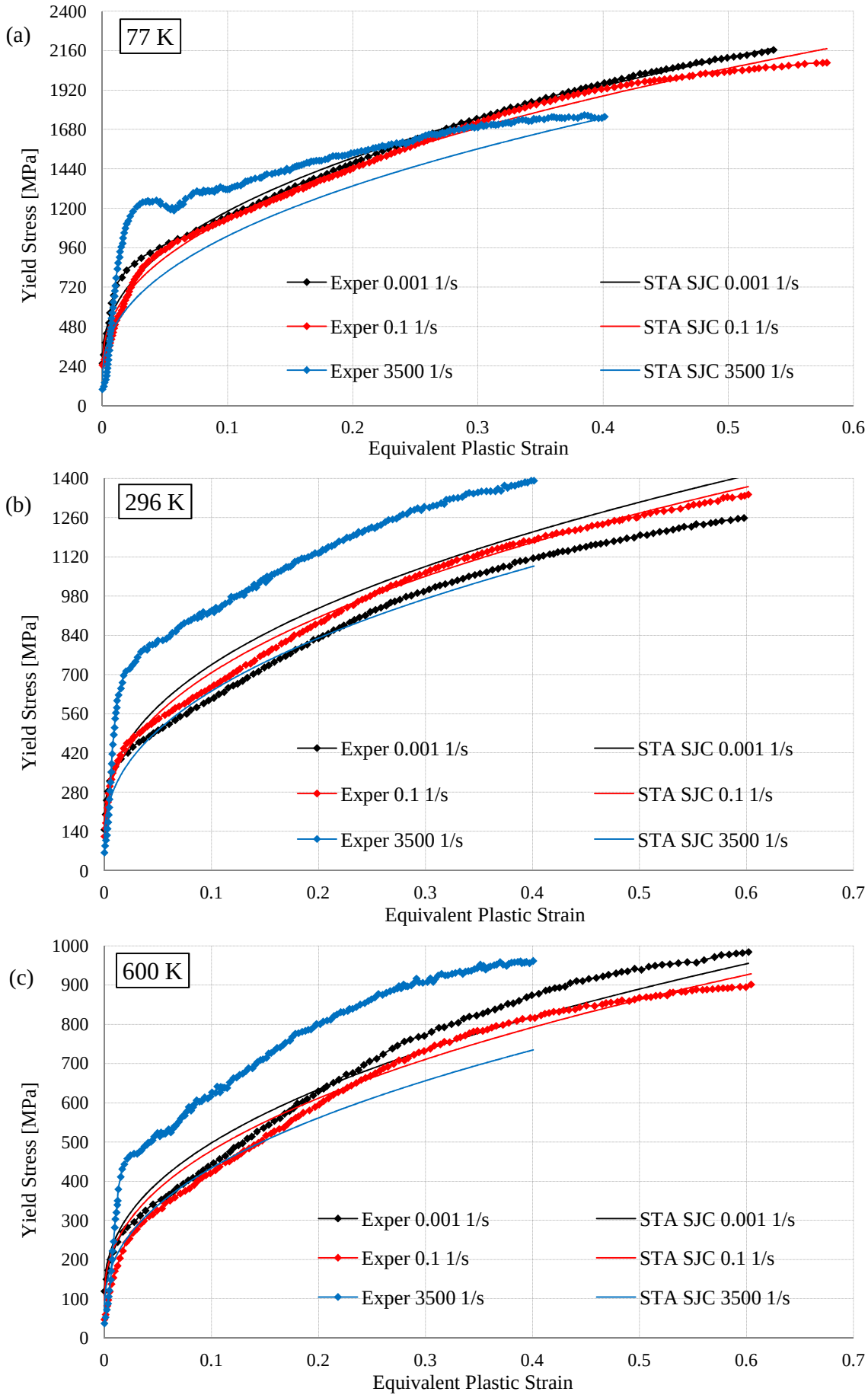

Figure 3. STA calibrated SJC fit for AL-6XN steel at 0.001 s^{-1}, 0.1 s^{-1}, 3500 s^{-1} and at (a) 77 K, (b) 296 K, (c) 600 K.

Following Table 4 compares the STA calibrated SJC model lower yield stress predictions to experimental results, for the three material cases, with absolute and percentage error measure indications and their averages. Values in Table 4 are identical to those from plain JC by LYS calibration (Gambirasio and Rizzi, 2014) and are reported for the ease of comparison among all the treated cases.

	Experimental value [MPa]	**STA SJC value [MPa]**	**Error absolute value [MPa]**	**Percentage error value**
DH-36 steel				
0.001 s^{-1}; 77 K	915.56	915.56	0	0%
0.1 s^{-1}; 77 K	974.57	981.32	6.7500	0.693%
3000 s^{-1}; 77 K	1150.5	1128.5	22.000	1.912%
0.001 s^{-1}; 296 K	282.46	340.01	57.550	20.37%
0.1 s^{-1}; 296 K	305.46	364.44	56.980	18.65%
3000 s^{-1}; 296 K	630.14	419.12	211.00	33.48%
0.001 s^{-1}; 800 K	190.35	160.97	29.380	15.43%
0.1 s^{-1}; 800 K	200.21	172.53	27.680	13.83%
3000 s^{-1}; 800 K	305.35	198.42	106.93	35.02%
Average			*57.587*	*15.49%*
Niobium				
0.001 s^{-1}; 296 K	76.345	76.345	0	0%
3300 s^{-1}; 296 K	375.95	395.82	19.870	5.285%
8000 s^{-1}; 296 K	435.70	414.67	21.030	4.827%
0.001 s^{-1}; 500 K	67.110	68.329	1.2190	1.816%
3300 s^{-1}; 500 K	172.84	354.26	181.42	105.0%
8000 s^{-1}; 500 K	238.39	371.13	132.74	55.68%
0.001 s^{-1}; 700 K	62.910	61.457	1.4530	2.310%
3300 s^{-1}; 700 K	135.09	318.63	183.54	135.86%
8000 s^{-1}; 700 K	154.35	333.80	179.45	116.26%
Average			*80.080*	*47.45%*
AL-6XN stainless steel				
0.001 s^{-1}; 77 K	256.86	256.86	0	0%
0.1 s^{-1}; 77 K	246.67	227.66	19.010	7.707%
3500 s^{-1}; 77 K	99.109	161.31	62.201	62.76%
0.001 s^{-1}; 296 K	146.49	160.30	13.810	9.427%
0.1 s^{-1}; 296 K	122.49	142.07	19.580	15.99%
3500 s^{-1}; 296 K	64.884	100.67	35.786	55.15%
0.001 s^{-1}; 600 K	119.32	108.60	10.720	8.984%
0.1 s^{-1}; 600 K	47.307	96.251	48.944	103.5%
3500 s^{-1}; 600 K	37.090	68.200	31.110	83.88%
Average			*26.800*	*38.59%*

Table 4. STA calibrated SJC model lower yield stress predictions for the three material cases. Values coincide with those from plain JC by LYS calibration (Gambirasio and Rizzi, 2014) and are reported for the ease of comparison.

For a complete evaluation of the errors introduced with a particularly calibrated SJC model over the considered equivalent plastic strain ranges, the Root Mean Square (RMS) error on the yield stress can be evaluated as

$$\bar{s}_{err} = \sqrt{\frac{\sum_{i=1}^{n}\left(\bar{s}_i^{SJC} - \bar{s}_i^{EXP}\right)^2}{n}}, \tag{32}$$

where $\bar{s}_i^{SJC}$ and $\bar{s}_i^{EXP}$ are the i-th yield stress SJC prediction and measurement of the same equivalent plastic strain, respectively, and n is the number of digitalized samples.

A further assessment error measure for a particularly-calibrated SJC model can be stated in percentage RMS error form as

$$\bar{s}_{\%err} = \sqrt{\frac{\sum_{i=1}^{n}\left(100 \cdot \frac{\bar{s}_i^{SJC} - \bar{s}_i^{EXP}}{\bar{s}_i^{EXP}}\right)^2}{n}}. \tag{33}$$

Considering results from STA calibration, Table 5 shows the error measures and their average for the nine considered hardening functions and three material cases. Their algebraic average is presented too.

	$\bar{s}_{err}$ **[MPa]**	$\bar{s}_{\%\,err}$		$\bar{s}_{err}$ **[MPa]**	$\bar{s}_{\%\,err}$		$\bar{s}_{err}$ **[MPa]**	$\bar{s}_{\%\,err}$
DH-36 steel			**Niobium**			**AL-6XN stainless steel**		
0.001 s^{-1}; 77 K	19.589	1.784%	**0.001 s^{-1}; 296 K**	13.960	8.078%	**0.001 s^{-1}; 77 K**	34.392	4.674%
0.1 s^{-1}; 77 K	43.997	3.529%	**3300 s^{-1}; 296 K**	44.059	7.299%	**0.1 s^{-1}; 77 K**	51.817	8.907%
3000 s^{-1}; 77 K	57.925	4.976%	**8000 s^{-1}; 296 K**	51.986	7.923%	**3500 s^{-1}; 77 K**	207.78	28.16%
0.001 s^{-1}; 296 K	51.788	8.728%	**0.001 s^{-1}; 500 K**	13.578	8.463%	**0.001 s^{-1}; 296 K**	70.214	9.024%
0.1 s^{-1}; 296 K	111.36	15.74%	**3300 s^{-1}; 500 K**	128.75	34.11%	**0.1 s^{-1}; 296 K**	24.844	6.141%
3000 s^{-1}; 296 K	440.60	49.01%	**8000 s^{-1}; 500 K**	86.834	19.68%	**3500 s^{-1}; 296 K**	265.49	30.09%
0.001 s^{-1}; 800 K	97.036	21.55%	**0.001 s^{-1}; 700 K**	18.659	9.086%	**0.001 s^{-1}; 600 K**	61.891	8.299%
0.1 s^{-1}; 800 K	176.62	32.44%	**3300 s^{-1}; 700 K**	126.12	39.43%	**0.1 s^{-1}; 600 K**	37.530	22.71%
3000 s^{-1}; 800 K	383.03	62.07%	**8000 s^{-1}; 700 K**	123.90	41.71%	**3500 s^{-1}; 600 K**	196.21	31.91%
Average	*153.55*	*22.20%*	***Average***	*67.538*	*19.53%*	***Average***	*105.57*	*16.66%*

Table 5. STA calibrated SJC model yield stress errors, for the three material cases.

The predictions of the STA calibrated SJC model match first yield and subsequent plastic flow for the hardening functions marked by one reference condition at least. Indeed, data used for calibration come only from such a subset. However, such an accomplishment is partially prevented if log and power law dependencies of the yield stress are not really apparent. Conversely, fittings for the four hardening curves not referring to at least one reference condition may display considerable mismatches. This is due to having considered reference conditions only in the calibration of parameters C_1, m_1, C_2 and m_2. Indeed, data from the four hardening curves not referring to at least one reference state are never employed for STA calibration, as for LYS and EPS calibrations of plain JC. Hence, heavy errors may be involved in the

prediction, and at random.

In particular, fitting incoherencies appear for the two hardening curves of DH-36 steel at 3000 s^{-1} and 296 K, and at 3000 s^{-1} and 800 K, since parameter C_2 is calibrated by considering only data at temperature 77 K, which present material softening at 3000 s^{-1}. Therefore, the calibration of parameter C_2 tries to fit this softening trend, which is completely different for the two hardening trends at 3000 s^{-1} and 296 K, and at 3000 s^{-1} and 800 K. Hence, considerable mismatches arise.

The various comments above are confirmed when inspecting the achieved fittings for the three considered material cases. In fact, lower yield stresses and plastic flow predictions are precise for the five hardening curves referring to at least one reference state, while on the four other ones wide errors may be introduced, with the worst case being represented by the DH-36 steel, due to the issues above.

3.2.2. OPT Calibration Strategy

The OPT (OPTimized) approach goal is that of improving the previous STA approach by further optimizing the value of parameters C_1, C_2, m_1 and m_2. given fixed the other STA parameters. This approach uses results from hardening curves not referring to one reference state at least, with the goal of calculating values of C_1, C_2, m_1 and m_2 achieving the best fit among all available hardening curves. The OPT calibration strategy plays the same role as that outlined for the OPTLYS and OPTEPS calibration procedures of plain JC.

The first step regards lower yield stress parameters C_1 and m_1. To involve a complete lower yield stress information from all the available hardening curves, the SJC model, Eq. (19), is called a number of times as that of the hardening curves that do not refer to reference conditions, that is all hardening data except for the one referring to the reference values of lower yield stress equivalent plastic strain rate and temperature. Such a strategy leads to a nonlinear overdetermined system of equations, with parameters C_1 and m_1 as unknowns. Clearly, the equivalent plastic strain keeps set to zero, because only the lower yield stress is considered. Therefore, the plastic flow factor vanishes. Such system is then reported as

$$\bar{s}_i = A \cdot \left(1 + C_1 \cdot \ln \frac{\dot{\bar{\varepsilon}}_{p_i}}{\dot{\bar{\varepsilon}}^0_{p_1}} \right) \cdot \left(1 - \left(\frac{T_i - T_{0_1}}{T_m - T_{0_1}} \right)^{m_1} \right). \tag{34}$$

where subscript i marks values of the i-th hardening function. Considering the three analyzed material cases, index i goes up to 8, for the hardening curves not referring to reference lower yield stress states. This system is analogous to that derived in the OPTLYS calibration of plain JC. Solution may be obtained by nonlinear least squares. Since such overdetermined system typically presents a limited number of equations and only two unknowns (target parameters C_1 and m_1), no particular solving problems should arise, like for instance the appearance of local minima. This is recorded for the material cases analyzed here.

The second step targets plastic flow parameters C_2 and m_2. Using all hardening curves, the SJC hardening prediction function, Eq. (19), is used for all the investigated equivalent plastic strain ranges. Reference is made to all available hardening curves apart from that referring to plastic flow reference on equivalent plastic strain rate and temperature. This leads to a large overdetermined nonlinear system in unknown parameters C_2 and m_2, with a number of equations that corresponds to the number of yield stress/equivalent plastic strain couples. Such a number is ruled not only by the number of hardening curves but also by the digitalized sampling frequency. To avoid too large systems, decimation on test data may be used. The system discussed above may be represented as

$$\bar{s}_i = A \cdot \left(1 + C_1 \cdot \ln \frac{\dot{\bar{\varepsilon}}_{p_i}}{\dot{\bar{\varepsilon}}^0_{p_1}}\right) \cdot \left(1 - \left(\frac{T_i - T_{0_1}}{T_m - T_{0_1}}\right)^{m_1}\right) + B \cdot \bar{\varepsilon}^n_{p_i} \cdot \left(1 + C_2 \cdot \ln \frac{\dot{\bar{\varepsilon}}_{p_i}}{\dot{\bar{\varepsilon}}^0_{p_2}}\right) \cdot \left(1 - \left(\frac{T_i - T_{0_2}}{T_m - T_{0_2}}\right)^{m_2}\right). \quad (35)$$

in terms of the i-th yield stress-equivalent plastic strain couples for a specific equivalent plastic strain rate and temperature. For the three analyzed material cases, subscript i goes up to: 664 for DH-36 steel; 761 for niobium; 1199 for AL-6XN stainless steel. These are the numbers of experimental scores not referring to reference stages of plastic flow of equivalent plastic strain rate and temperature. Despite the high number of involved equations, nonlinear least square solutions for target parameters C_2 and m_2 are found effectively, independently from the initial guess on C_2 and m_2, around wide ranges centered on values coming from the previous STA calibration.

Experimental tests needed for the OPT calibration of the SJC parameters are resumed as follows, given the melting temperature to be known:

1. A test at the reference value of lower yield stress temperature and equivalent plastic strain rate. The attached results are used to determine lower yield stress quasi-static parameter A.
2. A series of tests where at least one among equivalent plastic strain and temperature differs from their reference yield stress values. The corresponding scores are adopted to compute parameters C_1 and m_1.
3. A test at the reference value of plastic flow temperature and equivalent plastic strain rate. The associated markings are employed to calibrate parameters B and n.
4. A series of tests where at least one among equivalent plastic strain and temperature differs from their reference plastic flow values. The corresponding points are sampled to evaluate parameters C_2 and m_2.

Concerning points 2 and 4, notice that OPT calibration does not require to conduct separate tests at the reference value of lower yield stress (plastic flow) temperature but at different equivalent plastic strain rates and then at the reference value of the lower yield stress (plastic flow) equivalent plastic strain rate but at different temperature values, to characterize parameters C_1 and m_1 (C_2 and m_2). Rather, any hardening curve that is not referring to reference conditions for the lower yield stress (plastic flow) for both equivalent plastic strain rate and temperature is indeed useful to achieve parameters C_1 and m_1 (C_2 and m_2).

Since the reference values of lower yield stress and plastic flow temperature are taken equal in the OPT strategy, cases where the reference values of the lower yield stress and plastic flow equivalent plastic strain rate are equal too imply that experimental results used for point 4 are the same as those adopted for point 2. Also, about points 2 and 4, the more hardening curves are available, the more temperature and equivalent plastic strain rate ranges are covered with good resolution. Moreover, if the reference parameters of lower yield stress and plastic flow are the same, the hardening curves required for OPT calibration are the same as those needed for the OPTLYS or OPTEPS calibrations of plain JC.

Here the OPT calibration is applied to the three material cases. The reference values of lower yield stress and plastic flow equivalent plastic strain rate and temperature are set equal. The regression needed for getting parameters C_1, m_1, C_2 and m_2 has been implemented within MathWorks MatLab. Two algorithms are tried, namely a nonlinear least squares trust-region-reflective one (see, e.g., Coleman and Li, 1984) and a Levenberg-Marquardt one (see Levenberg, 1944, and Marquardt, 1963), with a 10^{-8} tolerance and same achieved outcomes. Wide overdetermined solution systems of 664 (DH-36 steel), 761 (niobium) and 1199 (AL-6XN stainless steel) nonlinear equations in two unknowns are assembled and solved, with determined material parameters as exposed in Table 6.

DH-36 steel	$\dot{\bar{\varepsilon}}^{0}_{p_1}$ **[s^{-1}]**	T_{0_1} **[K]**	T_m **[K]**	**A [MPa]**	C_1	m_1
	0.001	77	1773	915.56	0.0205	0.2637
	$\dot{\bar{\varepsilon}}^{0}_{p_2}$ **[s^{-1}]**	T_{0_2} **[K]**	**n**	**B [MPa]**	C_2	m_2
	0.001	77	0.6010	760.782	-0.0258	3175.4
Niobium	$\dot{\bar{\varepsilon}}^{0}_{p_1}$ **[s^{-1}]**	T_{0_1} **[K]**	T_m **[K]**	**A [MPa]**	C_1	m_1
	0.001	296	2750	76.345	0.2780	0.2748
	$\dot{\bar{\varepsilon}}^{0}_{p_2}$ **[s^{-1}]**	T_{0_2} **[K]**	**n**	**B [MPa]**	C_2	m_2
	0.001	296	0.2877	390.84	-0.0025	1.8256
Al-6XN steel	$\dot{\bar{\varepsilon}}^{0}_{p_1}$ **[s^{-1}]**	T_{0_1} **[K]**	T_m **[K]**	**A [MPa]**	C_1	m_1
	0.001	77	1673	256.87	-0.0386	0.4228
	$\dot{\bar{\varepsilon}}^{0}_{p_2}$ **[s^{-1}]**	T_{0_2} **[K]**	**n**	**B [MPa]**	C_2	m_2
	0.001	77	0.4340	2511.9	0.0123	0.5126

Table 6. OPT calibration strategy: SJC parameters for the three material cases.

If the reference parameters of lower yield stress and plastic flow are the same, ten out of the twelve OPT calibrated SJC parameters could be taken from those calibrated by the OPTLYS calibration of plain JC. Indeed, all OPT SJC parameters are the OPTLYS JC ones, except for C_2 and m_2, while C_1 and m_1 coincide with C and m for OPTLYS JC.

Figs. 4 to 6 display the achieved hardening predictions by the OPT calibrated SJC, for the three material cases.

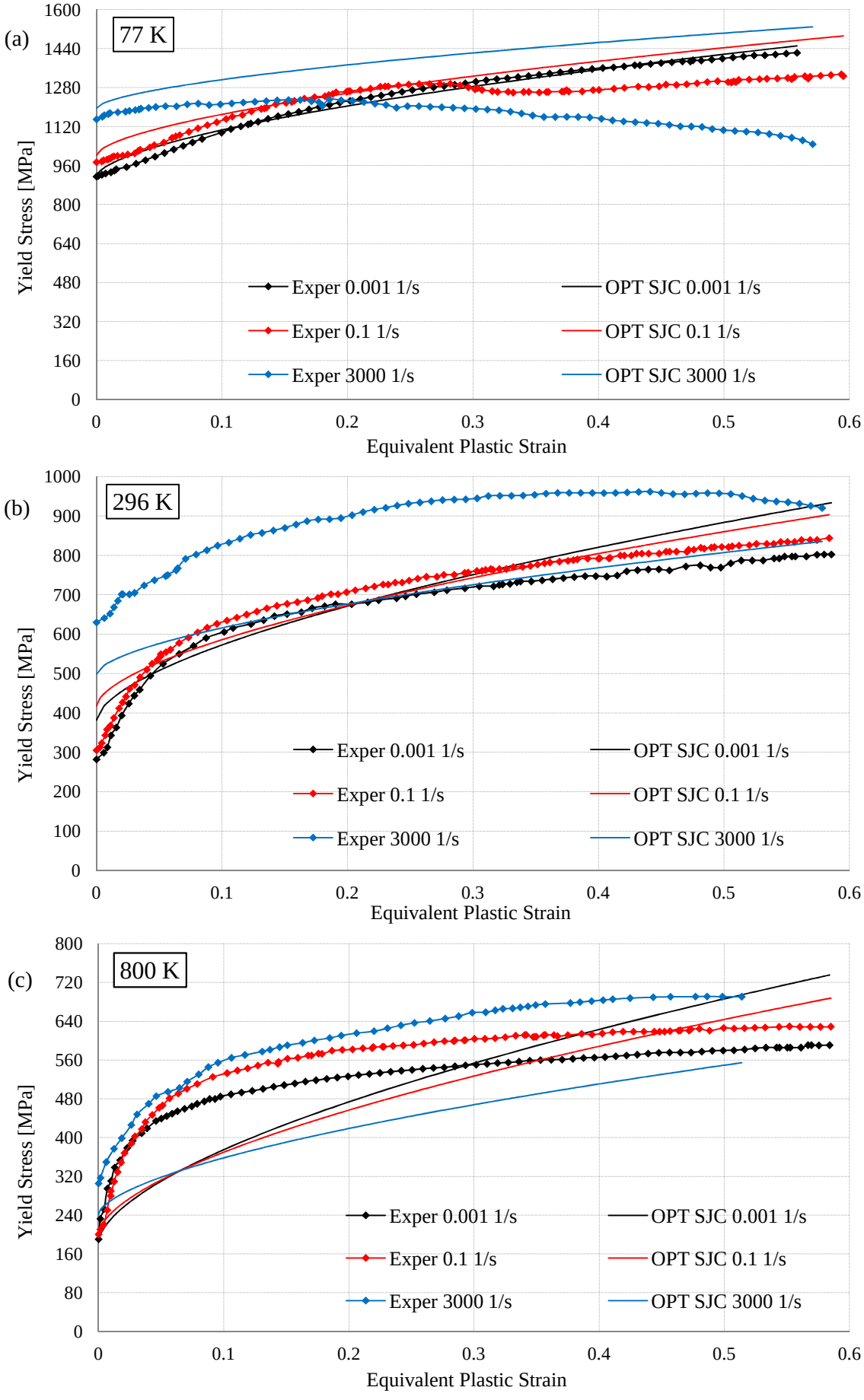

Figure 4. OPT calibrated SJC fit for DH-36 steel at 0.001 s^{-1}, 0.1 s^{-1}, 3000 s^{-1} and at (a) 77 K, (b) 296 K, (c) 800 K.

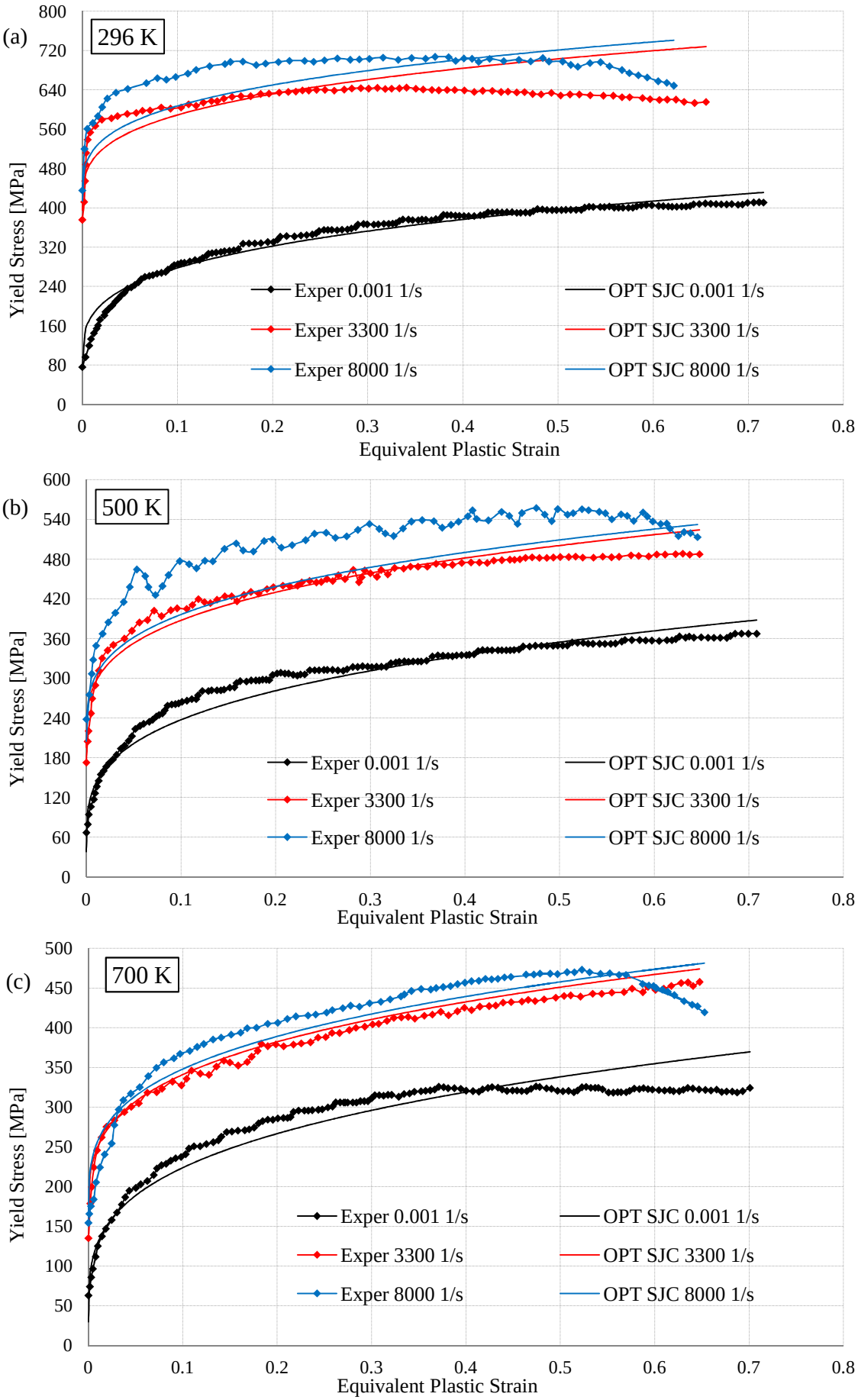

Figure 5. OPT calibrated SJC fit for niobium at 0.001 s^{-1}, 3300 s^{-1}, 8000 s^{-1} and at (a) 296 K, (b) 500 K, (c) 700 K.

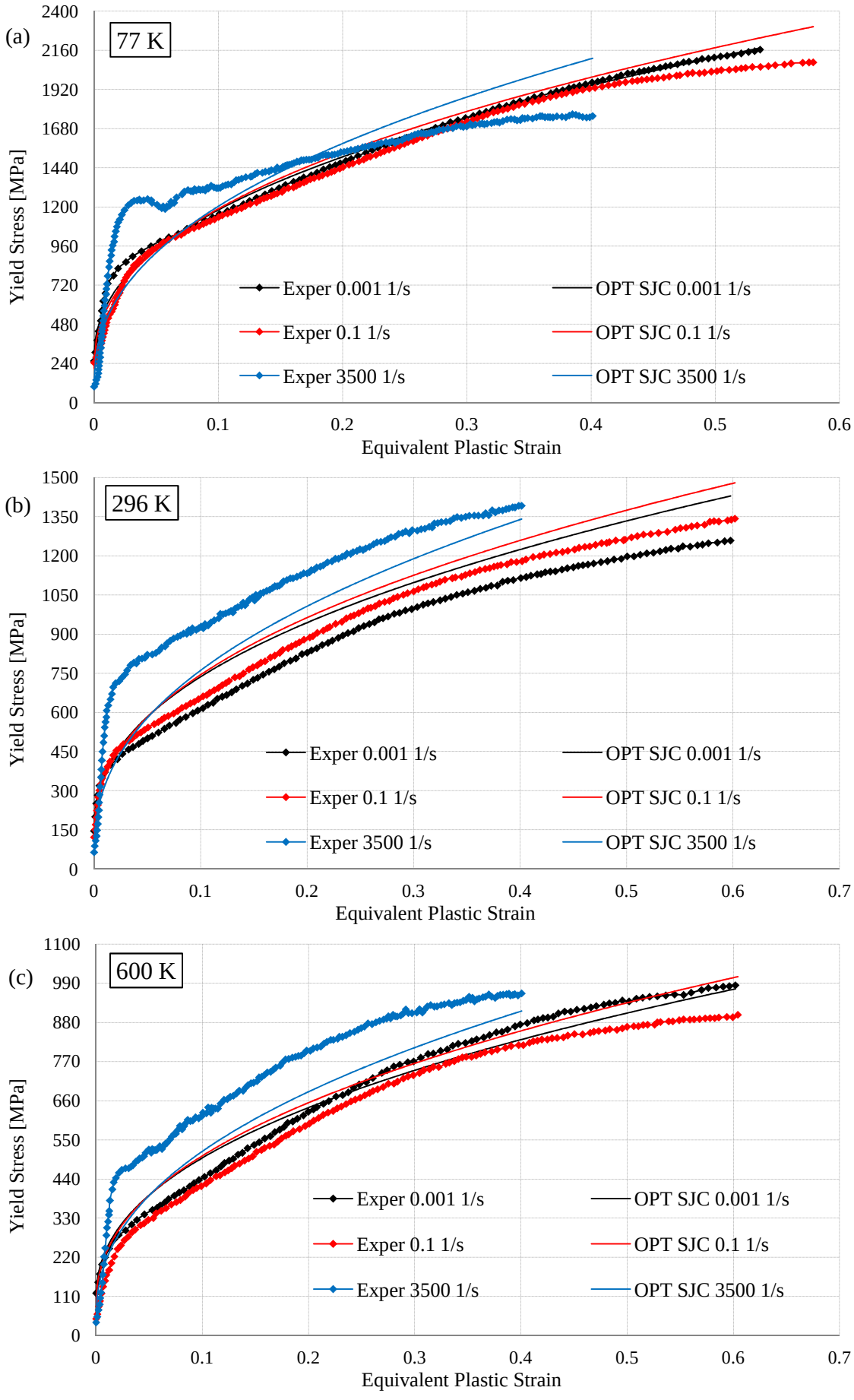

Figure 6. OPT calibrated SJC fit for AL-6XN steel at 0.001 s^{-1}, 0.1 s^{-1}, 3500 s^{-1} and at (a) 77 K, (b) 296 K, (c) 600 K.

Table 7 illustrates the prediction of lower yield stress data for the SJC model by OPT calibration. Table 8 reports yield stress and percentage yield stress RMS errors.

	Experimental value [MPa]	**OPT SJC value [MPa]**	**Error absolute value [MPa]**	**Percentage error value**
DH-36 steel				
0.001 s^{-1}; 77 K	915.56	915.56	0	0%
0.1 s^{-1}; 77 K	974.57	1001.9	27.330	2.804%
3000 s^{-1}; 77 K	1150.5	1195.3	44.800	3.894%
0.001 s^{-1}; 296 K	282.46	381.87	99.410	35.19%
0.1 s^{-1}; 296 K	305.46	417.90	112.44	36.81%
3000 s^{-1}; 296 K	630.14	498.56	131.58	20.88%
0.001 s^{-1}; 800 K	190.35	184.33	6.020	3.163%
0.1 s^{-1}; 800 K	200.21	201.72	1.5100	0.754%
3000 s^{-1}; 800 K	305.35	240.66	64.690	21.19%
Average			*54.198*	*13.85%*
Niobium				
0.001 s^{-1}; 296 K	76.345	76.345	0	0%
3300 s^{-1}; 296 K	375.95	394.94	18.990	5.051%
8000 s^{-1}; 296 K	435.70	413.74	21.960	5.040%
0.001 s^{-1}; 500 K	67.110	37.805	29.305	43.67%
3300 s^{-1}; 500 K	172.84	195.57	22.730	13.15%
8000 s^{-1}; 500 K	238.39	204.87	33.520	14.06%
0.001 s^{-1}; 700 K	62.910	29.843	33.067	52.56%
3300 s^{-1}; 700 K	135.09	154.38	19.290	14.28%
8000 s^{-1}; 700 K	154.35	161.73	7.3800	4.781%
Average			*20.694*	*16.95%*
AL-6XN stainless steel				
0.001 s^{-1}; 77 K	256.86	256.86	0	0
0.1 s^{-1}; 77 K	246.67	211.23	35.440	14.37
3500 s^{-1}; 77 K	99.109	107.56	8.4510	8.527
0.001 s^{-1}; 296 K	146.49	145.95	0.5400	0.369
0.1 s^{-1}; 296 K	122.49	120.02	2.4700	2.016
3500 s^{-1}; 296 K	64.884	61.113	3.7710	5.812
0.001 s^{-1}; 600 K	119.32	96.600	22.720	19.04
0.1 s^{-1}; 600 K	47.307	79.439	32.132	67.92
3500 s^{-1}; 600 K	37.090	40.449	3.3590	9.056
Average			*12.098*	*14.12%*

Table 7. OPT calibrated SJC model lower yield stress predictions for the three material cases.

	$\bar{s}_{err}$ [MPa]	$\bar{s}_{\%\,err}$		$\bar{s}_{err}$ [MPa]	$\bar{s}_{\%\,err}$		$\bar{s}_{err}$ [MPa]	$\bar{s}_{\%\,err}$
DH-36 steel			**Niobium**			**AL-6XN stainless steel**		
0.001 s^{-1}; 77 K	19.589	1.784	**0.001 s^{-1}; 296 K**	13.960	8.078%	**0.001 s^{-1}; 77 K**	34.392	4.674
0.1 s^{-1}; 77 K	89.606	7.070	**3300 s^{-1}; 296 K**	52.778	8.615%	**0.1 s^{-1}; 77 K**	89.531	9.659
3000 s^{-1}; 77 K	248.45	22.01	**8000 s^{-1}; 296 K**	48.206	7.387%	**3500 s^{-1}; 77 K**	211.52	25.14
0.001 s^{-1}; 296 K	72.761	12.45	**0.001 s^{-1}; 500 K**	15.845	7.029%	**0.001 s^{-1}; 296 K**	113.32	12.92
0.1 s^{-1}; 296 K	41.457	9.365	**3300 s^{-1}; 500 K**	18.019	5.160%	**0.1 s^{-1}; 296 K**	80.276	9.303
3000 s^{-1}; 296 K	188.09	21.54	**8000 s^{-1}; 500 K**	51.779	10.74%	**3500 s^{-1}; 296 K**	155.76	21.18
0.001 s^{-1}; 800 K	90.174	18.47	**0.001 s^{-1}; 700 K**	21.641	8.682%	**0.001 s^{-1}; 600 K**	35.679	7.234
0.1 s^{-1}; 800 K	93.193	18.06	**3300 s^{-1}; 700 K**	11.646	3.977%	**0.1 s^{-1}; 600 K**	64.365	22.73
3000 s^{-1}; 800 K	174.68	29.61	**8000 s^{-1}; 700 K**	23.517	8.277%	**3500 s^{-1}; 600 K**	104.22	21.25
Average	*113.11*	*15.60%*	***Average***	*28.599*	*7.549%*	***Average***	*98.785*	*14.90%*

Table 8. OPT calibrated SJC model yield stress errors, for the three material cases.

OPT calibrated SJC hardening trends match as best as possible all nine experimental curves over the ranges of equivalent plastic strain ranges, compatibly with the assumption of log and power law dependencies brought about by the SJC prediction. Another issue that may prevent perfect fitting on the real material behavior is the fact that hardening parameters B and n are determined as those apt to fit best only hardening curves attached to reference conditions.

A compromise is reached for the fitting among all the nine adopted hardening curves. This remark implies that the fitting achieved with at least one satisfied reference condition becomes less effective than that obtainable by STA SJC calibration. Conversely, concerning the achieved reproduction of the four hardening curves that do not refer to one reference state at least, errors are lower, both on lower yield stress and plastic flow.

The achieved fits for the three material cases on lower yield stress and plastic flow are quite acceptable on all the nine hardening curves. Specifically, the matching for the two DH-36 steel curves at 3000 s^{-1} and 296 K, and at 3000 s^{-1} and 800 K shows a strong improvement when comparing to STA calibration results.

3.2.3. GOPT Calibration Strategy

The GOPT (Global OPTimization) calibration procedure for SJC seeks the best material parameter set by a multi-objective optimization for (up to) eleven out of the twelve SJC parameters, that is all parameters except for the melting temperature, which is supposed to be given from scratch and not involved in the optimization process. All experimental curves are involved, towards obtaining the eleven parameters apt to provide the best fit on all hardening function data, over all involved ranges of equivalent plastic strain and plastic strain rate and temperature. This calibration plays the same role as that covered by GOPTEPS calibration for plain JC. Optimization is achieved by solving an overdetermined nonlinear system of equations in eleven unknowns.

A remark can be issued about the reference values of lower yield stress and plastic flow equivalent plastic strain rate and temperature. For the two earlier calibrations, these references were selected by choosing among the values of one of the hardening curves, that was then identified as reference, either for lower yield stress or plastic flow, or for both. In the present GOPT calibration, these references may be different from those set by one specific hardening curve, since the competent parameters are kept as optimization variables. However, their values still fix the reference states of lower yield stress and plastic flow, although as unknowns in the process. Same as for the GOPTEPS approach for plain JC, this should allow much degree of freedom towards achieving a better overall fitting.

Concerning calculation of the eleven optimized SJC parameters, the method is comparable to the OPT approach, although more complicated in computation, not only for the augmented number of unknowns (now eleven) but also because the number of equations increases, since all hardening curves are taken into account, including the one which was previously excluded because referring to a predetermined plastic flow reference condition and therefore not useful to determine parameters C_2 and m_2.

Again, towards preventing the assembly of too large systems, decimation of experimental measurements could be applied. The nonlinear system is similar to that exposed in Eq. (35), but now with eleven targeted optimization variables as unknowns. For the three material cases, subscript i in Eq. (35) goes now up to: 739 for DH-36 steel; 917 for niobium; 1305 for AL-6XN stainless steel.

A key solving issue concerns now the enforcement of appropriate constraints on the eleven optimization variables, leading to a constrained multi-objective nonlinear optimization. Therefore, the reference values of lower yield stress and plastic flow equivalent plastic strain rate are set to be positive, since in the SJC hardening model, logarithms of negative numbers cannot be computed. Moreover, the reference values of lower yield stress and plastic flow temperature are constrained to be lower or equal to the lowest tested temperature, towards preventing power law computation of negative lower yield stress or plastic flow homologous temperatures. The reference values of lower yield stress and plastic flow temperature are also imposed to be positive, not as a mathematical constraint but simply since temperatures lower than zero Kelvin are not physical. No further constraints are set on the other calibration parameters.

The assembled system is much complicated than that for the OPT procedure, because of the extension of the optimization variables from two to eleven. Again, solution is attempted by nonlinear least squares. However, some solution issues may appear. Specifically, the solver may not easily converge to a solution. Besides, even if the solver gets to a solution, it may be on a local minimum. If this occurs, results may present an average RMS error higher than for the earlier calibrations. In such instances, the following additional directions are able to improve performance, in particular by getting to a minimum that may be local, but always with better performance than that achieved through the other calibrations.

A first point concerns the initialization of the eleven optimization variables, i.e. the eleven SJC material parameters to be calibrated (all, except for the malting temperature). Appropriate initial guesses may correspond to previous calibrations, specifically for cases that produced the lower average errors, likely by the previous OPT strategy.

A second and more important issue consists in setting a priori some of the eleven material parameters. The parameters that may be fixed could be one or more of the four material parameters attached to reference conditions, i.e. the reference values of lower yield stress and plastic flow equivalent plastic strain rate and temperature. These may come from previous calibrations, e.g. a testing equivalent plastic strain rate, typically the lowest, and the lowest testing temperature. This allows to strongly reduce the computational burden, since such reference parameters enter four nonlinear terms in the SJC hardening function. Eliminating unknowns from these terms favors the achievement of better results. Anyway, a new overdetermined system needs to be prepared for each case in which one or more reference parameters are fixed a priori.

In order to avoid setting-up too many cases, a convenient approach may be that of carrying-out the GOPT strategy by considering a total number of *four different cases*, i.e.:

- no fixed parameters and thus eleven unknowns;
- both reference equivalent plastic strain rates fixed, thus nine unknowns;
- both reference temperatures fixed, thus nine unknowns;
- all reference values of equivalent plastic strain rate and temperature fixed, thus seven unknowns.

The present work follows this approach. Hence, four overdetermined systems are set-up and solved. After their solving, the kept solution is that leading to the lowest average RMS mismatch. For the present three

material cases, this way to proceed has been able to achieve the best SJC calibration, among all the three considered calibrations, by locating the set of material parameters apt to provide the lowest average error.

If the calibration did not produce satisfactory results yet, a third point may involve the enforcement of bounds on the optimization variables. These bounding constraints may be identified based on the values of the material parameters from other calibrations, typically the OPT one. The target would be that of constraining the eleven target parameters into specific boundaries centered on this already achieved solution, with the aim to further refine it. One or more parameters may also be fixed, specifically those suspected for unsatisfactory matching, by setting optimum previously-calibrated values. Anyway, contraindications may be present, since an arbitrary setting of the boundaries or the fixing of some optimization variable, may run against the scope of falling on the lowest error estimate.

A last option consists in comparing results from diverse solution procedures, for identifying the best solving strategy. Here, solutions by a trust-region-reflective algorithm and a Levenberg-Marquardt algorithm have been assessed, with same results. Moreover, the adopted solvers may be properly set-up by adjusting various features like, e.g., tolerances in the solution process, and so on.

About the experimental results needed for GOPT calibration, these are the same as those necessary for the OPT technique, namely the same data needed for calibrating plain JC by OPTLYS, OPTEPS and GOPTEPS calibrations.

Below, the GOPT calibration technique is adopted by a MathWorks MatLab implementation through the above-mentioned two algorithms, with tolerance set to 10^{-8}, achieving the same results. Wide overdetermined nonlinear systems of 739 (DH-36 steel), 917 (niobium) and 1305 (AL-6XN stainless steel) equations on eleven unknowns are set-up and iteratively solved. On the basis of the comments above, three other overdetermined systems have been assembled, by setting fixed either both reference equivalent plastic strain rates or both reference temperatures or all four reference parameters, with values enforced in the other two calibration techniques.

Table 9 reports the achieved GOPT results for the three analyzed material cases. Some convergence problems appear. In particular, the solvers do not converge to a solution when the reference temperatures are not fixed a priori. This may be related to the presence in the overdetermined systems of the reference temperatures, which are located in power nonlinear terms. This implies difficulties in converging to a solution. Hence, for each analyzed material case, only two out of the four set-up overdetermined systems actually provide a solution.

	Lower yield stress average error [MPa]	Lower yield stress average % error	Average $\bar{s}_{err}$ [MPa]	Average $\bar{s}_{\%\,err}$
DH-36 steel				
No fixed material parameters	NC	NC	NC	NC
$\dot{\bar{\varepsilon}}^{0}_{p_1}$ **and** $\dot{\bar{\varepsilon}}^{0}_{p_2}$ **fixed to 0.001 s^{-1}**	NC	NC	NC	NC
T_{0_1} **and** T_{0_2} **fixed to 77 K**	143.16	25.58%	63.98	10.19%
$\dot{\bar{\varepsilon}}^{0}_{p_1}$ **and** $\dot{\bar{\varepsilon}}^{0}_{p_2}$ **fixed to 0.001 s^{-1},** T_{0_1} **and** T_{0_2} **fixed to 77 K**	143.21	25.59%	63.98	10.19%
Niobium				
No fixed material parameters	NC	NC	NC	NC
$\dot{\bar{\varepsilon}}^{0}_{p_1}$ **and** $\dot{\bar{\varepsilon}}^{0}_{p_2}$ **fixed to 0.001 s^{-1}**	NC	NC	NC	NC
T_{0_1} **and** T_{0_2} **fixed to 296 K**	32.797	32.01%	26.031	8.853%
$\dot{\bar{\varepsilon}}^{0}_{p_1}$ **and** $\dot{\bar{\varepsilon}}^{0}_{p_2}$ **fixed to 0.001 s^{-1},** T_{0_1} **and** T_{0_2} **fixed to 296 K**	32.928	32.16%	26.038	8.861%
AL-6XN stainless steel				
No fixed material parameters	NC	NC	NC	NC
$\dot{\bar{\varepsilon}}^{0}_{p_1}$ **and** $\dot{\bar{\varepsilon}}^{0}_{p_2}$ **fixed to 0.001 s^{-1}**	NC	NC	NC	NC
T_{0_1} **and** T_{0_2} **fixed to 77 K**	90.446	81.70%	83.332	15.40%
$\dot{\bar{\varepsilon}}^{0}_{p_1}$ **and** $\dot{\bar{\varepsilon}}^{0}_{p_2}$ **fixed to 0.001 s^{-1},** T_{0_1} **and** T_{0_2} **fixed to 77 K**	89.308	80.67%	84.106	15.74%

Table 9. Results from the four solving systems for the three material cases. No Convergence is marked by NC.

For the case of AL-6XN stainless steel, further convergence problems appear. In particular, it was not possible to get the system converging to a solution at 10^{-8} tolerance. Instead, the system with both reference temperatures fixed was solved with a tolerance of $5\cdot10^{-7}$ and that with reference values of equivalent plastic strain rate and temperature fixed with a tolerance of $5\cdot10^{-6}$. These are symptoms of convergence problems. Indeed, for the four considered cases regarding AL-6XN stainless steel, while the plastic flow obtained errors are sensibly lower than those relative to the OPT case, the lower yield stress errors are quite higher. Further strategies have been pursued, by fixing parameter A or all three lower yield stress parameters A, C_1 and m_1. Anyway, these approaches lead to the achievement of worse results, comparing to those relative to the case with both reference temperatures fixed and those relative to the case with all four reference parameters fixed. Therefore, these results are discarded.

For each material case, the solution producing the lower discrepancies throughout the whole plastic flow is chosen. For all the three material cases, this corresponds to the system with fixed reference temperatures and free reference equivalent plastic strain rates, although such results are very similar to those referring to fixed reference equivalent plastic strain rates and temperatures.

The best eleven SJC parameters calculated by the GOPT procedure are resumed in Table 10, along with the given melting temperatures.

DH-36 steel	$\dot{\bar{\varepsilon}}^{0}_{p_1}$ **[s^{-1}]**	T_{0_1} **[K]**	T_m **[K]**	**A [MPa]**	C_1	m_1
	$2.3452 \cdot 10^{-3}$	77	1773	855.87	-0.0108	0.2538
	$\dot{\bar{\varepsilon}}^{0}_{p_2}$ **[s^{-1}]**	T_{0_2} **[K]**	**n**	**B [MPa]**	C_2	m_2
	$3.9780 \cdot 10^{-4}$	77	0.2223	487.74	0.0277	3175.0
Niobium	$\dot{\bar{\varepsilon}}^{0}_{p_1}$ **[s^{-1}]**	T_{0_1} **[K]**	T_m **[K]**	**A [MPa]**	C_1	m_1
	0.0010	296	2750	33.012	0.7008	0.3302
	$\dot{\bar{\varepsilon}}^{0}_{p_2}$ **[s^{-1}]**	T_{0_2} **[K]**	**n**	**B [MPa]**	C_2	m_2
	0.4098	296	0.2172	390.02	-0.0101	1.1684
Al-6XN steel	$\dot{\bar{\varepsilon}}^{0}_{p_1}$ **[s^{-1}]**	T_{0_1} **[K]**	T_m **[K]**	**A [MPa]**	C_1	m_1
	$9.9986 \cdot 10^{-4}$	77	1673	148.09	-0.0405	$5.7746 \cdot 10^{-5}$
	$\dot{\bar{\varepsilon}}^{0}_{p_2}$ **[s^{-1}]**	T_{0_2} **[K]**	**n**	**B [MPa]**	C_2	m_2
	0.0073	77	0.3714	2511.0	0.0092	0.5634

Table 10. GOPT calibration strategy: SJC parameters for the three material cases.

Figs. 7 to 8 report the hardening curves predicted by the GOPT calibrated SJC, for the three material cases.

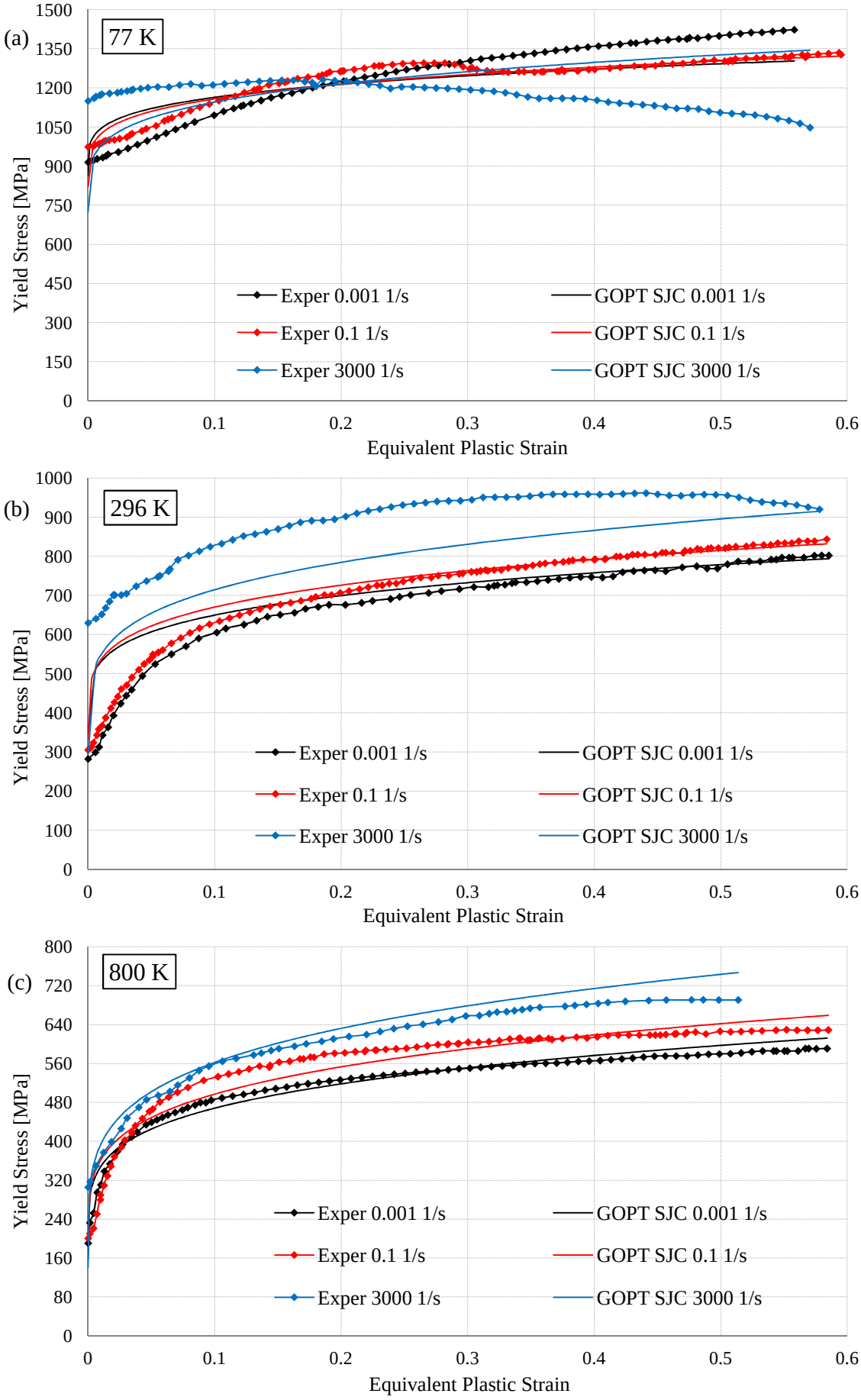

Figure 7. GOPT calibrated SJC fit for DH-36 steel at 0.001 s^{-1}, 0.1 s^{-1}, 3000 s^{-1} and at (a) 77 K, (b) 296 K, (c) 800 K.

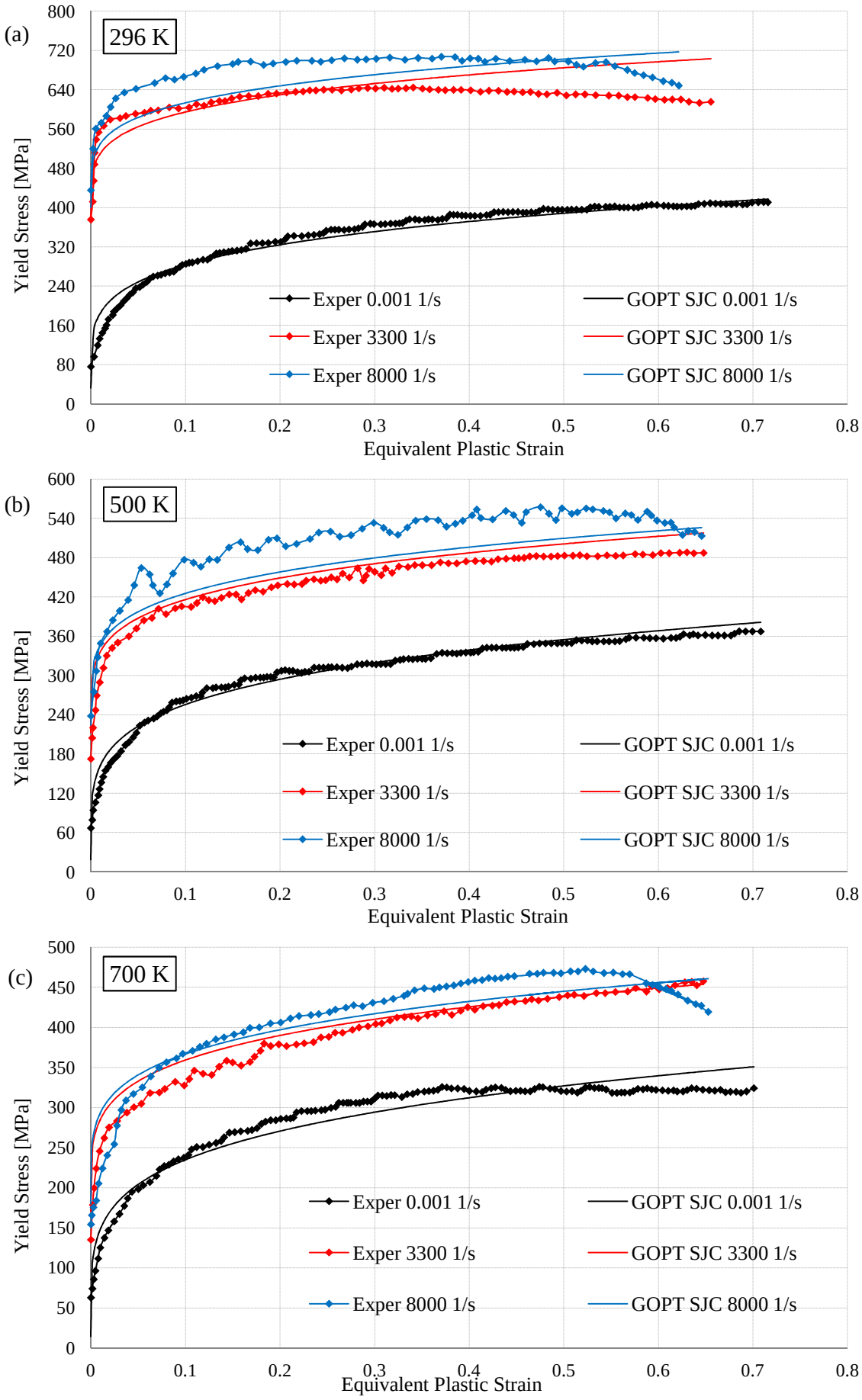

Figure 8. GOPT calibrated SJC fit for niobium at 0.001 s^{-1}, 3300 s^{-1}, 8000 s^{-1} and at (a) 296 K, (b) 500 K, (c) 700 K.

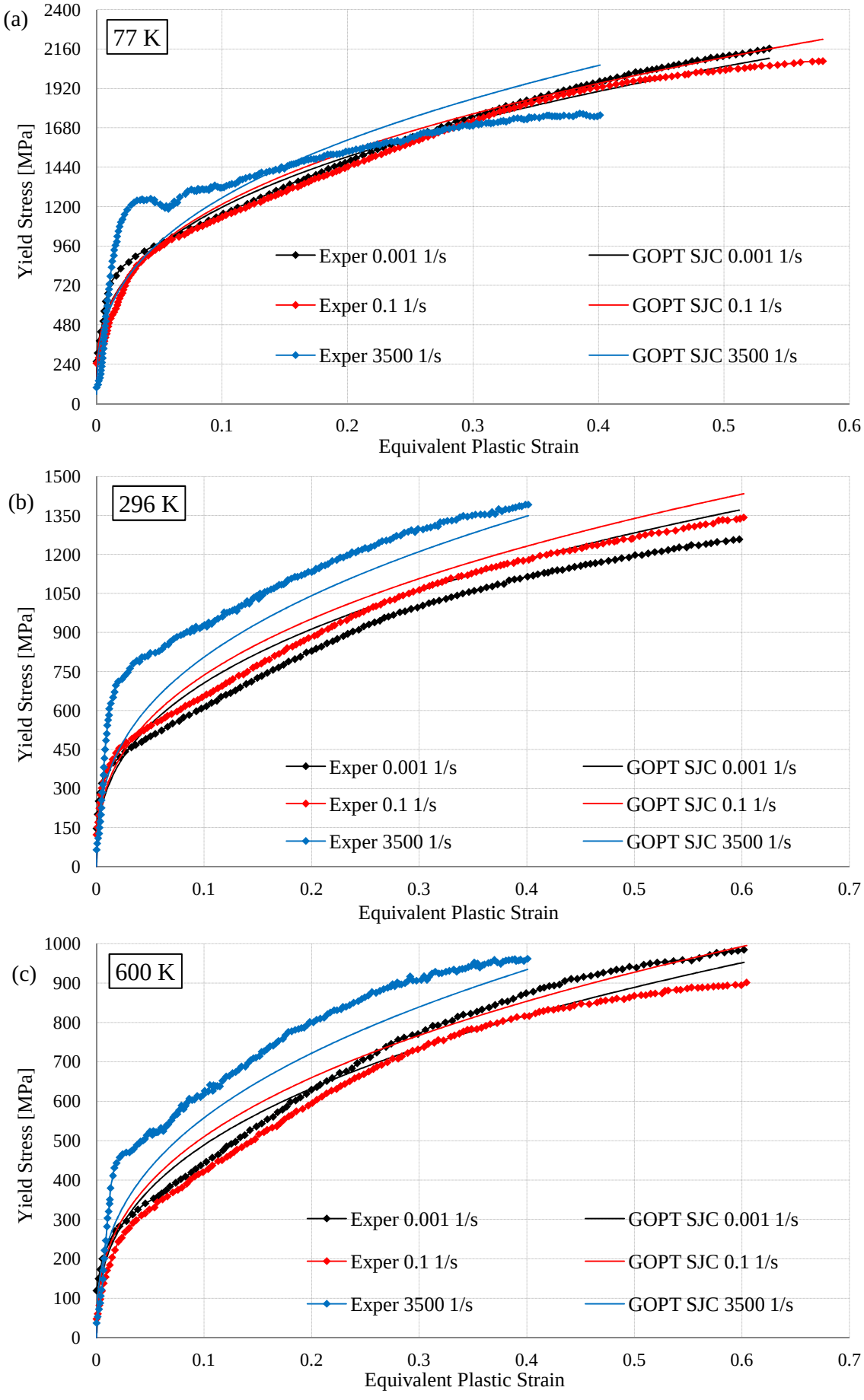

Figure 9. GOPT calibrated SJC fit for AL-6XN steel at 0.001 s^{-1}, 0.1 s^{-1}, 3500 s^{-1} and at (a) 77 K, (b) 296 K, (c) 600 K.

Table 11 compares lower yield stress predictions from the GOPT calibrated SJC, with the usual error measures.

	Experimental value [MPa]	**GOPT SJC value [MPa]**	**Error absolute value [MPa]**	**Percentage error value**
DH-36 steel				
0.001 s^{-1}; 77 K	915.56	863.78	51.780	5.656%
0.1 s^{-1}; 77 K	974.57	821.03	153.54	15.75%
3500 s^{-1}; 77 K	1150.5	725.33	425.17	36.96%
0.001 s^{-1}; 296 K	282.46	350.05	67.590	23.93%
0.1 s^{-1}; 296 K	305.46	332.72	27.260	8.924%
3500 s^{-1}; 296 K	630.14	293.94	336.20	53.35%
0.001 s^{-1}; 600 K	190.35	168.11	22.240	11.68%
0.1 s^{-1}; 600 K	200.21	159.78	40.430	20.19%
3500 s^{-1}; 600 K	305.35	141.16	164.190	53.77%
Average			*143.160*	*25.58%*
Niobium				
0.001 s^{-1}; 296 K	76.345	32.413	43.932	57.54%
3300 s^{-1}; 296 K	375.95	379.68	3.7300	0.992%
8000 s^{-1}; 296 K	435.70	400.17	35.530	8.155%
0.001 s^{-1}; 500 K	67.110	18.158	48.952	72.94%
3300 s^{-1}; 500 K	172.84	212.69	39.850	23.06%
8000 s^{-1}; 500 K	238.39	224.17	14.220	5.965%
0.001 s^{-1}; 700 K	62.910	14.549	48.361	76.87%
3300 s^{-1}; 700 K	135.09	170.42	35.330	26.15%
8000 s^{-1}; 700 K	154.35	179.62	25.270	16.37%
Average			*32.797*	*32.01%*
AL-6XN stainless steel				
0.001 s^{-1}; 77 K	256.86	148.09	108.77	42.35%
0.1 s^{-1}; 77 K	246.67	120.44	126.23	51.17%
3500 s^{-1}; 77 K	99.109	57.621	41.488	41.86%
0.001 s^{-1}; 296 K	146.49	0.0170	146.47	99.99%
0.1 s^{-1}; 296 K	122.49	0.0138	122.48	99.99%
3500 s^{-1}; 296 K	64.884	0.0066	64.877	99.99%
0.001 s^{-1}; 600 K	119.32	0.0095	119.31	99.99%
0.1 s^{-1}; 600 K	47.307	0.0078	47.299	99.98%
3500 s^{-1}; 600 K	37.090	0.0037	37.086	99.99%
Average			*90.446*	*81.70%*

Table 11. GOPT calibrated SJC model lower yield stress predictions for the three material cases.

Considering GOPT calibration results, Table 12 shows the adopted error measures for the three material cases and for each of the nine hardening curves.

	$\bar{s}_{err}$ [MPa]	$\bar{s}_{\%\,err}$		$\bar{s}_{err}$ [MPa]	$\bar{s}_{\%\,err}$		$\bar{s}_{err}$ [MPa]	$\bar{s}_{\%\,err}$
DH-36 steel			**Niobium**			**AL-6XN stainless steel**		
0.001 s^{-1}; 77 K	82.034	6.972	**0.001 s^{-1}; 296 K**	14.864	9.827%	**0.001 s^{-1}; 77 K**	51.940	6.008
0.1 s^{-1}; 77 K	35.947	3.234	**3300 s^{-1}; 296 K**	40.011	6.606%	**0.1 s^{-1}; 77 K**	73.306	10.42
3000 s^{-1}; 77 K	150.21	13.30	**8000 s^{-1}; 296 K**	41.166	6.272%	**3500 s^{-1}; 77 K**	181.28	26.82
0.001 s^{-1}; 296 K	64.415	17.56	**0.001 s^{-1}; 500 K**	11.674	9.494%	**0.001 s^{-1}; 296 K**	79.080	14.30
0.1 s^{-1}; 296 K	57.035	14.35	**3300 s^{-1}; 500 K**	23.468	8.449%	**0.1 s^{-1}; 296 K**	62.559	11.70
3000 s^{-1}; 296 K	105.61	13.10	**8000 s^{-1}; 500 K**	37.968	7.630%	**3500 s^{-1}; 296 K**	125.54	19.74
0.001 s^{-1}; 800 K	17.130	5.101	**0.001 s^{-1}; 700 K**	16.133	10.23%	**0.001 s^{-1}; 600 K**	41.581	11.82
0.1 s^{-1}; 800 K	29.772	9.693	**3300 s^{-1}; 700 K**	19.277	8.210%	**0.1 s^{-1}; 600 K**	61.999	18.00
3000 s^{-1}; 800 K	33.655	8.406	**8000 s^{-1}; 700 K**	29.715	12.963%	**3500 s^{-1}; 600 K**	72.699	19.78
Average	*63.979*	*10.19%*	***Average***	*26.031*	*8.853%*	***Average***	*83.332*	*15.40%*

Table 12. GOPT calibrated SJC model yield stress errors, for the three material cases.

The GOPT calibrated trends match at best the nine hardening functions over the equivalent plastic strain ranges. As said, this is partially prevented when the material does not trace true log and power dependencies. Comparing to the other two SJC calibration procedures, the fittings throughout the plastic flows are now improved. This positive result is a consequence of the large number of optimization variables adopted during identification. Also, this is in part a consequence of having created four overdetermined systems, therefore locating the best solution when moving from eleven to seven SJC material variables. Conversely, the fittings to the lower yield stresses are sometimes worse, comparing to STA and OPT. This may be expected, since the GOPT calibration optimizes several SJC parameters at the same time by attempting the best global fit throughout the whole plastic flow, without setting any specific importance at tracing the lower yield stress. Therefore, comparing to the other two calibration strategies, the fitting on the plastic flow is better, but this improvement may sometimes be hindered by a worsening of the lower yield stress description.

Average errors over the plastic flow are lower than those for STA and OPT, for all the three material cases. In particular, DH-36 steel and niobium results present a much lower absolute average error over the plastic flow. However, AL-6XN stainless steel outcomes show a slight increase in the average error, comparing to OPT calibration results, even though the absolute average error is sensibly lower. This is because OPT errors result greater in absolute value but they are recorded at higher yield stresses, resulting then in smaller percentage errors. Of course, the solving of the considered overdetermined systems minimizes the absolute value of the error rather than its percentage.

3.2.4. Calibration Strategies Assessment and Comparison with the Original Johnson-Cook model

This section aims at comparing the different hardening prediction outcomes that have been achieved on the SJC model by the three developed calibrations. To favor confrontation also with results provided by plain JC, additional results from five calibration procedures on plain JC from the same material data are presented too (Gambirasio and Rizzi, 2014).

Figs. 10 to 18 report plain JC and enhanced SJC hardening predictions for the three material cases. Some trends displayed in Figs. 10 to 18 depict calibration fittings that may be the same for different calibrations, at specific equivalent plastic strain rates and temperatures. This may result in apparent curve overlapping, although each of the following plots truly reports nine hardening trends (one experimental, five from plain JC and three from SJC).

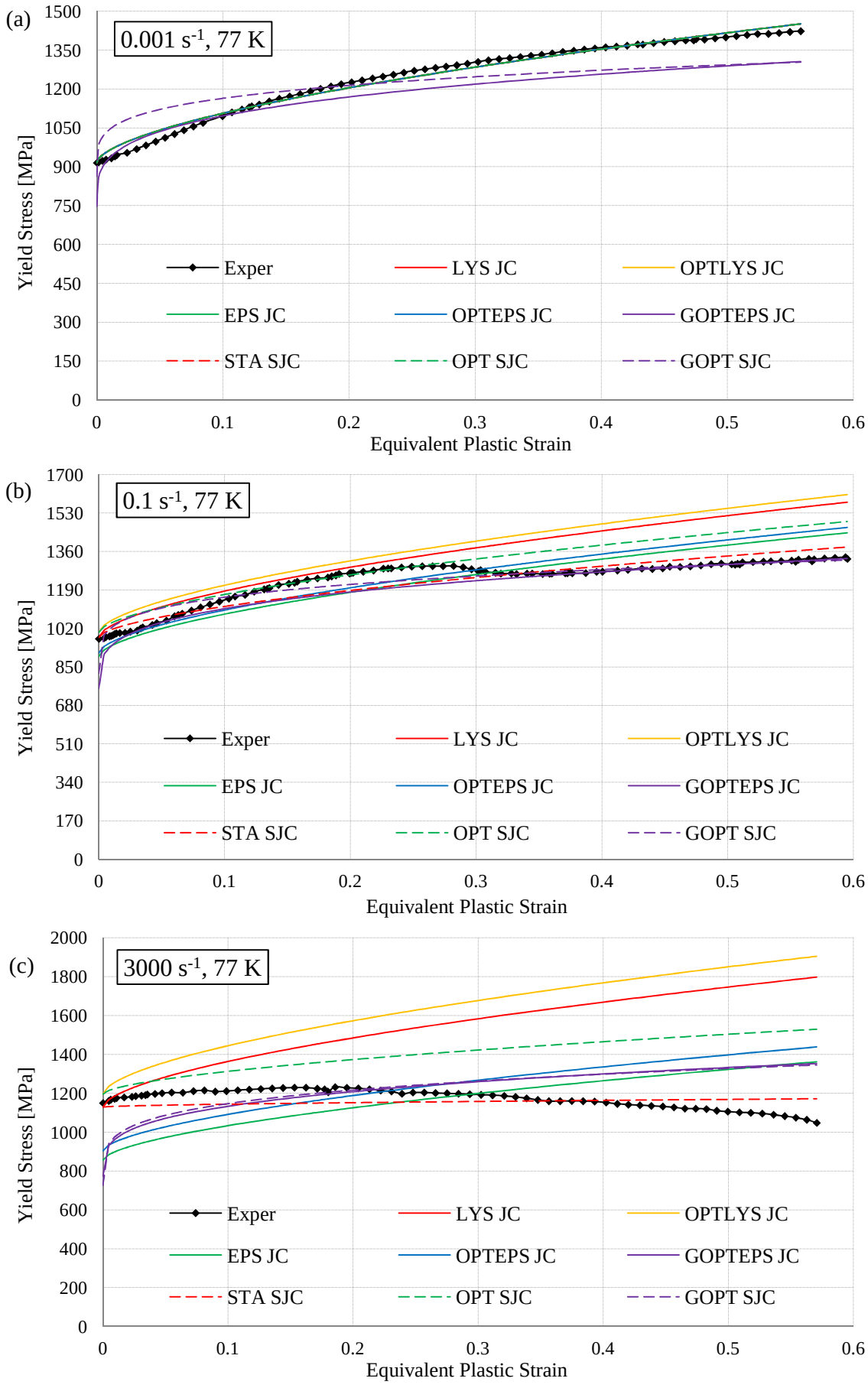

Figure 10. Five JC and three SJC calibrations for DH-36 steel at (a) 0.001 s^{-1}, 77 K, (b) 0.1 s^{-1}, 77 K, (c) 3000 s^{-1}, 77 K.

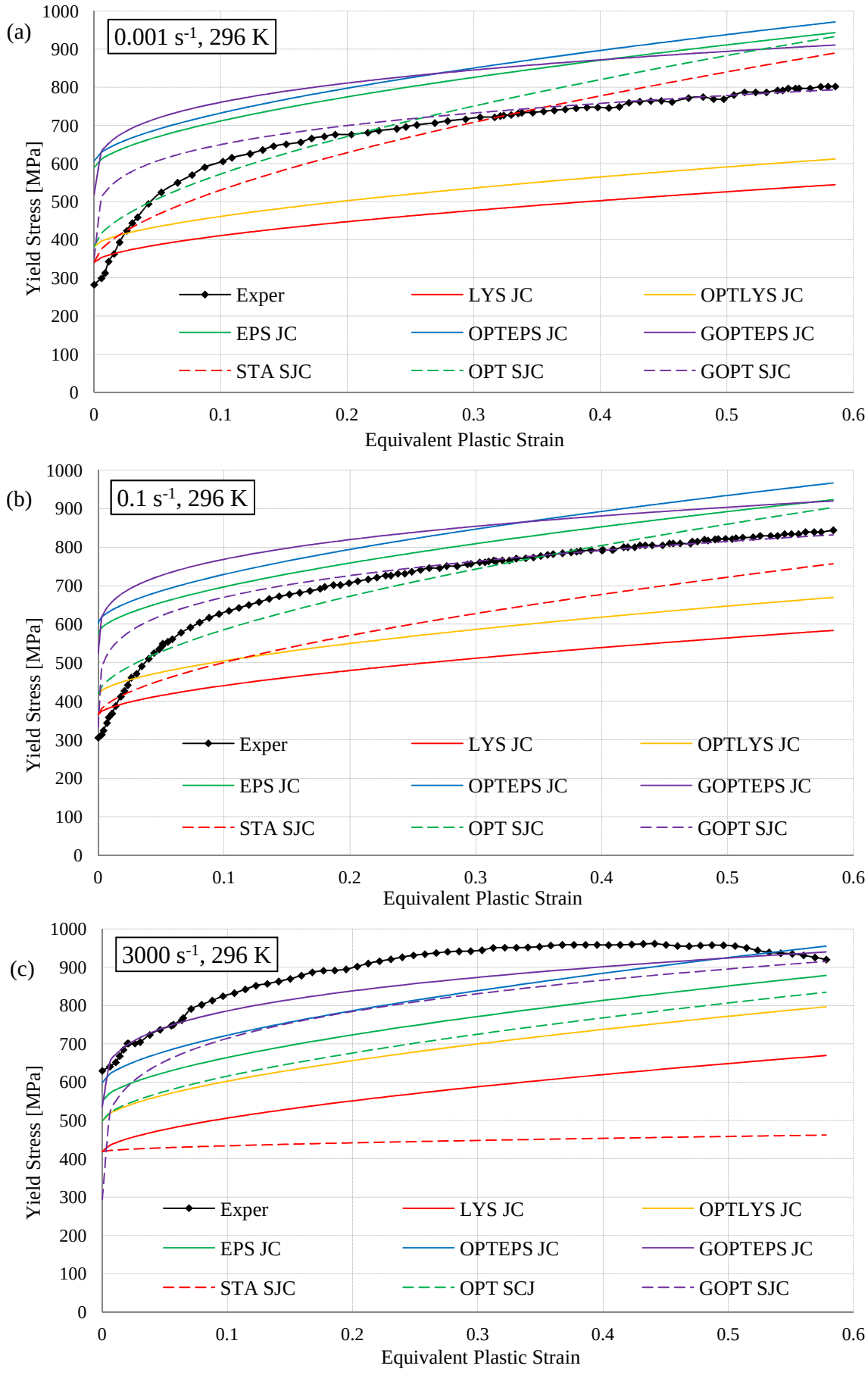

Figure 11. Five JC and three SJC calibrations for DH-36 steel at (a) 0.001 s^{-1}, 296 K, (b) 0.1 s^{-1}, 296 K, (c) 3000 s^{-1}, 296 K.

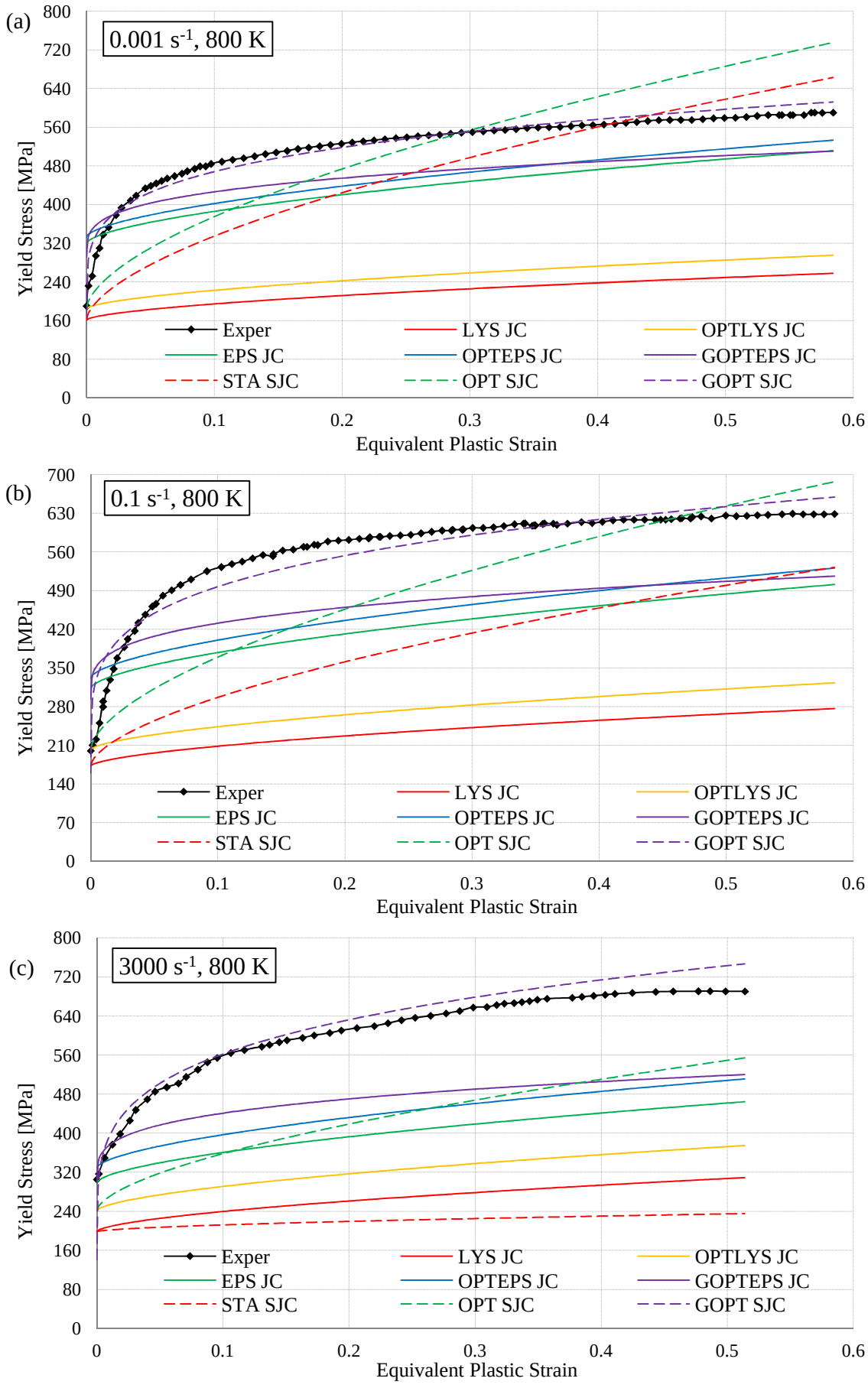

Figure 12. Five JC and three SJC calibrations for DH-36 steel at (a) 0.001 s^{-1}, 800 K, (b) 0.1 s^{-1}, 800 K, (c) 3000 s^{-1}, 800 K.

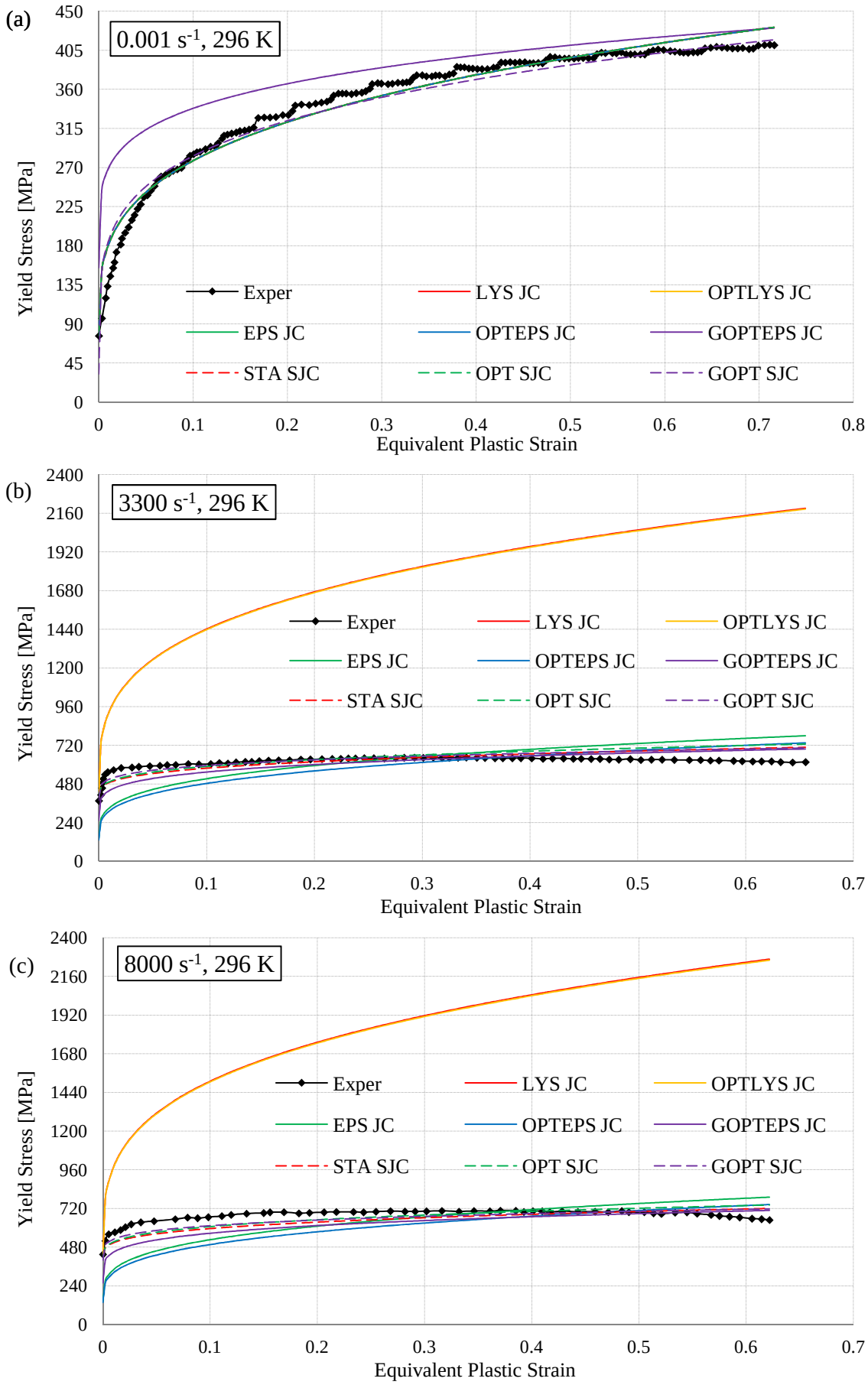

Figure 13. Five JC and three SJC calibrations for niobium at (a) 0.001 s^{-1}, 296 K, (b) 3300 s^{-1}, 296 K, (c) 8000 s^{-1}, 296 K.

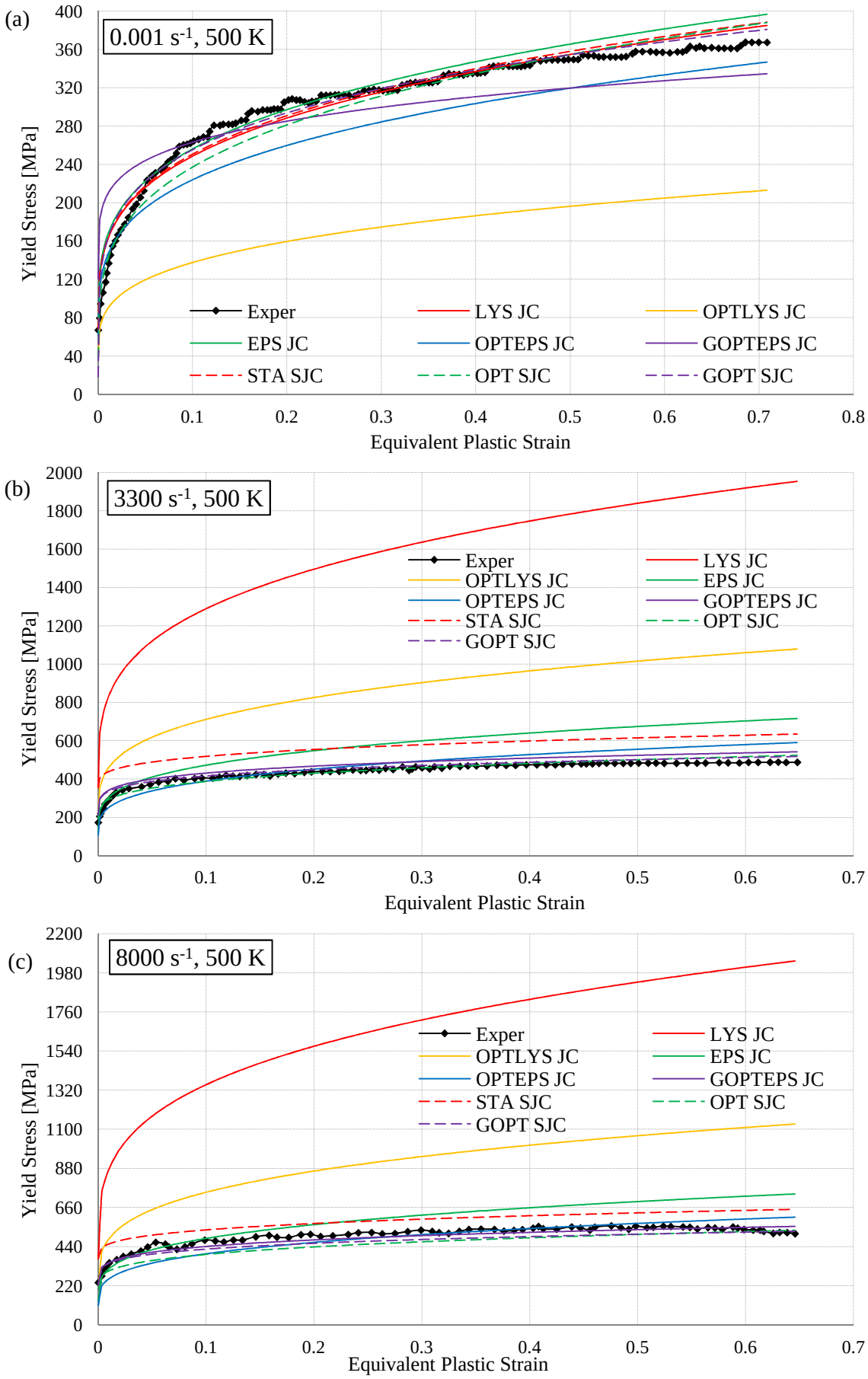

Figure 14. Five JC and three SJC calibrations for niobium at (a) 0.001 s^{-1}, 500 K, (b) 3300 s^{-1}, 500 K, (c) 8000 s^{-1}, 500 K.

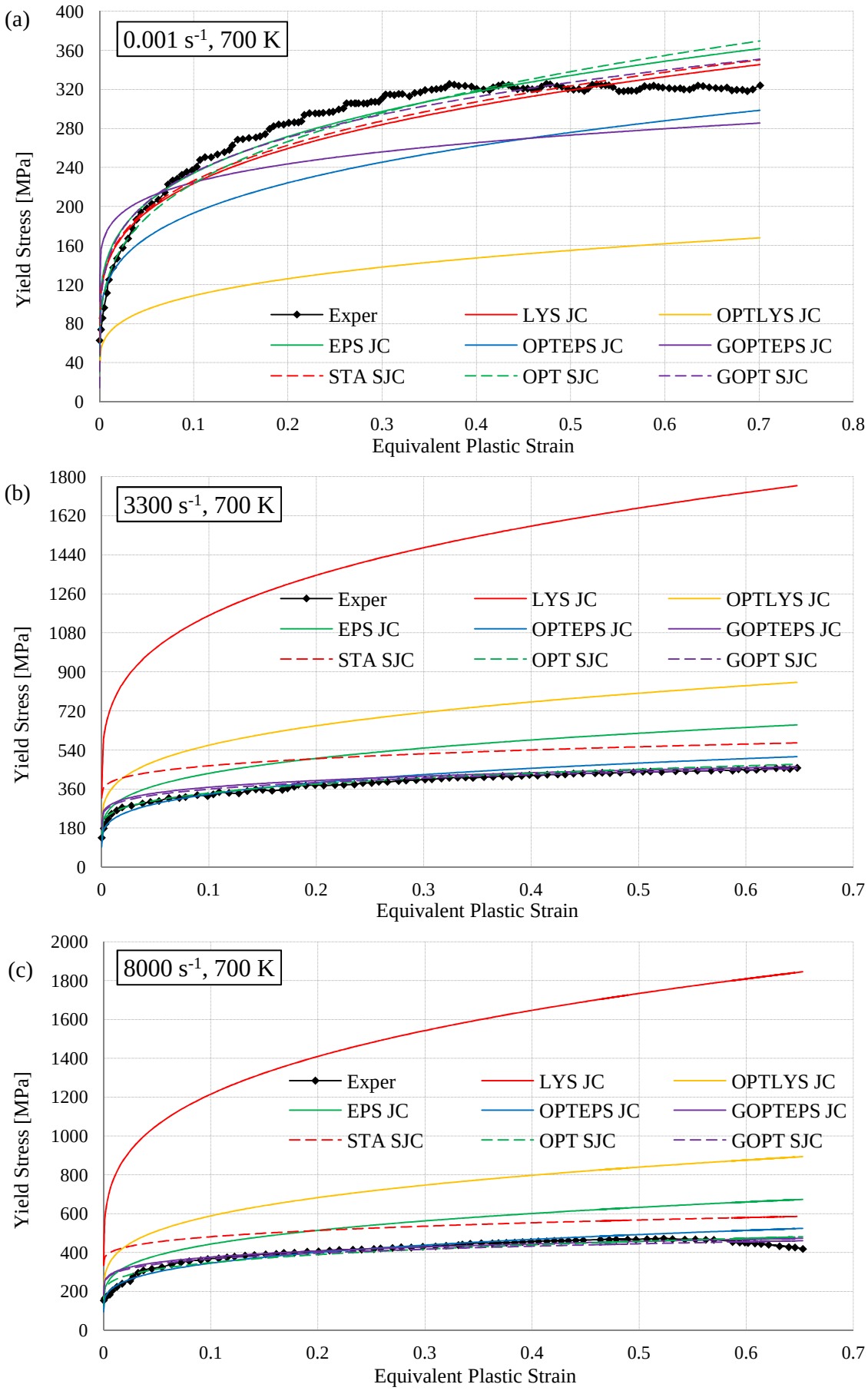

Figure 15. Five JC and three SJC calibrations for niobium at (a) 0.001 s^{-1}, 700 K, (b) 3300 s^{-1}, 700 K, (c) 8000 s^{-1}, 700 K.

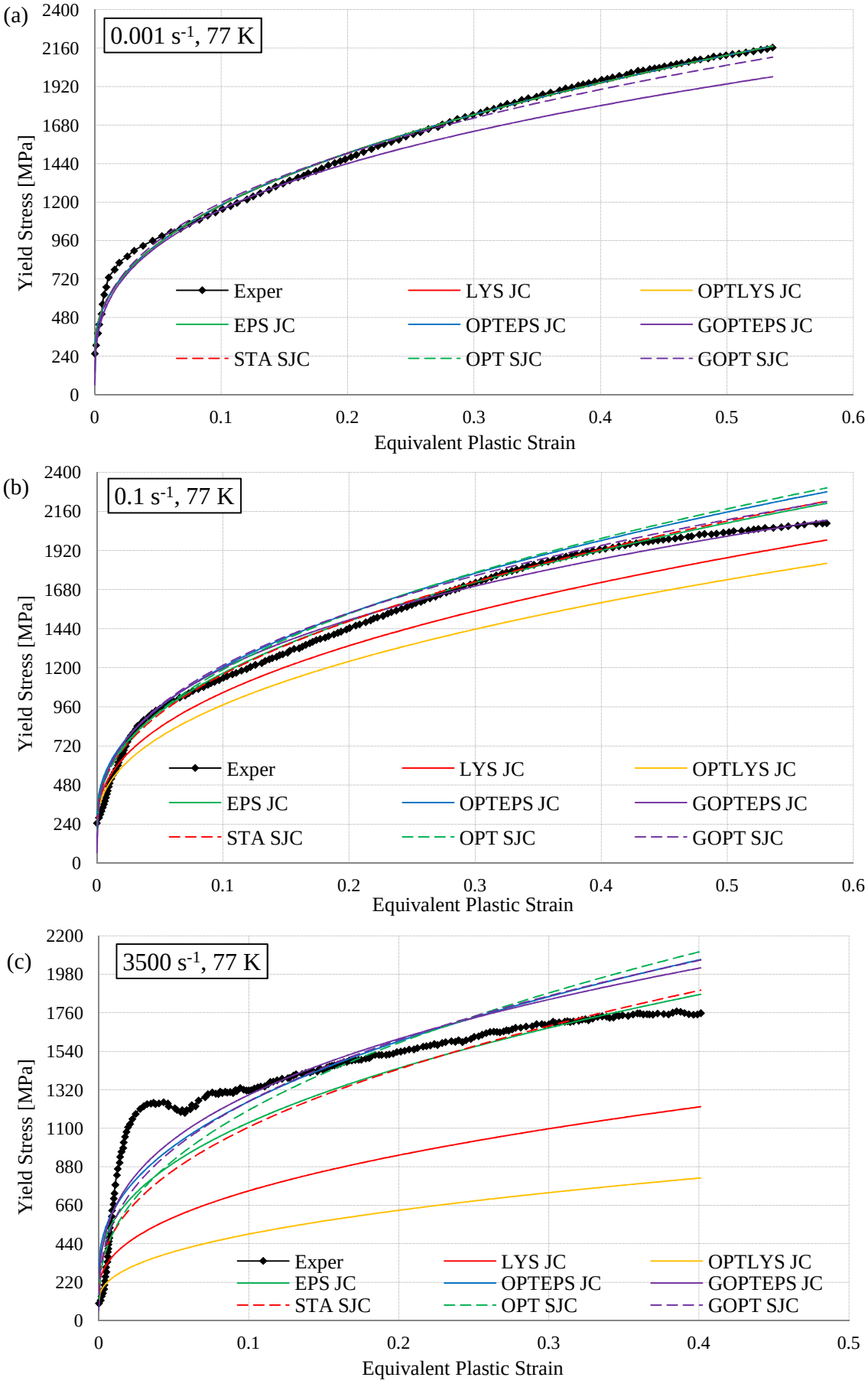

Figure 16. Five JC and three SJC calibrations for AL-6XN steel at (a) 0.001 s^{-1}, 77 K, (b) 0.1 s^{-1}, 77 K, (c) 3500 s^{-1}, 77 K.

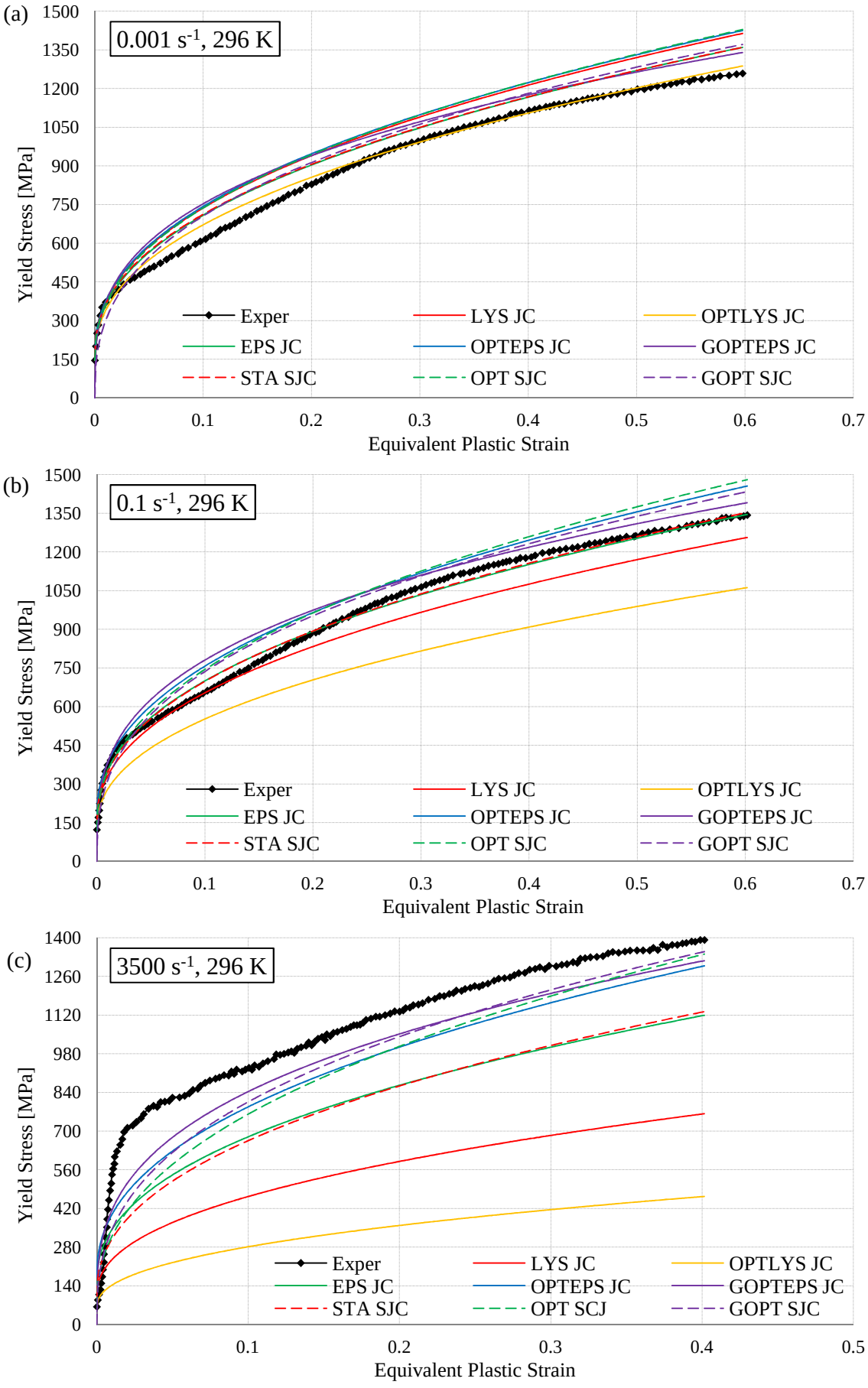

Figure 17. Five JC and three SJC calibrations for AL-6XN steel at (a) 0.001 s^{-1}, 296 K, (b) 0.1 s^{-1}, 296 K, (c) 3500 s^{-1}, 296 K.

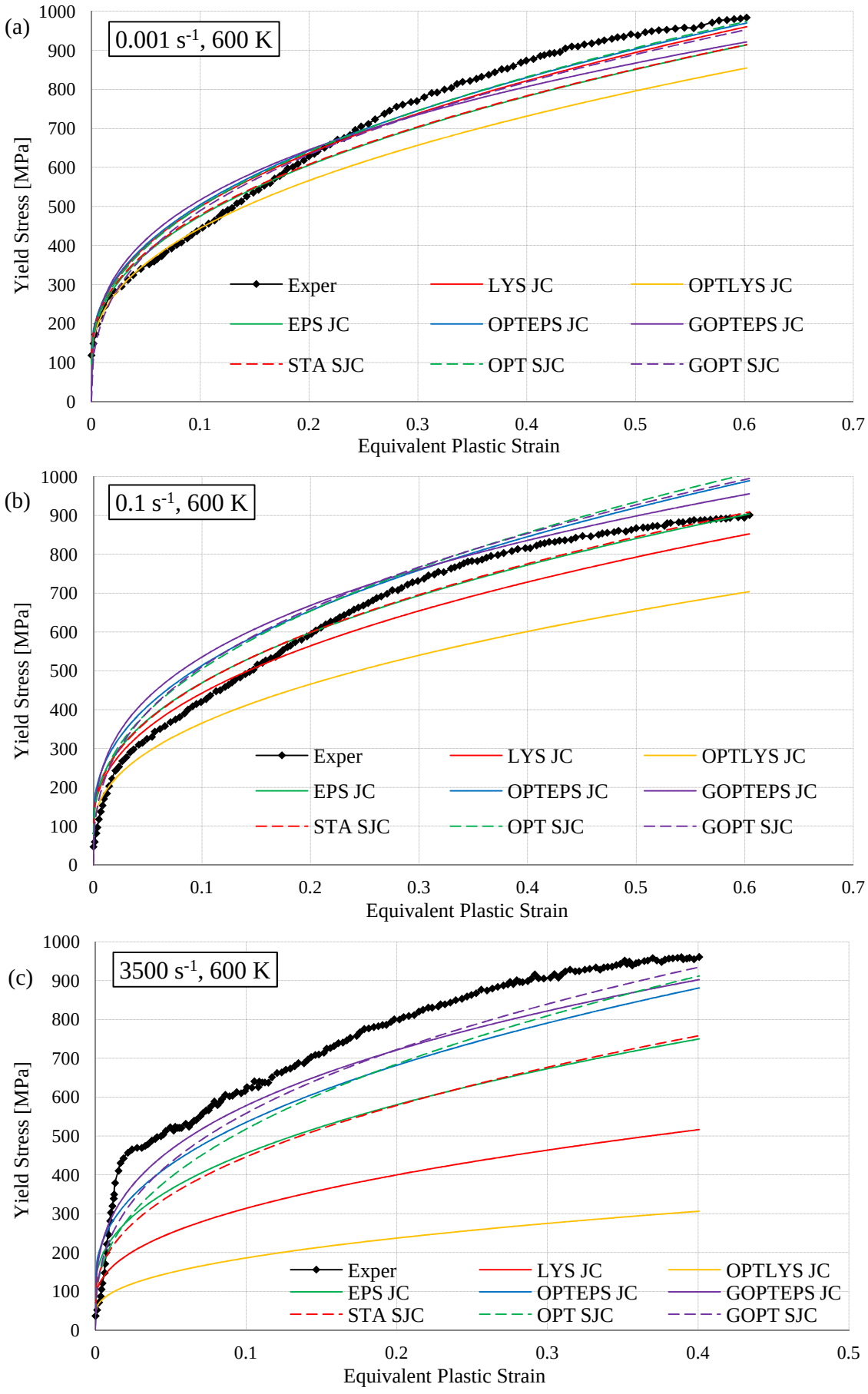

Figure 18. Five JC and three SJC calibrations for AL-6XN steel at (a) 0.001 s^{-1}, 600 K, (b) 0.1 s^{-1}, 600 K, (c) 3500 s^{-1}, 600 K.

Table 13 gathers the adopted error measures for each JC and SJC calibration strategy, as applied to the three considered material cases.

	Lower yield stress average error [MPa]	Lower yield stress average % error	Average $\bar{s}_{err}$ [MPa]	Average $\bar{s}_{\%err}$
DH-36 steel				
LYS JC	57.587	15.49%	253.86	34.85%
OPTLYS JC	54.198	13.85%	226.29	30.31%
EPS JC	142.20	41.12%	121.78	19.23%
OPTEPS JC	140.09	43.68%	113.92	18.21%
GOPTEPS JC	168.06	38.31%	105.49	16.86%
STA SJC	57.587	15.49%	153.55	22.20%
OPT SJC	54.198	13.85%	113.11	15.60%
GOPT SJC	143.160	25.58%	63.979	10.19%
Niobium				
LYS JC	80.080	47.45%	759.21	154.0%
OPTLYS JC	20.694	16.95%	457.89	87.53%
EPS JC	80.830	26.50%	91.920	21.06%
OPTEPS JC	94.980	35.51%	56.571	13.55%
GOPTEPS JC	64.771	42.65%	41.386	14.61%
STA SJC	80.080	47.45%	67.538	19.53%
OPT SJC	20.694	16.95%	28.599	7.549%
GOPT SJC	32.797	32.01%	26.031	8.853%
AL-6XN stainless steel				
LYS JC	26.800	38.59%	209.09	23.06%
OPTLYS JC	12.098	14.12%	314.72	30.88%
EPS JC	45.190	67.15%	103.09	18.66%
OPTEPS JC	56.108	83.02%	93.670	20.93%
GOPTEPS JC	81.483	53.83%	88.386	18.64%
STA SJC	26.800	38.59%	105.57	16.66%
OPT SJC	12.098	14.12%	98.785	14.90%
GOPT SJC	90.446	81.70%	83.332	15.40%

Table 13. Fitting matching from five original JC (reported from Gambirasio and Rizzi, 2014, for the ease of comparison) and three SJC calibration strategies for the three material cases.

As for plain JC, the calibration procedure for the SJC model displays chief importance towards achieving an eventual hardening function apt to manifest proper coherence over all ranges of equivalent plastic strain, equivalent plastic strain rate and temperature. To better interpret the implications of choosing a particular SJC calibration strategy or another, some considerations are outlined below.

3.2.5. Considerations on the Choice of the Calibration Strategy

Concerning the overall plastic flow fittings, the GOPT calibration strategy certainly provides the best results, considering the average absolute errors. If percentage values are considered, the average error of the GOPT approach may be higher than that obtained for the OPT calibration strategy, as happens for the niobium and AL-6XN stainless steel cases. As previously mentioned, this is because the errors of the SJC model calibrated with the OPT strategy turn-out higher in absolute value but appear at higher yield stresses, producing then smaller percentage errors. Nonetheless, the average error absolute values involved in the GOPT results may sometimes be strongly lower than that for the OPT strategy, like for DH-36 and AL-6XN steels. The STA approach provides sensibly higher average RMS errors, comparing to the OPT and GOPT strategies. This is mainly due to the random errors associated to the fitting of the hardening curves that do not refer to one reference condition at least, whether it is the reference value of equivalent plastic strain rate or of temperature, for both lower yield stress and plastic flow terms, whose data are never used for calibration.

Conversely, regarding the predictions of the lower yield stress, the GOPT SJC calibration strategy may sometimes provide the worst fit, comparing to the STA and OPT approaches. As previously mentioned, this issue is a consequence of the fact that the GOPT strategy determines the SJC parameters by trying to get the best overall fit over the whole range of equivalent plastic strains, giving to the lower yield stress the same importance as for any other available point. This may lead to quite bad fittings of the lower yield stresses, as a price to be paid for achieving the best overall plastic flow fittings. For what it concerns the STA and OPT calibration strategies, the lower yield stress fittings are usually much better than those relative to the GOPT strategy, since the parameters relative to its prediction are directly determined by relying on lower yield stress data, giving them much importance than for the other data. On the other hand, this choice is paid by a higher average error throughout the plastic flows, comparing to GOPT results. However, the overall plastic flow errors from the OPT calibration strategy may be not too far from those of the GOPT approach, but providing a much better lower yield stress fittings. This point is indeed true for the two material cases of niobium and AL-6XN steel. Therefore, taking into account the fittings of both lower yield stress and plastic flow, the OPT calibration strategy may sometimes be capable to provide better results than the GOPT approach. In order to select the best results, both cases should then be analyzed.

Regarding the easiness of implementation of each calibration strategy, comments may be advanced on the computations required by each approach and on the possible need of preliminary treatment of the experimental data. The STA method turns out the simplest, since it needs a regression on parameters B and n, together with straightforward computations for parameters C_1 and m_1, plus some other nonlinear regressions necessary for parameters C_2 and m_2. The STA strategy may require inverse analyses of all the hardening curves referring to at least one plastic flow reference condition, because they are thoroughly used for the determination of plastic flow parameters C_2 and m_2. The OPT method requires more computations, since two overdetermined systems of nonlinear equations have to be assembled and solved, one for determining parameters C_1 and m_1 and the other for getting parameters C_2 and m_2. Furthermore, all the hardening data may require inverse analyses treatment, for filtering possible structural effects at the sample scale. Lastly, the GOPT method further complicates the scene. This time, there are more unknowns in the considered overdetermined system, up to eleven, producing a problem that is harder to be solved. Besides, when the procedure defined in Section 3.2.3 is used, four overdetermined systems have to be analyzed, instead of a single one.

The three SJC model calibration strategies require experimental data in terms of complete hardening functions, i.e. not only data attached to the lower yield stress. The more the experimental data, the better for SJC calibration. All the available data can fruitfully be introduced in the SJC calibration procedures. Anyway, it may happen that the SJC hardening prediction may display difficulties in fitting intricate material behaviors, when more experimental data are introduced in the calibration process. Data that may not be interpreted well by the lower yield stress and plastic flow log and power dependencies may appear. As an

example, the experimental curves of DH-36 steel presented more complex dependencies on plastic strain rate and temperature than what it is considered by the present model generalizing plain JC. Indeed, if data at 500 K are considered, the yield stress does not strictly increase at increasing equivalent plastic strain rate, which makes the conceived log dependence of the yield stress on the two dimensionless equivalent plastic strain rates quite unsuitable to fit such experimental data. If the SJC model appears to fit poorly the experimental curves, a substitution of one or more of the lower yield stress and plastic flow strain rate and temperature factors may be pondered, in order to alleviate fitting difficulties. In this regard, the various proposed modified versions of such terms from the literature, some of them widely presented and discussed in Section 2, could be considered within the present framework. This aspect is actually another positive point of the present SJC model. Indeed, having maintained a form quite similar to that of plain JC, with specific reference to the nature of strain rate and temperature factors, allows for replacing some of these terms, either for the lower yield stress or for the plastic flow factors, or even for both.

As a matter of fact, the just mentioned problem arises for the original JC model as well, with even worse implications. In fact, the SJC model capability to separately describe the lower yield stress and plastic flow dependencies on plastic strain rate and temperature allows for alleviating this issue. However, these incoherencies cannot be totally eliminated, when maintaining a very simple modeling framework is an aim, as previously stated in Section 3.1. If the results are still unsatisfactory when one or more strain rate and temperature terms have been changed, other strength models could be considered. In particular, materials that present a heavy dependence of plastic flow parameters B and n on equivalent plastic strain rate and temperature may further worsen this aspect.

The SJC model appears capable to provide a significant improvement comparing to plain JC. This statement relies on the average errors on lower yield stress and plastic flow reported in Table 13, together with trends reported in Figs. 10 to 18. By comparing the best calibrated original JC results to the best calibrated SJC results, sensible improvements can be noted. In this regard, some considerations specifically related to each of the three material instances are presented below.

For the DH-36 steel material, the best original JC calibration strategy, i.e. the GOPTEPS, provides an average lower yield stress error of 168.06 MPa (38.31%) and an average error throughout the plastic flows of 105.49 MPa (16.86%). Respectively, these values are lowered down to 143.160 MPa (25.58%) and 63.979 MPa (10.19%) for the SJC GOPT results. The OPT calibrated SJC results are interesting as well, providing a much lower error for the average lower yield stress error, i.e. 54.198 MPa (13.85%), even though the average error throughout the plastic flows is higher, equal to 113.11 MPa (15.60%). Moreover, if SJC outcomes are checked against plain JC results calibrated with likely the most popular calibration strategy, i.e. the LYS approach, improvements are even much higher, since this calibration strategy provides an average lower yield stress error of 57.587 MPa (15.49%) and an average error throughout the plastic flows of 253.86 MPa (34.85%), i.e. more than four times the absolute plastic flow error provided by the GOPT calibrated SJC model.

The niobium case further exacerbates this situation. In fact, the best original JC model results, i.e. those due to the GOPTEPS approach, provide an average lower yield stress error of 64.771 MPa (42.65%) and an average error throughout the plastic flows of 41.386 MPa (14.61%). Respectively, these values are lowered down to 32.797 (32.01%) and 26.031 MPa (8.853%) for the GOPT calibrated SJC model. The OPT calibrated SJC model provides even more interesting results, i.e. an average lower yield stress error of 20.694 MPa (16.95%) and an average error throughout the plastic flows of 28.559 MPa (7.549%). Comparing to the LYS calibrated original JC model, the improvements are huge, since this case involves an average lower yield stress error of 80.080 MPa (47.45%) and an average error throughout the plastic flows of 759.21 MPa (154.0%), that is more than twenty-nine times higher than the absolute plastic flow error of the GOPT calibrated SJC model.

Comparing to plain JC results, the SJC description of the AL-6XN stainless steel case does not provide as strong improvements as those involved in the two previous cases. In fact, the best original JC results obtained are those referring to the OPTEPS and GOPTEPS cases. The former provides an average lower

yield stress error of 56.108 MPa (83.02%) and an average error throughout the plastic flows of 93.670 MPa (20.93%), while the latter gives an average lower yield stress error of 81.483 MPa (53.83%) and an average error throughout the plastic flows of 88.386 MPa (18.64%). The best SJC results are those referring to the OPT and GOPT approaches. The OPT strategy provides an average lower yield stress error of 12.098 MPa (14.12%) and an average error throughout the plastic flows of 98.785 MPa (14.90%). The GOPT approach gives an average lower yield stress error of 90.446 MPa (81.70%) and an average error throughout the plastic flows of 83.332 MPa (15.40%). The reduced efficiency of the SJC model is due to the fact that this material presents lower yield stress and plastic flow variations on plastic strain rate and temperature appearing fairly similar. As a matter of fact, the more these two dependencies are similar, the more the SJC model provides results similar to those of the JC model. Indeed, it is recalled that the Split JC model is a generalization of the original JC model, which is actually recovered if lower yield stress and plastic flow dependencies are exactly equal. The consideration that the AL-6XN steel material presents this behavior explains also why the LYS calibrated original JC model provides results not too far from those provided by the other calibration strategies of both original JC and SJC models, by involving an average lower yield stress error of 26.800 MPa (38.59%) and an average error throughout the plastic flows of 209.09 MPa (23.06%). Indeed, the LYS calibration strategy determines the original JC parameters by using lower yield stress experimental data only. Nevertheless, the obtained results do not present heavy fitting worsening, comparing to those relative to calibration strategies that use all experimental data. Anyway, the SJC outcomes arise still better than those for plain JC.

Concerning the STA SJC calibration strategy, the obtained results are always quite good, for the fittings of both lower yield stress and plastic flow. Also, if calibration complexities are taken into consideration, STA results should better be compared with those of the original JC model LYS and EPS calibration strategies, since these strategies are similar and involve more or less the same calculation burden to achieve appropriate calibration. Hence, when both average errors on lower yield stress and plastic flows are considered, STA results provide a sensible improvement for all the three examined material cases, comparing to the OPT and LYS results, as shown in Table 13.

In general, comparing to the original JC model, the SJC model appears capable to offer a remarkable improvement in the fitting capabilities, leading to results more acceptable from the engineering standpoint. Beyond the reported errors, the trends shown in the plots demonstrate that calibration is now much improved. The SJC model efficiently tackles the so-called second drawback of the original JC model, previously discussed in Sections 1 and 2, at least for the fact that the effects of plastic strain rate and temperature no longer need to be assumed as equal for each equivalent plastic strain. More in detail, the new model aims at relieving the problem of having to choose between coherently model either the lower yield stress scores, through the original JC LYS or OPTLYS calibration procedures, or the plastic flows, through the original JC EPS, OPTEPS or GOPTEPS calibration techniques. Also, the SJC model keeps at the same time the original JC best results obtainable for the fittings of lower yield stress and plastic flow, instead of having to pick either of the two, with the risk of introducing unacceptably high errors. The good qualities of the original JC OPTLYS and OPTEPS strategies are preserved together and even improved with the OPT SJC strategy. Furthermore, the GOPT SJC strategy appears capable to further improve the results for some practical case, in particular for the plastic flow fittings, although the fitting of the lower yield stress may sometimes be quite high. Having the possibility to coherently model at the same time lower yield stress and plastic flow trends allows to keep a good prediction throughout the whole plastic flow but to avoid negative consequences due to a possibly bad lower yield stress fittings, such as strongly erroneous computations of the equivalent plastic strain. This last point may actually produce unacceptable errors when damage and failure models are used, in particular for models which calculate the damage variables as driven by the equivalent plastic strain, such as the damage and failure model by Johnson-Cook (Johnson and Cook, 1985), not analyzed in the present context.

In the very worst case, the SJC model provides results at least equal to those of the original JC model. This happens when the considered material presents exactly equal lower yield stress and plastic flow

dependencies on plastic strain rate and temperature. Clearly, a case like this appears quite difficult to be manifested in practice, whatever material may be considered. On the other hand, the modeling of material cases in which lower yield stress and plastic flow present quite different dependencies on plastic strain rate and temperature are no longer a problem, differently from what happens with the original JC model. Rather, such cases can be successfully reproduced thanks to the features of the new SJC model. The more these dependencies are different from each other, the more the SJC model provides better results comparing to those for plain JC.

The present analysis shows that the adoption of the SJC model determines significant improvements comparing to the original JC. Also, the adoption of the SJC model does not introduce any strong negative consequence. The following considerations aim at explaining this important point.

The calibration of the proposed enhanced model requires the availability of the same type of experimental data needed for plain JC calibration, although the model parameters are now increased from eight to twelve. At the same time, the enlargement of the number of material parameters does not appear to be a problematic issue. Indeed, the calibration procedures for original JC and for enhanced SJC require a similar effort in terms of data recovering, processing and calculation. Furthermore, when the STA and OPT calibration strategies are adopted, the SJC model may rely on some parameters already calculated for the original JC model.

The SJC model maintains the same appeal of the original JC model towards computational implementations, with particular reference to applications in FEM codes. In fact, the model uses the same driving variables used by the original JC model, namely equivalent plastic strain, equivalent plastic strain rate and temperature. These variables are usually already available in most FEM codes. In fact, it is common that these variables are inserted among the information provided for each timestep.

Regarding the computational heaviness of the implementation, the only point that differs from the original JC model consists in the fact that the SJC model implies a slight increase in the number of algebraic operations necessary to compute the current yield stress, since the proposed model contains two split additive terms, rather than a single one. Comparing to the computational requirements necessary to run an analysis with the original JC model, this aspect does not appear to be crucial in further burdening the computational requirements necessary for carrying-out FEM analyses.

4. Conclusions

A new strength model, named SJC model, has been presented. It has been formulated as a convenient generalization of the original JC model. The aims were those of improving the original JC hardening function, in order to mitigate shortcomings such as the issue that the effects of equivalent plastic strain, equivalent plastic strain rate and temperature on the yield stress are totally independent from each other. More in detail, the SJC model allows to separately model the dependencies of lower yield stress and plastic flow on the equivalent plastic strain rate and temperature.

The salient achievements of the present paper, specifically in terms of novelties and superior outcomes by the proposed SJC modeling shall be synoptically summarized as follows:

- The various characteristic features of the enhanced SJC model have been widely investigated, together with the presentation of a comprehensive discussion on its calibration strategies. Through a reasoned treatment, three different calibration approaches have been presented and thoroughly discussed, thus providing a guide for calculating the model parameters, by relying on experimental data consisting of a set of hardening curves carried-out at various conditions of equivalent plastic strain rate and temperature.
- The new SJC model has been consistently applied to the description of three real material cases. The results have allowed to discuss and evaluate all positive and negative aspects of the different calibration strategies.

- The obtained results have been checked against those provided by the original JC model, considering the same three material cases under consideration, developed in an earlier companion work (Gambirasio an Rizzi, 2014). In this regard, the replacement of the original JC model with the new model appears to introduce appreciable positive consequences. The SJC model has proven capable to remarkably improve the description of the experimental data, for both lower yield stress and plastic flow predictions.
- The SJC model characteristic of presenting a form very similar to that of plain JC allows for further interesting options, such as the possibility to substitute one or more of the SJC model lower yield stress and plastic flow strain rate and temperature factors with some of the substitutive terms already proposed in the literature, some of which have been reviewed in Section 2. Furthermore, displaying a form very similar to that of plain JC allows to partially reuse some of the material parameters of such a model, that may be already known from previous calibrations.
- The SJC model presents strong scientific and technologic foundations. From the scientific point of view, it provides an efficient way to describe temperature and strain rate dependent behavior of materials, with a much better coherence than that provided by the plain JC model. Regarding the technologic point of view, the SJC model can be successfully used in many industrial contexts and attached computational modeling, whenever temperature and strain rate become important for the description of the involved materials, like, e.g., for impact problems, perforating phenomena, thermal analyses and so on.
- Negative implications, if really any, appear to be very limited. Even though the model requires four extra material parameters, the need of experimental data, heaviness of calibration and computational weight remain almost unchanged, comparing to those for the original JC model. Furthermore, the SJC model has been conceived to maintain the same computational appeal of the original JC model. Indeed, it operates by requiring only the knowledge of equivalent plastic strain, equivalent plastic strain rate and temperature, thus allowing for perfect fitting within the same computational framework of the JC model.

By considering the listed positive consequences, the SJC strength model is deemed as a promising option for modeling strain rate and temperature dependent hardening behavior of elastoplastic materials. Also, it may be considered as a very valid replacement for the original JC model, no matter which material is under consideration, since the new model always provides better fitting results. This point becomes truer the more the considered material presents different dependencies of lower yield stress and plastic flow on equivalent plastic strain rate and temperature. Surely, the proposed model is intended to be considered when empirical approaches are feasible. Whenever the need to use more physically-based models takes importance, other hardening functions that address this aspect should be considered.

As a future development, the new model may be implemented into FEM codes. Structural results may then be compared to those provided by the original JC model, in particular by considering some benchmark reference cases. Another future investigation may regard the possibility to calibrate the SJC model by relying on different experimental results, i.e. not only on a bunch of hardening functions for several equivalent plastic strain rates and temperatures. Procedures apt to identify the model parameters from experimental tests such as Taylor impact tests, flyer plate impact tests (see, e.g., Meyers, 1994, and Zukas, 2004) or through virtual fields methods (see, e.g., Notta-Cuvier et al., 2013) may be defined, similarly to what already discussed for the original JC model in Gambirasio and Rizzi, 2014.

Acknowledgments

The authors gratefully acknowledge funding from "Fondi di Ricerca d'Ateneo ex 60%" at the University of Bergamo, Dept. of Engineering and Applied Sciences.

References

[1] Abotula, S., Shukla, A., Chona, R., (2011), *"Dynamic constitutive behavior of Hastelloy X under thermo-mechanical loads"*, Journal of Materials Science, 46(14), pp. 4971-4979.

[2] Akbari Mousavi, S.A.A., Shahab, A.R., Mastoori, M., (2008), *"Computational study of Ti–6Al–4V flow behaviors during the twist extrusion process"*, Materials & Design, 29(7), pp. 1316-1329.

[3] Allen, D.J., Rule, W.K., Jones, S.E., (1997), *"Optimizing material strength constants numerically extracted from Taylor impact data"*, Experimental Mechanics, 37(3), pp. 333-338.

[4] Batra, R.C., Kim, C.H., (1991), *"Effect of thermal conductivity on the initiation, growth and bandwidth of adiabatic shear bands"*, International Journal of Engineering Science, 29(8), pp. 949-960.

[5] Benson, D.J., (1992), *"Computational methods in Lagrangian and Eulerian hydrocodes"*, Computer Methods in Applied Mechanics and Engineering, 99(2-3), pp. 235-394.

[6] Bigoni, D., (2012), *"Nonlinear Solid Mechanics. Bifurcation Theory and Material Instability"*, ISBN 987-1-107-02541-7.

[7] Børvik, T., Hopperstad, O.S., Berstad, T., (2003), *"On the influence of stress triaxiality and strain rate on the behaviour of a structural steel. Part II. Numerical study"*, European Journal of Mechanics, A/Solids, 22(1), pp. 15-32.

[8] Børvik, T., Hopperstad, O.S., Berstad, T., Langseth, M., (2001), *"A computational model of viscoplasticity and ductile damage for impact and penetration"*, European Journal of Mechanics, A/Solids, 20(5), pp. 685-712.

[9] Brünig, M., Driemeier, L., (2007), *"Numerical simulation of Taylor impact tests"*, International Journal of Plasticity, 23(12), pp. 1979-2003.

[10] Cadoni, E., Dotta, M., Forni, D., Tesio, N., Albertini, C., (2013), *"Mechanical behaviour of quenched and self-tempered reinforcing steel in tension under high strain rate"*, Materials & Design, 49, pp. 657-666.

[11] Cai, J., Wang, K., Zhai, P., Li, F., Yang, J., (2015), *"A modified Johnson-Cook constitutive equation to predict hot deformation behavior of Ti-6Al-4V alloy"*, Journal of Materials Engineering and Performance, 24(1), pp. 32-44.

[12] Camacho, G.T., Ortiz, M., (1997), *"Adaptive Lagrangian modelling of ballistic penetration of metallic targets"*, Computer Methods in Applied Mechanics and Engineering, 142(3-4), pp. 269-301.

[13] Chaboche, J.L., (2008), *"A review of some plasticity and viscoplasticity constitutive theories"*, International Journal of Plasticity, 24(10), pp. 1642-1693.

[14] Chen, A.Y., Ruan, H.H., Wang, J., Chan, H.L., Wang, Q., Li, Q., Lu, J., (2011), *"The influence of strain rate on the microstructure transition of 304 stainless steel"*, Acta Materialia, 59(9), pp. 3697-3709.

[15] Clausen, A.H., Børvik, T., Hopperstad, O.S., Benallal, A., (2004), *"Flow and fracture characteristics of aluminium alloy AA5083-H116 as function of strain rate, temperature and triaxiality"*, Materials Science and Engineering A, 364(1-2), pp. 260-272.

[16] Coleman, T.F., Li, Y., (1994), *"On the convergence of interior-reflective Newton methods for nonlinear minimization subject to bounds"*, Mathematical Programming, 67(1-3), pp. 189-224.

[17] Couque, H.R., Boulanger, R., Bornet, F., (1995), *"A modified Johnson-Cook model for strain rates ranging from 10^{-3} to 10^{5} s^{-1}"*, Journal de Physique IV, 134, pp. 87-93.

[18] Dey, S., Børvik, T., Hopperstad, O.S., Langseth, M., (2007), *"On the influence of constitutive relation in projectile impact of steel plates"*, International Journal of Impact Engineering, 34(3), pp. 464-486.

[19] Gambirasio, L., (2013), *"Large Strain Computational Modeling of High Strain Rate Phenomena in Perforating Gun Devices by Lagrangian/Eulerian FEM Simulations"*, Doctoral Thesis, April 2013, Advisor Rizzi, E., University of Trento/University of Bergamo, 273 pp.

[20] Gambirasio, L., Chiantoni, G., Rizzi, E., (2014), *"On the consequences of the adoption of the Zaremba–Jaumann objective stress rate in FEM codes"*, Archives of Computational Methods in Engineering, published online 12 October 2014, DOI 10.1007/s11831-014-9130-z.

[21] Gambirasio, L., Rizzi, E., (2014), *"On the calibration strategies of the Johnson-Cook strength model: Discussion and applications to experimental data"*, Materials Science and Engineering A, 610, pp. 370-413.

[22] Grązka, M., Janiszewski, J., (2012), *"Identification of Johnson-Cook equation constants using finite element method"*, Engineering Transactions, 60(3), pp. 215-223.

[23] Gruben, G., Fagerholt, E., Hopperstad, O.S., Børvik, T., (2011), *"Fracture characteristics of a cold-rolled dual-phase steel"*, European Journal of Mechanics, A/Solids, 30(3), pp. 204-218.

[24] Hähner, P., Rizzi, E., (2003), *"On the kinematics of Portevin-Le Chatelier bands: theoretical and numerical modelling"*, Acta Materialia, 51(12), pp. 3385-3397.
[25] Hawkyard, J.B., (1969), *"A theory for the mushrooming of flat-ended projectiles impinging on a flat rigid anvil, using energy considerations"*, International Journal of Mechanical Sciences, 11(3), pp. 313-333.
[26] Hawkyard, J.B., Eaton, D., Johnson, W.B., (1968), *"The mean dynamic yield strength of copper and low carbon steel at elevated temperatures from measurements of the "mushrooming" of flat-ended projectiles"*, International Journal of Mechanical Sciences, 10(12), pp. 929-948.
[27] He, A., Xie, G., Zhang, H., Wang, X., (2013), *"A comparative study on Johnson–Cook, modified Johnson–Cook and Arrhenius-type constitutive models to predict the high temperature flow stress in 20CrMo alloy steel"*, Materials & Design, 52, pp. 677-685.
[28] Hill, R., (1950), *"The Mathematical Theory of Plasticity"*, Clarendon Press.
[29] Hoge, K.G., Mukherjee, A.K., (1977), *"The temperature and strain rate dependence of the flow stress of tantalum"*, Journal of Materials Science, 12(8), pp. 1666-1672.
[30] Holmquist, T.J., Johnson, G.R., (1988), *"Determination of Constitutive Model Constants from Cylinder Impact Tests"*, Report NSWC TR 88-250, Naval Surface Warfare Center. Defense Technical Information Center (DTIC), U.S. Department of Defense.
[31] Holmquist, T.J., Johnson, G.R., (1991), *"Determination of constants and comparison of results for various constitutive models"*, Journal de Physique IV, 1(C3), pp. 853-860.
[32] Hopkinson, B., (1914), *"A method of measuring the pressure produced in the detonation of high explosive or by the impact of bullets"*, Proceedings of the Royal Society A: Mathematical, Physical and Engineering Sciences, 89(612), pp. 411-413.
[33] Hopperstad, O.S., Børvik, T., Langseth, M., Labibes, K., Albertini, C., (2003), *"On the influence of stress triaxiality and strain rate on the behaviour of a structural steel. Part I. Experiments"*, European Journal of Mechanics, A/Solids, 22(1), pp. 1-13.
[34] Hou, Q.Y., Wang, J.T., (2010), *"A modified Johnson-Cook constitutive model for Mg-Gd-Y alloy extended to a wide range of temperatures"*, Computational Materials Science, 50(1), pp. 147-152.
[35] House, J.W., (1989), *"Taylor Impact Testing"*, Report AFATL-TR-89-41, U.S. Air Force Armament Laboratory, University of Kentucky. Defense Technical Information Center (DTIC), U.S. Department of Defense.
[36] Hussain, G., Hameed, A.S.H., Hetherington, J.G., Barton, P.C., Malik, A.Q., (2013), *"Hydrocode simulation with modified Johnson-Cook model and experimental analysis of explosively formed projectiles"*, Journal of Energetic Materials, 31(2), pp. 143-155.
[37] Jiang, F., Vecchio, K.S., (2009), *"Hopkinson bar loaded fracture experimental technique: a critical review of dynamic fracture toughness tests"*, Applied Mechanics Reviews, 62(6), pp. 1-39.
[38] Johnson, G.R., Cook, W.H., (1983), *"A constitutive model and data for metals subjected to large strains, high strain rates and high temperatures"*, Proceedings of the 7th International Symposium on Ballistics, April 19-21, 1983, The Hague, South Holland, The Netherlands, pp. 541-547.
[39] Johnson, G.R., Cook, W.H., (1985), *"Fracture characteristics of three metals subjected to various strains, strain rates, temperatures and pressures"*, Engineering Fracture Mechanics, 21(1), pp. 31-48.
[40] Johnson, G.R., Holmquist, T.J., (1988), *"Evaluation of cylinder-impact test data for constitutive model constants"*, Journal of Applied Physics, 64(8), pp. 3901-3910.
[41] Johnson, G.R., Holmquist, T.J., Anderson Jr., C.E., Nicholls, A.E., (2006), *"Strain-rate effects for high-strain-rate computations"*, Journal de Physique IV, 134, pp. 391-396.
[42] Kachanov, L.M., (1971), *"Foundations of the Theory of Plasticity, English Translation of the Second Edition"*, ISBN 0-7204-2363-5, monograph in the series *"North-Holland Series in Applied Mathematics and Mechanics"*, Number 12, Series Editors Lauwerier, H.A, Koiter, W.T.
[43] Kajberg, J., Sundin, K.G., Melin, L.G., Ståhle, P.W., (2004), *"High strain-rate tensile testing and viscoplastic parameter identification using microscopic high-speed photography"*, International Journal of Plasticity, 20(4-5), pp. 561-575.
[44] Kajberg, J., Wikman, B., (2007), *"Viscoplastic parameter estimation by high strain-rate experiments and inverse modelling – Speckle measurements and high-speed photography"*, International Journal of Solids and Structures, 44(1), pp. 145-164.
[45] Kang, W.J., Cho, S.S., Huh, H., Chung, D.T., (1999), *"Modified Johnson-Cook model for vehicle body crashworthiness simulation"*, International Journal of Vehicle Design, 21(4-5, Special Issue), pp. 424-435.

[46] Kapoor, R., Nemat-Nasser, S., (1998), *"Determination of temperature rise during high strain rate deformation"*, Mechanics of Materials, 27(1), pp. 1-12.
[47] Khan, A.S., Suh, Y.S., Kazmi, R., (2004), *"Quasi-static and dynamic loading responses and constitutive modeling of titanium alloys"*, International Journal of Plasticity, 20(12), pp. 2233-2248.
[48] Kolsky, H., (1949), *"An investigation of the mechanical properties of materials at very high rates of loading"*, Proceedings of the Physical Society. Section B, 62(11), pp. 676-700.
[49] Kotkunde, N., Deole, A.D., Gupta, A.K., Singh, S.K., (2014a), *"Comparative study of constitutive modeling for Ti–6Al–4V alloy at low strain rates and elevated temperatures"*, Materials & Design, 55, pp. 999-1005.
[50] Kotkunde, N., Krishnamurthy, H.N., Puranik, P., Gupta, A.K., Singh, S.K., (2014b), *"Microstructure study and constitutive modeling of Ti–6Al–4V alloy at elevated temperatures"*, Materials & Design, 54, pp. 96-103.
[51] Krafft, A., Sullivan, A.M., Tipper, C.F., (1954), *"The effect of static and dynamic loading and temperature on the yield stress of iron and mild steel in compression"*, Proceedings of the Royal Society A: Mathematical, Physical and Engineering Sciences, 221(1144), pp. 114-127.
[52] Langrand, B., Geoffroy, P., Petitniot, J.L., Fabis, J., Markiéwicz, É., Drazétic, P., (1999), *"Identification technique of constitutive model parameters for crashworthiness modelling"*, Aerospace Science and Technology, 3(4), pp. 215-227.
[53] Lee, W.S., Lin, C.F., (1998), *"Plastic deformation and fracture behaviour of Ti-6Al-4V alloy loaded with high strain rate under various temperatures"*, Materials Science and Engineering A, 241(1-2), pp. 48-59.
[54] Lesuer, D., (1999), *"Experimental Investigation of Material Models for Ti-6Al-4V and 2024-T3"*, Report UCRL-ID-134691, Lawrence Livermore National Laboratory.
[55] Levenberg, K., (1944), *"A method for the solution of certain non-linear problems in least squares"*, Quarterly of Applied Mathematics, 2, pp. 164-168.
[56] Li, H.Y., Li, Y.H., Wang, X.F., Liu, J.J., Wu, Y., (2013), *"A comparative study on modified Johnson Cook, modified Zerilli–Armstrong and Arrhenius-type constitutive models to predict the hot deformation behavior in 28CrMnMoV steel"*, Materials & Design, 49, pp. 493-501.
[57] Lin, Y.C., Chen, X.M., (2010a), *"A combined Johnson-Cook and Zerilli-Armstrong model for hot compressed typical high-strength alloy steel"*, Computational Materials Science, 49(3), pp. 628-633.
[58] Lin, Y.C., Chen, X.M., (2010b), *"Erratum to: "A combined Johnson-Cook and Zerilli-Armstrong model for hot compressed typical high-strength alloy steel" [Computational Materials Science (2010) 49(628-633)]"*, Computational Materials Science, 50(10), pp. 3073.
[59] Lin, Y.C., Chen, X.M., Liu, G., (2010), *"A modified Johnson-Cook model for tensile behaviors of typical high-strength alloy steel"*, Materials Science and Engineering A, 527(26), pp. 6980-6986.
[60] Lin, Y.C., Li, L.T., Jiang, Y.Q., (2012a), *"A phenomenological constitutive model for describing thermo-viscoplastic behavior of Al-Zn-Mg-Cu alloy under hot working condition"*, Experimental Mechanics, 52(8), pp. 993-1002.
[61] Lin, Y.C., Li, Q.F., Xia, Y.C., Li, L.T., (2012b), *"A phenomenological constitutive model for high temperature flow stress prediction of Al-Cu-Mg alloy"*, Materials Science and Engineering A, 534, pp. 654-662.
[62] Lin, Y.C., Li, L.T., Fu, Y.X., Jiang, Y.Q., (2012c), *"Hot compressive deformation behavior of 7075 Al alloy under elevated temperature"*, Journal of Materials Science, 47(3), pp. 1306-1318.
[63] Maheshwari, A.K., Pathak, K.K., Ramakrishnan, N., Narayan, S.P.A., (2010), *"Modified Johnson-Cook material flow for hot deformation processing"*, Journal of Materials Sciences, 45(4), pp. 859-864.
[64] Marquardt, D.W., (1963), *"An algorithm for least-squares estimation of nonlinear parameters"*, Journal of the Society for Industrial and Applied Mathematics, 11(2), pp. 431-441.
[65] Meyers, M.A., (1994), *"Dynamic Behavior of Materials"*, ISBN 0-471-58262-X.
[66] Mishra, A., Martin, M., Thadhani, N.N., Kad, B.K., Kenik, E.A., Meyers, M.A., (2008), *"High-strain rate response of ultra-fine-grained copper"*, Acta Materialia, 56(12), pp. 2770-2783.
[67] Nemat-Nasser, S., Guo, W.G., (2000), *"Flow stress of commercially pure niobium over a broad range of temperatures and strain rates"*, Materials Science and Engineering A, 284(1-2), pp. 202-210.
[68] Nemat-Nasser, S., Guo, W.G., (2003), *"Thermomechanical response of DH-36 structural steel over a wide range of strain rates and temperatures"*, Mechanics of Materials, 35(11), pp. 1023-1047.
[69] Nemat-Nasser, S., Guo, W.G., (2005), *"Thermomechanical response of HSLA-65 steel plates: experiments and modeling"*, Mechanics of Materials, 37(2-3 Special Issues), pp. 379-405.

[70] Nemat-Nasser, S., Guo, W.G., Kihl, D.P., (2001), *"Thermomechanical response of Al-6XN stainless steel over a wide range of strain rates and temperatures"*, Journal of the Mechanics and Physics of Solids, 49(8), pp. 1823-1846.
[71] Nguyen, D.T., Bahn, T.L., Jung, D.W., Yang, S.H., Kim, Y.S., (2012), *"A modified Johnson-Cook model to predict stress-strain curves of boron steel sheets at elevated and cooling temperatures"*, High Temperature Materials and Processes, 31(1), pp. 37-45.
[72] Notta-Cuvier, D., Langrand, B., Markiéwicz, É., Lauro, F., Portemont, G., (2013), *"Identification of Johnson-Cook's viscoplastic model parameters using the virtual fields method: application to titanium alloy Ti6Al4V"*, Strain, 49(1), pp. 22-45.
[73] Nussbaum, J., Faderl, N., (2011), *"Evaluation of strength model parameters from Taylor impact tests"*, Procedia Engineering, 10, pp. 3453-3458.
[74] Pappu, S., Murr, L.E., (2002), *"Hydrocode and microstructural analysis of explosively formed penetrators"*, Journal of Materials Science, 37(2), pp. 233-248.
[75] Qingdong, Z., Qiang, C., Xiaofeng, Z., (2014), *"A modified Johnson-Cook model for advanced high-strength steels over a wide range of temperatures"*, Journal of Materials Engineering and Performance, 23(12), pp. 4336-4341.
[76] Rakvåg, K.G., Børvik, T., Hopperstad, O.S., (2014), *"A numerical study on the deformation and fracture modes of steel projectiles during Taylor bar impact tests"*, International Journal of Solids and Structures, 51(3-4), pp. 808-821.
[77] Ramesh, K.T., Narasimhan, S., (1996), *"Finite deformations and the dynamic measurement of radial strains in compression Kolsky bar experiments"*, International Journal of Solids and Structures, 33(25), pp. 3723-3728.
[78] Rizzi, E., Hähner, P., (2004), *"On the Portevin–Le Chatelier effect: theoretical modeling and numerical results"*, International Journal of Plasticity, 20(1), pp. 121-165.
[79] Rohr, I., Nahme, H., Thoma, K.A.T., Anderson Jr., C.E., (2008), *"Material characterisation and constitutive modelling of a tungsten-sintered alloy for a wide range of strain rates"*, International Journal of Impact Engineering, 35(8), pp. 811-819.
[80] Roth, C.C., Mohr, D., (2014), *"Effect of strain rate on ductile fracture initiation in advanced high strength steel sheets: Experiments and modeling"*, International Journal of Plasticity, 56, pp. 19-44.
[81] Rule, W.K., (1997), *"A numerical scheme for extracting strength model coefficients from Taylor test data"*, International Journal of Impact Engineering, 19(9-10), pp. 797-810.
[82] Rule, W.K., Jones, S.E., (1998), *"A revised form for the Johnson-Cook strength model"*, International Journal of Impact Engineering, 21(8), pp. 609-624.
[83] Rusinek, A., Rodríguez-Martínez, J.A., Klepaczko, J.R., Pęcherski, R.B., (2009), *"Analysis of thermo-visco-plastic behaviour of six high strength steels"*, Materials & Design, 30(5), pp. 1748-1761.
[84] Rusinek, A., Zaera, R., Klepaczko, J.R., (2007), *"Constitutive relations in 3-D for a wide range of strain rates and temperatures – Application to mild steels"*, International Journal of Solids and Structures, 44(17), pp. 5611-5634.
[85] Rusinek, A., Zaera, R., Klepaczko, J.R., Cheriguene, R., (2005), *"Analysis of inertia and scale effects on dynamic neck formation during tension of sheet steel"*, Acta Materialia, 53(20), pp. 5387-5400.
[86] Samantaray, D., Mandal, S., Bhaduri, A.K., (2009), *"A comparative study on Johnson Cook, modified Zerilli-Armstrong and Arrhenius-type constitutive models to predict elevated temperature flow behaviour in modified 9Cr-1Mo steel"*, Computational Materials Science, 47(2), pp. 568-576.
[87] Schwer, L.E., (2007), *"Optional strain-rate forms for the Johnson Cook constitutive model and the role of the parameter epsilon_0[1]"*, Proceedings of the 6th European LS-DYNA Users Conference, May 29-30, 2007, Gothenburg, Götaland, Sweden.
[88] Seidt, J.D., Gilat, A., (2013), *"Plastic deformation of 2024-T351 aluminum plate over a wide range of loading conditions"*, International Journal of Solids and Structures, 50(10), pp. 1781-1790.
[89] Šlais, M., Dohnal, I., Forejt, M., (2012), *"Determination of Johnson-Cook equation parameters"*, Acta Metallurgica Slovaca, 18(2-3), pp. 125-132.
[90] Symonds, P.S., (1967), *"Survey of Methods of Analysis for Plastic Deformation of Structures Under Dynamic Loading"*, Report BU/NSRDC/1-67, Division of Engineering, Brown University. Defense Technical Information Center (DTIC), U.S. Department of Defense.
[91] Taylor, G., (1948), *"The use of flat-ended projectiles for determining dynamic yield stress. I. Theoretical considerations"*, Proceedings of the Royal Society A: Mathematical, Physical and Engineering Sciences, 194(1038), pp. 289-299.

[92] Teng, X., Wierzbicki, T., (2005), *"Transition of failure modes in round-nosed mass-to-beam impact"*, European Journal of Mechanics, A/Solids, 24(5), pp. 857-876.
[93] Teng, X., Wierzbicki, T., Hiermaier, S., Rohr, I., (2005), *"Numerical prediction of fracture in the Taylor test"*, International Journal of Solids and Structures, 42(9-10), pp. 2929-2948.
[94] Valerio-Flores, O.L., Murr, L.E., Hernandez, V.S., Quinones, S.A., (2004), *"Observations and simulations of the low velocity-to-hypervelocity impact crater transition for a range of penetrator densities into thick aluminum targets"*, Journal of Materials Science, 39(20), pp. 6271-6289.
[95] Wang, Y.P., Han, C.J., Wang, C., Li, S.K., (2011), *"A modified Johnson-Cook model for 30Cr2Ni4MoV rotor steel over a wide range of temperature and strain rate"*, Journal of Materials Science, 46(9), pp. 2922-2927.
[96] Whiffin, A.C., (1948), *"The use of flat-ended projectiles for determining dynamic yield stress. II. Tests on various metallic materials"*, Proceedings of the Royal Society A: Mathematical, Physical and Engineering Sciences, 194(1038), pp. 300-322.
[97] Wilkins, M.L., (1963), *"Calculation of Elastic-Plastic Flow"*, Report UCRL-7322, Lawrence Radiation Laboratory. Defense Technical Information Center (DTIC), U.S. Department of Defense.
[98] Wilkins, M.L., (1978), *"Mechanics of penetration and perforation"*, International Journal of Engineering Science, 16(11), pp. 793-807.
[99] Wilkins, M.L., Guinan, M.W., (1973), *"Impact of cylinders on a rigid boundary"*, Journal of Applied Physics, 44(3), pp. 1200-1206.
[100] Zerilli, F.J., Armstrong, R.W., (1987), *"Dislocation-mechanics-based constitutive relations for material dynamics calculations"*, Journal of Applied Physics, 61(5), pp. 1816-1825.
[101] Zukas, J.A., (2004), *"Introduction to Hydrocodes"*, ISBN 0-08-044348-6, monograph in the series *"Studies in Applied Mechanics"*, Number 49, Series Editor Elishakoff, I.